NANYANG TECHNOLOGICAL UNIVERSITY

SYNTHESIS OF POLY(*N*-ISOPROPYLACRYLAMIDE)-BASED STAR-BLOCK AND DENDRITIC COPOLYMERS AND THEIR THERMAL AND PH DUAL-RESPONSIVE BEHAVIORS

Bai Yu

SCHOOL OF MATERIALS SCIENCE & ENGINEERING

2013

SYNTHESIS OF POLY(*N*-ISOPROPYLACRYLAMIDE)-BASED STAR-BLOCK AND DENDRITIC COPOLYMERS AND THEIR THERMAL AND PH DUAL-RESPONSIVE BEHAVIORS

Bai Yu

SCHOOL OF MATERIALS SCIENCE & ENGINEERING

A thesis submitted to the Nanyang Technological University in partial fulfilment of the requirement for the degree of

Doctor of Philosophy

2013

ACKNOWLEDGEMENTS

I am greatly indebted to my advisor Associate Professor Lu Xuehong, Division of Materials Technology, School of Materials Science and Engineering for all the guidance, support and inspiration provided me over the years. I also wish to thank Dr. He Chaobin, Dr. Liu Ye and Dr. Chakravarthy S. Gudipati, Institute of Materials Research and Engineering, for all their research instruction and guidance.

I would like to acknowledge the technical executives, especially the Organic Materials Service Laboratory for their significant technical help and support.

I would like to thank all my fellow colleagues, in particular Dr. Yang Liping, Dr. Wei Jia, Ms. Cher Ling Toh Joan, Dr. Teo Jun Kai Herman and Dr. Xiao Yang for their valuable assistance and suggestions.

I want to thank Nanyang Technological University, Singapore, for providing my Ph.D. scholarship.

I am eternally grateful to my parents for believing in me and to my dear wife Ms. Zhan Ying for the tremendous support and understanding throughout the years.

TABLE OF CONTENTS

LIST OF FIGURES, SCHEMES AND TABLES

LIST OF ABBREVIATIONS

AAm	Acrylamide
AFM	Atomic Force Microscopy
ATRP	Atom Transfer Radical Polymerization
bpy	Bipyridine
CTA	Chain Transfer Agent
CRP	Controlled Living Polymerization
DMA	Dimethylacrylamide
DMF	Dimethylformamide
DLS	Dynamic Light Scattering
DBSA	Dodecylbenzene Sulphonic Acid
ECP	Ethyl-2-chloropropionate
EMI	2-Ethyl-4-methylimidazole
EBIB	Ethyl-2-bromoisobutyrate
FTIR	Fourier Transform Infrared
LCST	Lower Critical Solution Temperature
Me_6TREN	Tris(2-dimethylaminoethyl)-amine
NMR	Nuclear Magnetic Resonance
OAPS	Octa-aminophenyl Silsesquioxane
OpePOSS	Octa-glycidyl Silsesquioxane
PAMAM	Poly(amidoamine)
PBMA	Poly(butylmethacrylate)
PCL	Poly(ε-caprolactone)

PDMAEMA	Poly(*N*,*N*-dimethylaminoethyl methacrylate)
PEG	Poly(ethylene glycol)
PEO	Poly(ethylene oxide)
PEPyM	Poly(*N*-ethylpyrrolidine methacrylate)
PLA	Poly(lactic acid)
PMDETA	*N*,*N*,*N*',*N*'',*N*''-pentamethyldiethylenetriamine
PMMA	Poly(methyl methacrylate)
PNIPAm	Poly(*N*-isopropylacrylamide)
POSS	Polyhedral Oligomeric Silsesquioxane
PS	Polystyrene
PSS	Poly(4-styrene sulfonic acid)
PVCL	Poly(*N*-vinylcaprolactam)
PVME	Poly(vinylmethylether)
RAFT	Reversible Addition-Fragmentation Chain Transfer
R_g	Radius of Gyration
R_h	Hydrodynamic Radius
ROP	Ring Opening Polymerization
THF	Tetrahydrofuran
TMS	Tetramethylsilane
UVRR	Ultraviolet Resonance Raman Spectroscopy

ABSTRACT

Thermal responsive polymers have aroused extensive research interest due to their potential applications in areas such as controlled drug release and gene delivery, molecular switch and separation membranes. Poly (*N*-isopropylacrylamide) (PNIPAm) is probably the most widely investigated thermal responsive polymer. PNIPAm can be dissolved in aqueous solution at low temperature and exhibit an inverse soluble-insoluble phase transition at *ca*. 34 ˚C, well-known as the lower critical solution temperature (LCST) or cloud point (T_c). At the transition the PNIPAm chains change from extended random coils to collapsed globules, expelling water and small molecules. The transition temperature of PNIPAm and its copolymers is of great importance for scientific research and technical applications and is affected by many factors such as solution's ionic strength, molecular weight, polymer architecture, hydrophilicity of the copolymer and the end groups, etc. This work is focused on synthesis of PNIPAm-based star-block and dendritic copolymers and study of the effects of molecular architecture and chain length on the solution phase transition behaviors of the copolymers.

Star-shaped PNIPAm with short arms was successfully synthesized by "core first" atom transfer radical polymerization (ATRP) using a multi-functional polyhedral oligomeric silsesquioxane (POSS) initiator. The star architecture of POSS-PNIPAm was verified by molecular weight analysis of the star polymers and the corresponding linear arms produced by hydrolysis. POSS-PNIPAm exhibits T_c which is found to be much lower than that of the linear counterpart having similar chain length. It could be attributed to the high local chain density in the near-core region that significantly increased intra-molecular interaction among the neighbour arms. On the other hand, such interactions are

inhibited in solutions of low molecular weight linear PNIPAm that adopts a rigid rod-like conformation when their lengths are close to the persistent length.

To reveal the influence of the high local chain density in the near-core region on temperature and pH dual-response behavior of PNIPAm-based copolymers, short blocks of pH sensitive poly(acrylic acid) (PAAc) are inserted between the POSS core and the PNIPAm block via sequential steps of ATRP. By changing the length of PAAc block and pH of the solution, the hydrophilicity of the molecules and intra-molecular interaction can be manipulated. It is found that when PAAc block is very short, T_c of the star-block copolymers varies in a wide temperature range while when PAAc block is relatively long the phase transition is broad and the T_c had almost no response to pH. The results suggest that with high local chain density in the near-core region, the intra-molecular interaction is significantly enhanced between PAAc and PNIPAm blocks to lower the T_c, whereas the synergic effect is weakened when the PAAc block is longer.

To improve biocompatibility of temperature and pH dual-responsive polymers, dendritic POSS-PNIPAm with a peripheral poly(2-hydroxyethyl methacrylate) (PHEMA) layer are successfully synthesized via the combination of ATRP and click reaction. The dendritic architecture is constructed by clicking between POSS-PNIPAm and Y-shape PNIPAm or PHEMA precursors. The dendrimers with a peripheral layer of short PHEMA chains (DN2H) is found to be temperature and pH sensitive. Its T_c decreases with decreasing pH from 10.0 to 5.0, whereas exhibits a small increase from pH 5.0 to 4.0 due to better solvation of PHEMA at highly acidic condition. Dynamic light scattering studies reveal that DN2H forms large aggregations at high pH values, while at pH 4.0 it has a mono-dispersed distribution with R_h of about 5 nm. The controlled release experiments at different temperature and pH demonstrate that dendritic PNIPAm-PHEMA is a promising candidate for thermal and pH dual responsive nanocarrier.

1. INTRODUCTION

1.1 Background

Smart or intelligent materials have been around us for many years, attracting lots of research interest and having its significant applications in automotive, aerospace, biomedical and many other fields. Generally, a smart material can be recognized as a kind of material that is responsive to changes in conditions such as temperature, pH, ionic strength, magnetic or electric field [1-3]. As compared with traditional materials, the field of smart materials is multidisciplinary and interdisciplinary, and is becoming increasingly important for development of functional devices/systems such as transducers, actuators and controlled drug release systems.

Thermal responsive polymers are often described as “smart” or “intelligent” materials. These polymers have been regarded as “smart” because they can undergo conformational changes in response to environmental temperature variation to induce a reversible phase transition. Poly(*N*-isopropylacrylamide) (PNIPAm) is probably the most widely investigated thermal responsive polymer [4]. The aqueous solution of PNIPAm undergoes a coil-to-globule conformational transition at *ca*. 34 ℃, which is known as the lower critical transition temperature (LCST) or cloud point (T_c). At LCST PNIPAm solutions show an increase in turbidity because the polymer chains switch from hydrophilic to hydrophobic conformation and collapse from an extended random coil into a compact state. LCST of PNIPAm is affected by many factors such as polymer tacticity, end groups, molecular weight and molecular architecture. Understanding of how these factors affect the transition is of great scientific and technical interest as different phase transition

behaviors may be favorable for applications in different areas, such as controlled drug delivery, molecular sensors or membrane separation.

Another kind of smart polymers that contains ionizable groups can change their conformation or solvation state upon a change in the pH value of their environment. This kind of pH responsive polymers, including poly(acrylic acid) (PAAc), poly(butylmethacrylate) (PBMA) and poly(*N*,*N*-dimethylaminoethyl methacrylate) (PDMAEMA), are also important for applications such as sensors and controlled drug delivery as they have different dissolving or swelling states under different pH conditions, *e.g.* neutral pH in intestinal tract or acidic pH in gastric environment. Recently, a well-known polymer with good biocompatibility, poly(2-hydroxyethyl methacrylate) (PHEMA), which is non-ionizable in water, has also been reported to have pH-dependent solvation behavior when its molecular weight is relatively low.

The combination of smart polymers responsive to different stimuli is an efficient and promising way to develop novel products with new behaviors or functions. In this thesis the research is focused on temperature and pH dual-responsive polymers formed via chemical combination of thermal and pH responsive polymers. The dual-responsive behaviors of such copolymers again are strongly influenced by the copolymer structures at different levels.

Since polymers began to play an essential and ubiquitous role in our daily life in the 19th century, numerous investigations have been concentrated on developing new structures and architectures to achieve better properties. Figure 1.1 illustrates major polymer architectures arranged in an increasing complexity way from left to right and top to bottom. For temperature and pH dual-responsive polymers, the molecular architectures play an important role in affecting their solution behaviors. For example, PNIPAm-PAAc random copolymers have a higher cloud point than PNIPAm homopolymer and the T_c is dependent on PAAc content because of the hydrophilic character of PAAc, while graft

PNIPAm-PAAc copolymers exhibit constant cloud points independent of PAAc content at pH 4.0 and 7.4, respectively, due to the hydrogen bonds between PAAc and PNIPAm [5]. In Figure 1.1 it can be found that star polymers and dendrimers have the most complex architectures. With their well-defined architectures, these polymers may have unique solution properties. For example, star-shaped PNIPAm with four arms has been reported to have significant lower T_c than linear PNIPAm due to the increased local chain density by tethering four chains on the core and the combined effects of the hydrophobic core and end groups [6]. Similar behavior has also been found with hyper-branched PNIPAm with hydrophobic end groups [7]. However, to date, although much research has been conducted on temperature and pH dual-responsive polymers, most of the investigation focused on linear or other types of polymers with relatively simple architectures [5, 8-10] and few was carried out on star-block and dendritic copolymers [11].

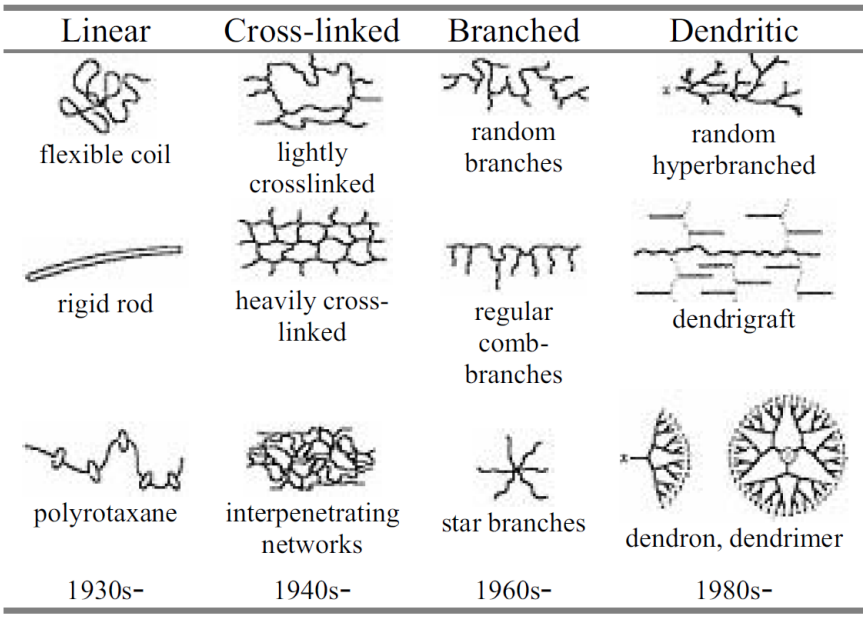

Figure 1.1. Classes of polymer architectures. The complexity is increasing from left to right (classes) and top to bottom (subclasses).

Molecular weight is another important factor affecting a polymer's various properties. When the molecular weight is sufficiently large, polymers exhibit relatively stable macroscopic chemical and physical properties. However, when the molecular weight is very low, the properties of the oligomers may be greatly dependent on their molecular weight. T_c of high-molecular-weight PNIPAm is well known at *ca*. 34 ℃ but it is much higher than this value or even disappears when the degree of polymerization (DP) drops to about 10 [12]. It is believed that PNIPAm short chains with lengths not much longer than its persistence length exhibit a rigid-rod conformation that hinders intra-chain hydrophobic interactions.

Fundamentally, thermal and pH sensitivities of a polymer in solution are mainly controlled by intra-chain and inter-chain hydrophobic interactions and that between the chains and solvent molecules. Such interactions could be much more complex in star and dendritic copolymers. Being significantly different from linear polymers, the adoption of star or dendritic architectures not only alters the molecular shape, changing inter-molecular interactions and possibly also the interactions of the polymers with solvents, but also induces different chemical environments for the chain segments in the same molecule, altering intra-molecular hydrophobic interactions. As mentioned earlier, although some research has been conducted on thermal responsive star PNIPAm, the influences of star architecture on temperature and pH dual-responsive behaviors of PNIPAm-based copolymers have not been systematically studied. It is hypothesized that the high local density created with the star molecular architecture would also affect the intra-molecular interactions among the pH-sensitive segments and/or that between PNIPAm and pH-sensitive segments in the star copolymers. Moreover, by varying the lengths of the thermal and pH responsive segments, these interactions may also vary and hence the dual-responsive behaviors of the copolymers may be further manipulated.

In recent years, with the progress of click chemistry and living radical polymerizations, including atom transfer radical polymerization (ATRP), reversible addition-fragmentation chain-transfer polymerization (RAFT) and nitroxide mediated radical polymerization (NMP), precise control of architectures of various kinds of star and dendritic polymers becomes possible. Previously reported star PNIPAm were synthesized using RAFT [6, 7], for which the hydrophobic chain transfer agent end groups inevitably affect the solution behaviors and T_c. To distinguish the effect of hydrophobic end groups and the effect induced by the star/dendritic architecture, ATRP is a better choice than RAFT. In an ATRP reaction, the polymer end groups are halogen atoms, bromine or chloride, which have much weaker hydrophobicity. On the other hand, star PNIPAm in previous reports have relatively large DP that reduces average local chain density and hence weakens the intra-molecular interactions. If short PNIPAm chains could be tethered onto a multi-functional core, *e.g*. octafunctional polyhedral oligomeric silsesquioxane (POSS), very high chain density may be achieved in the core region, significantly enhancing intra-molecular interactions. The arm length can also be controlled via ATRP as designed to investigate the effect of DP on solution behaviors. By precisely controlling the chain length and end groups, it is possible to understand the influences of the star architecture on the thermal responsive solution behaviors and the underlying mechanism better. On the basis of the star PNIPAm, temperature and pH dual-responsive star-block and dendritic copolymers could be further built up to investigate the influence of the star architecture and chain length, and their interplays, on dual-responsive behavior of the copolymers.

1.2 Objectives

With the hypothesis stated above, this research work is aimed at the synthesis of novel temperature and pH dual-responsive star-block and dendritic copolymers containing PNIPAm and investigation of the influence of the copolymer structures on solution properties in response to pH and thermal stimuli. The research is comprised of the following three parts:

- Synthesis and characterization of star PNIPAm with POSS as the core and investigation of the effect of arm length on thermal responsive behaviors.
- Synthesis and characterization of star-block PAAc-PNIPAm with POSS as the core and investigation of the effects of PAAc block length on temperature and pH dual-responsive behaviors.
- Synthesis and characterization of dendritic PNIPAm-PHEMA copolymers with POSS as the core and investigation of its dual-responsive behaviors as well as demonstration of their controlled release property.

1.3 Organization of the thesis

This thesis is divided into six chapters.

A brief description on the motivation and scope of the research is summarized in chapter 1.

In Chapter 2 the past research on topics related to this work are reviewed. After discussion of the preparation of POSS-PNIPAm polymers, the molecular weight and structural effects on their thermal response behaviors are investigated in Chapter 3. In Chapter 4, the synthesis and characterization of pH and thermal dual-responsive POSS-PAAc-PNIPAm star-block copolymers are reported. The dual responsive behaviors of the star-block copolymers are also studied, and the influences of the star architecture and

block lengths upon the transition temperatures are discussed in detail. In Chapter 5 the preparation of novel pH and thermal dual-responsive dendritic POSS-PNIPAm-PHEMA copolymers are reported. The influences of the dendritic architecture on its solution behaviors are discussed and the controlled release behaviors of these dendritic copolymers upon pH or thermal stimuli are demonstrated.

In Chapter 6 conclusions are drawn from this thesis and recommendations are proposed for future studies.

2. LITERATURE REVIEW

2.1 Thermal responsive polymers

In general, the solubilities of a majority of the polymers increase with increasing temperature. However, a number of polymers, such as poly(*N*-isopropylacrylamide) (PNIPAm) [4], poly(*N*,*N*-diethylacrylamide) (PDEA) [13], poly(*N*-vinylcaprolactam) (PVCL), and poly(vinylmethylether) (PVME) exhibit an opposite trend in this aspect. They undergo a soluble-insoluble transition when the environmental temperature is raised to a certain temperature known as the lower critical solution temperature (LCST) or cloud point (T_c). The T_c for a given homopolymer or copolymer system is dependent upon its intrinsic nature including the presence of ionic or potentially ionizable species, hydrogen bonding character and tacticity effects. Other factors such as the molecular weight and polydistribution of the polymer and the presence of other low molecular weight molecules and additives such as salts[13, 14], urea[15, 16] or surfactants[17-19] will all influence the cloud point.

The structure of a thermal responsive polymer typically shows a delicate balance between hydrophilic and hydrophobic moieties. For polymers that possess a LCST, the polymer chains exhibit an extended coil conformation surrounded by ordered water molecules in solution and/or water below the LCST. The hydration shell reduces the entropy of the system. Consequently, the free energy of swelling gel or solution is lowered by the formation of hydrogen bonds but is raised by the reduction of entropy. When the temperature is higher than the LCST, the solution is dominated by the entropy term and the polymer precipitates out of the solution or de-swelling of gel occurs[13]

(Figure 2.1). Therefore, very small changes in temperature can trigger drastic changes in the hydration layer[20] and lead to chain contraction and eventually to phase transition.

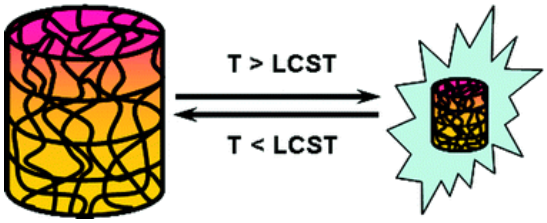

Figure 2.1. Coil-to-globule transition at LCST

Thermal responsive polymers have great scientific and technological importance as they serve as important additives in applications such as water treatment, enhanced oil recovery, controlled drug release, personal care coatings, etc. As PNIPAm is the most important and widely investigated thermal responsive polymer, the following review will focus on the structure, properties and applications of PNIPAm and its related copolymers.

2.1.1 Poly(*N*-isopropylacrylamide)

As the most well-known and widely studied thermal responsive polymer, PNIPAm (Figure 2.2) has fascinated scientists in both academia and industry since its thermal sensitivity was first observed by Heskins in 1968[21]. PNIPAm undergoes reversible hydrophilic to hydrophobic transition to form a turbid solution at *ca.* 34 ℃, i.e. the LCST or cloud point.

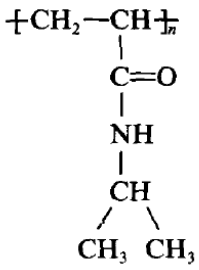

Figure 2.2. Structure of Poly(*N*-isopropylacrylamide) (PNIPAm)

Based on the coil-to-globule transition of a single linear polymer chain, Dusek predicted a possible discontinuous volume phase transition of a polymer gel in 1968 [22].

As a general and fundamental concept in polymer physics and solution dynamics, the coil-to-globule transition has attracted much research interest since then due to its implications in many biological systems such as protein folding and DNA packing.

In 1996, Zhou and his colleagues observed the coil-to-globule transition of a single PNIPAm chain for the first time in aqueous solution using light scattering techniques[23]. As an essential step to observe the coil-to-globule transition of a single chain, narrowly distributed high molecular weight PNIPAm was dissolved at an extremely low concentration to yield a stable homogeneous solution at all the temperatures investigated. Figure 2.3 illustrates the radius of gyration/hydrodynamic radius (R_h/R_g) values in response to the temperature during the coil-to-globule transition. A, B and C indicate different states during the transition: the rigid globule, the molten globule and the random coil, respectively. The R_h/R_g value changes from *ca*. 0.66 to 1.30 with temperature and agrees with the expected value for a random coil (~0.66) and a rigid sphere (~1.29) in good solvent. The unexpected maximum R_h/R_g value of ~1.61 at 32.2 ℃, which otherwise the value should follow the trend of the dashed line (Figure 2.3a), suggests that there is another physical state exists between the fully collapsed globule and the unfolded random coil. At the molten globule state B, the high R_h/R_g value indicates that R_h increases faster than R_g and the portion near the periphery of the globule melts faster than the inner core, i.e. the melting is not uniform (Figure 2.3b). Therefore, the R_h/R_g value increases instead of following the trend of the dashed line in Figure 2.3a.

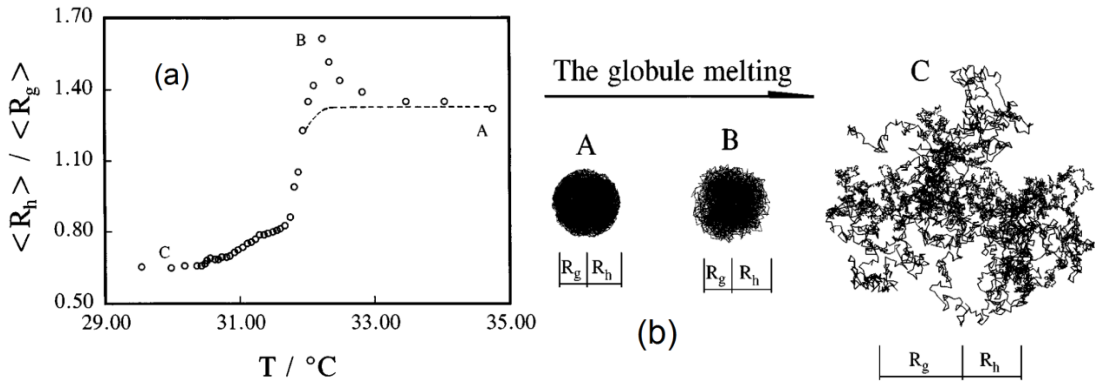

Figure 2.3. R_h and R_g changes during the coil-to-globule transition [23]. (a) R_h/R_g of individual PNIPAm chains in response to temperature changes; (b) the three different states of single PNIPAm chains in coil-to-globule transition. A: globule before melting; B: molten globule; C: random coil.

Maeda investigated the hydration state changes of PNIPAm during the coil-to-globule transition by FTIR spectroscopy [24]. During the transition, the differences in amide I, amide II, C-H stretching and C-H bending bands are believed to be due to partial dehydration of the polymer chain and deformation of intra-chain and inter-chain hydrogen bonding between amide groups. However, most of the C=O⋯H_2O hydrogen bonding remains unchanged even in the globular state.

More recently Asher utilized dynamic light scattering (DLS), ^{1}H NMR and steady state time-resolved ultraviolet resonance Raman spectroscopy (UVRR) to investigate the PNIPAm hydrophobic collapse [25]. It was determined that the amide bonds are predominantly fully hydrogen bonded with water and C=O is bonded to two water molecules at temperature below LCST. However, one of the C=O hydrogen bonds was broken and the NH-water hydrogen bonds remained unperturbed in the collapsed state. On the basis of the results, PNIPAm was proposed to adopt an extended water exposed conformation at low temperature to stabilize large clusters of water molecules. On the other hand, entropy penalty for water molecules at the surface of isopropyl groups would cause hydrophobic collapse to minimize exposing hydrophobic surface area. The amide carbonyl and N-H are forced to invaginate during the structure alternation and the water clusters are expelled (Figure 2.4).

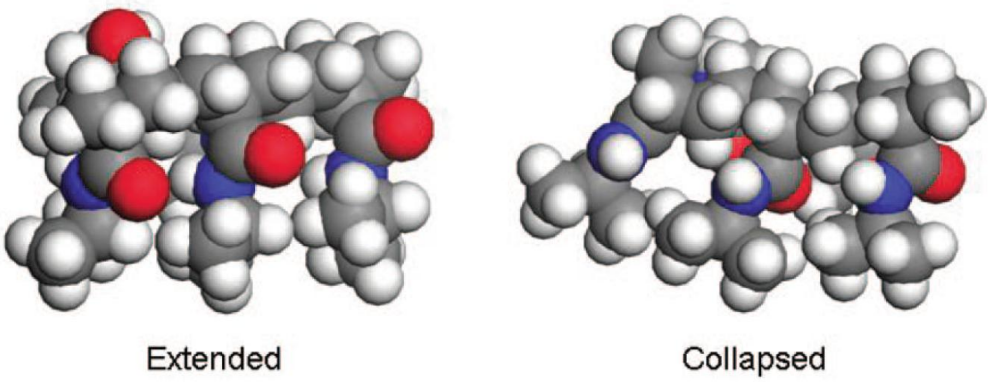

Figure 2.4. In the extended conformation the carbonyl groups are fully exposed, whereas in collapsed state they located inside the hydrophobic pocket (red: carbonyl oxygen; blue: nitrogen) [25].

The phase transition behaviors of PNIPAm have been widely studied and proved to be affected by various factors including: (1) intrinsic factors such as copolymer content ratio[5, 9], end groups[26-28], molecular weight[12, 25, 27-30], tacticity[31-33] and architecture[6, 7, 34-36] of the polymer, and (2) extrinsic factors such as concentration and ionic strength of solution[14, 37-39], surfactant[40, 41], etc.

Among these factors, the influence of molecular weight on LCST has been controversial for years. Researchers have diverse beliefs about the cloud point, i.e. it is either reversely dependent[42], independent [43-45], or dependent [27, 46, 47] on molecular weight. This meant that the molecular weight effect should not be considered individually and that the different polymer architecture, end groups and techniques to measure LCST may account for the variations. Additionally, in previous studies of the LCST, fractionated samples obtained from conventional radical polymerizations still often had broad mass distributions. As a result, the effects of M_w on measurement of LCST may be masked by either low or high molecular weight fractions. Therefore, a definitive solution would require a PNIPAm with well controlled molecular weight, distribution and end groups.

Stöver prepared narrowly dispersed PNIPAm by ATRP in alcohols and described the molecular weight dependence of cloud point for the first time [29]. The cloud point (50% transmission) decreases from 43.0 to 33.3 ℃ and approached the well-known value of 34 ℃ (Figure 2.5) when molecular weight ($M_{n,NMR}$) of narrowly dispersed PNIPAm increased from 2.8 to 26.5k. In comparison, broad dispersed samples of PNIPAm having 28.9k M_n and polydispersity of 2.0 made by conventional free radical polymerization exhibited cloud point of 31.2 ℃, i.e. about 2 ℃ lower than samples having similar M_n made by ATRP. The comparison clearly illustrates the importance of polydispersity in the studies of LCST behavior.

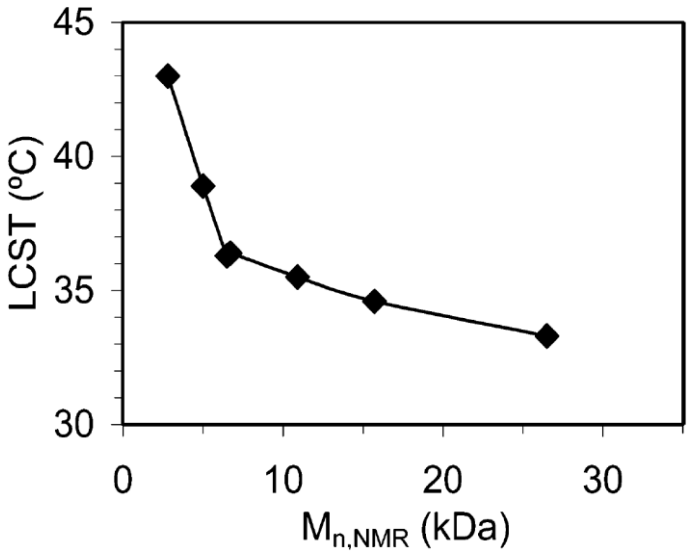

Figure 2.5. Effect of molecular weight ($M_{n,NMR}$) on cloud points of narrowly dispersed PNIPAm [29].

Asher observed the collapse rate of PNIPAm at approximately 10^6 s^{-1} and thus predicted an average persistence length of 10 repeating units by assuming diffusion limited collapse of PNIPAm [25]. If the polymer chain length is shorter than the persistence length, the PNIPAm is expected to behave like an elastic rod, while the polymer will behave like a random coil with polymer length longer than the persistence length. The persistence length is estimated about three times longer than the shortest polymer chain that can be sterically allowed to form a hydrophobic cluster. This implies

that the hydrophobic collapse is a cooperative process in which adjacent hydrophobic polymer segments coalesce through hydrophobic interactions to stabilize the collapsed particle.

More recently Ye prepared narrowly distributed PNIPAm by fractional precipitation. It was confirmed that the phase transition temperature agrees with the mean field theory of Flory which is a power law for the critical temperature(T_c) dependence on the degree of polymerization (N) [12].

$$T_c \propto N^{-1/2} \qquad N \to \infty$$

The phase transition temperature (T_p) was found to be proportional to $N^{-1/2}$ (Figure 2.6a). The data was also plotted in the form of $\ln(T_{p,0}\text{-}T_0)$ versus $\ln N$ to reveal the scaling relationship between $T_{p,0}$ and N (Figure 2.6b). The power was found to be -0.44 ±0.04 that is close to -1/2.

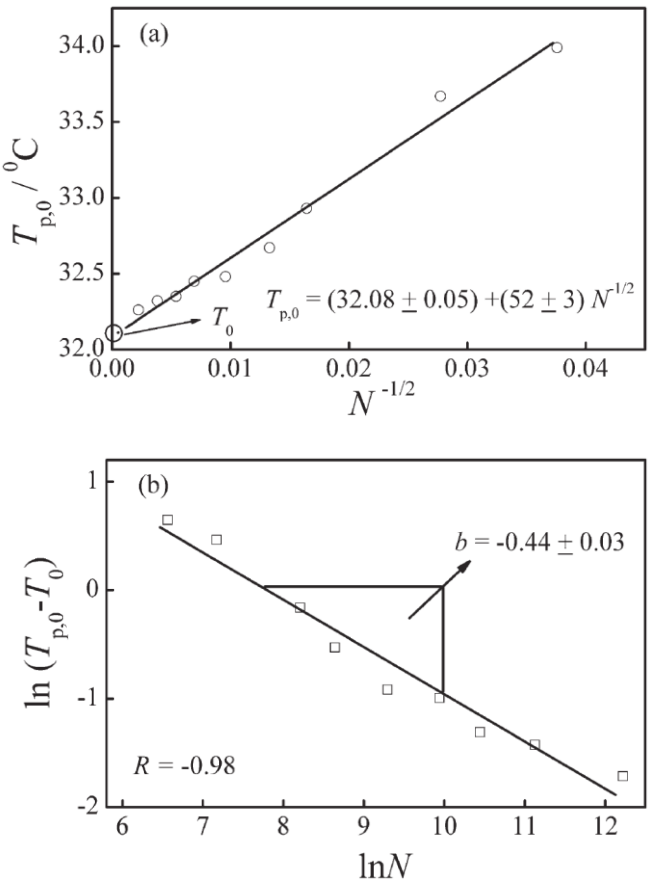

Figure 2.6. (a) Relationship of $T_{p,0}$ versus $N^{-1/2}$, where N is the DP of PNIPAm. (b) Plot of natural logarithm of ($T_{p,0}$-T_0) as a function of ln$N$ [12].

The end group may be an important factor in the phase transition of a polymer's solution. Hydrophobic end groups tend to decrease T_c of the polymer while hydrophilic end groups increase the T_c. St över prepared four series of narrow dispersed PNIPAm with different end groups by ATRP and studied the influences of molecular weight and end group on T_c of PNIPAm [27]. PNIPAm with various kinds of end groups all exhibited reverse molecular weight dependence of T_c (Figure 2.7). However, the end group effect was found to be more prominent for low molecular weight samples. The hydrophobic phenyl end groups caused an 8 ℃ decreasing for polymers having 3k molecular weight. The difference was less than 2 ℃ for polymers having 16-18k molecular weight.

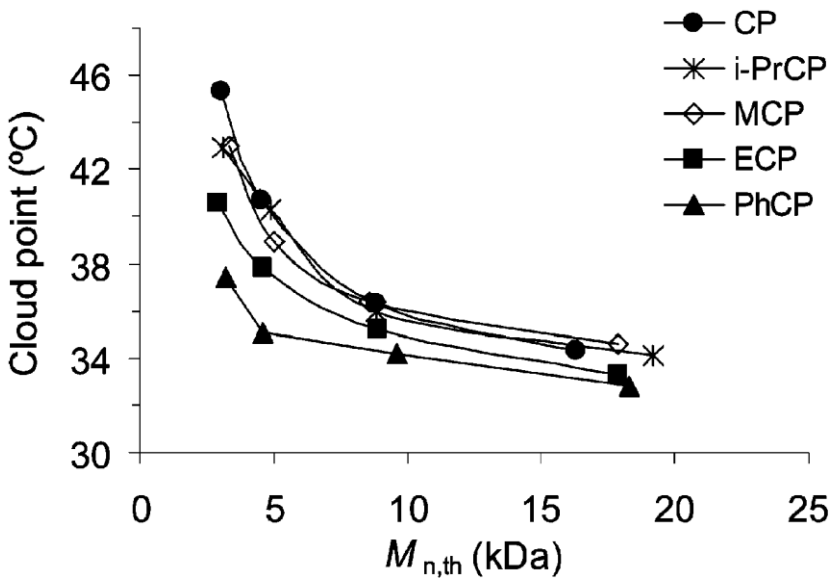

Figure 2.7. Cloud point of different molecular weight PNIPAm prepared by ATRP with different initiator: CP: 2-chloropropionamide; i-PrCP: isopropyl 2-chloropropionamide; MCP: methyl 2-chloropropionate; ECP: ethyl 2-chloropropionate; PhCP: phenyl 2-chloropropionamide [27].

Because of its hydrophobic-hydrophilic transition, PNIPAm is a promising material in surface modification, membrane and packaging applications. In these conditions, T_c of PNIPAm is also influenced by the graft chain density. Plunkett used surface initiated ATRP to graft PNIPAm on a self-assembled alkanethiol monolayer on gold [30] (Figure 2.8). The molecular weight of PNIPAm was controlled via reaction time and monomer

concentration. The temperature triggered chain collapse was found only evident at high molecular weight and high grafting density. The wettability above LCST was also found to be dependent on the grafting density and molecular weight. The author suggested a two-layer structure of the surface: a compressible outer phase and a dense, incompressible inner phase. These findings indicate that the inter- and intra- chain interactions strongly affect phase behavior of PNIPAm especially in compact structures.

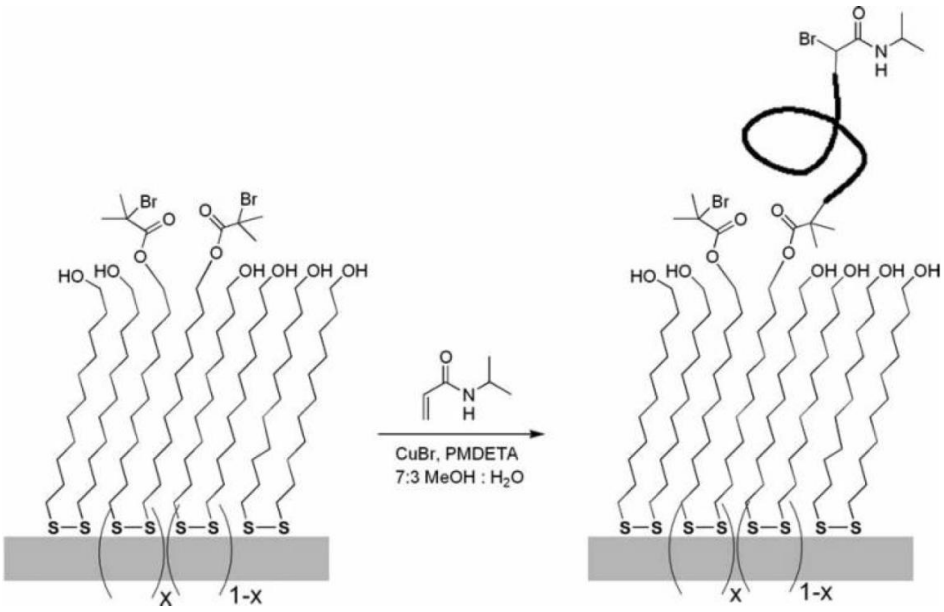

Figure 2.8. Illustration of grafted PNIPAm from alkanethiol monolayer on gold [30].

2.1.2 Other thermal responsive polymers

The amide groups in poly(*N*-substituted acrylamides) are important hydrophilic moieties and can form hydrogen bonds with water molecules below LCST. These hydrogen bonds can be broken to induce phase transition upon temperature increase. Ether groups in poly(ethylene oxide), poly(vinyl ether) and poly(propylene oxide) can also work as the polar sites to induce LCST.

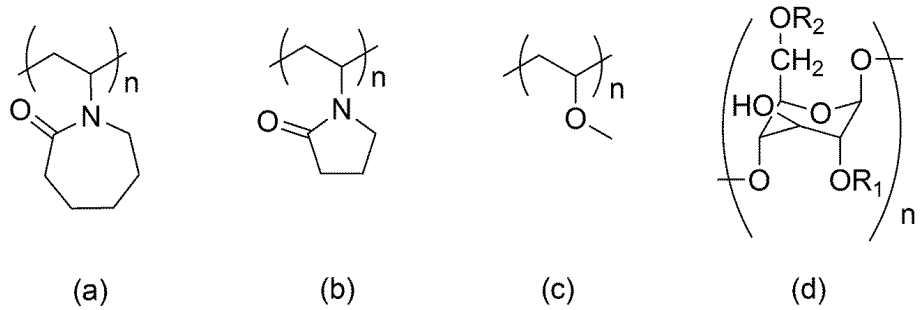

Figure 2.9. The structure of thermal responsive polymers. (a) poly(*N*-vinylcaprolactam) (PVCL), (b) poly(*N*-vinylpyrrolidone) (PVP), (c) poly(vinyl methyl ether) (PVME), (d) alkyl-substituted celluloses.

Figure 2.9 illustrates structures of some other well-known thermal responsive polymers. Poly(*N*-vinylcaprolactam) (PVCL) is a thermal responsive polymer which has been widely used in cosmetic and hair-care products. The LCST of PVCL is around 32 ℃. Therefore, it has similar thermal behavior to PNIPAm. Vihola prepared PVCL and PVCL-*g*-Poly(ethylene oxide) (PVCL-*g*-PEO) and evaluated their cytotoxicity in comparison to PNIPAm [48]. The effects of polymer concentration, incubation time and temperature were studied. PVCL-*g*-PEO exhibited the lowest cell toxicity when the temperature was close to physiological temperature which is higher than the polymer's LCST. The hydrophilic PEO is believed to reduce the aggregation of graft copolymer to diminish the polymer-cell contact.

Poly(*N*-vinylpyrrolidone) (PVP) is a close analog of PVCL and is widely used in pharmacology and medicine because of its good biocompatibility and low toxicity. PVP normally does not exhibit thermal sensitivity except when the pressure is higher than 1 kbar [49]. Both LCST and UCST can be observed when the pressure is in the 2-4 kbar range. The addition of salt or transition metal ions can also control the transition behavior of PVP solutions.

Poly(vinyl methyl ether) (PVME) has LCST at *ca*. 35 ℃. Maeda reported FTIR spectroscopic investigations to explain its phase transition in molecular terms[50]. The C-H stretching and C-O stretching bands were found to shift respectively toward a lower

wavelength and a higher wavelength upon phase transition. This is because the hydrogen bonds between ether oxygens and water molecules overcame the unfavorable decrease of entropy and form a structure around the hydrophobic moiety to stabilize the solution below LCST. On the other hand, the hydrogen bonds break when temperature increased to above LCST. Consequently, hydrophobic interactions between apolar moieties became dominant and induced phase separation.

Alkyl-substituted cellulose is another important kind of thermal responsive polymer which is often used in biomedical related applications. They are usually functionalized natural polymers and can be dissolved in aqueous solution because of the hydrophilic hydroxyl groups and ether linkages in their structure. The LCST of alkyl-substituted celluloses, such as methylcellulose, ethyl(hydroxyethyl) cellulose or hydroxypropyl-cellulose, locate at 50, 65 and 42 ℃, respectively.

2.1.3 Applications of thermal responsive polymers

PNIPAm is a potential candidate for biomedical carriers because its phase transition temperature is close to the human body temperature. Chilkoti prepared a copolymer of PNIPAm and acrylamide (AAm) having LCST slightly above 37 ℃ [51, 52]. A significant increase in delivery to solid tumors was achieved when the polymer hydrogel was combined with hyperthermia, comparing to the same polymers without hyperthermia or non-thermal responsive polymers with hyperthermia. The thermal targeting system is a promising method to increase the accumulation of polymer carriers in tumors and to enhance delivery of therapeutics by optimizing the molecular weight, inject dose, polymer's LCST and other factors.

Thermal responsive micelles can be used to solubilise hydrophobic molecules and enable targeted release of drugs upon stimuli within the body. There have been many

reports on self-assembly of amphiphilic PNIPAm block copolymers into polymer micelles in aqueous solutions [53-55]. The core can be formed by hydrophobic blocks such as PMMA or PCL, while PNIPAm constitutes the responsive shell. Hydrophobic drugs can be absorbed within the core which is stable at room temperature. The release of the drug is triggered at the LCST of PNIPAm when the collapse of the macromicelles occurs.

Thermal responsive block copolymers have been widely studied for protein delivery. Liu reported the PNIPAm-*b*-PLA microspheres prepared by a water-in-oil-in-water double emulsion method [56]. Bovine serum albumin (BSA) was loaded in the microspheres at a high encapsulation efficiency and sustained released over a period of three weeks at 37 ℃. Higher portion of PNIPAm was found to provide increased release speed. On the other hand, this system is favorable for biomedical applications because the PLA block is biodegradable.

Niu reported a high performance chiral resolution membrane by grafting PNIPAm on porous nylon-6 membrane [57]. Plasma-graft pore-filling polymerization was used to prepare the membrane and β-cyclodextrin (β-CD) was then grafted on PNIPAm chains as chiral selectors. It is found that the association of β-CD with guest molecules can be altered by the phase transition of PNIPAm. The selectivity is also found to be closely related to temperature. Thus, by using this thermal responsive membrane, high selective chiral resolution can be achieved by simply tuning the environmental temperature.

2.2 pH responsive polymers

Polymers responsive to pH stimuli consist of ionizable groups as pendants. These ionizable groups can accept and donate protons in response to pH changes. The degree of

ionization of the polymers can be dramatically altered at a specific pH value, which is the pKa point.

The main types of pH responsive polymers include, namely, polyacids, polybases, degradable pH responsive polymers, biopolymers and artificial polypeptides[58]. Weak polyacids and polybases can form polyelectrolytes in aqueous solutions. Weak polyacids withdraw protons at low pH and release them at neutral and high pH. On the contrary, weak polybases are protonated at basic conditions and positively ionized at neutral and low pH. For both polyacids and polybases, electrostatic repulsion forces dominate when the acidic or basic groups are ionized. When the ionizable groups are protonated, electrostatic repulsion forces diminish and hydrophobic interactions dominate, which cause the aggregation of polymer chains in aqueous solutions. Another collapse mechanism of pH responsive polymer is dependent on the hydrogen bonding status between the hydrogen and an electron donating atom, such as oxygen and nitrogen, in another functional group.

2.2.1 Poly(acrylic acid)

Poly (acrylic acid) (PAAc) (Figure 2.10a) and its analog acrylicacids (Figure 2.10, b-d) are the most representative pH responsive polyacids. Their ionization/deionization transitions occur from pH 4 to 8. The pendant carboxylic groups can withdraw protons at lower pH and release them at higher pH. The poly-(acrylicacid)s are transformed into polyelectrolytes upon ionization and electrostatic repulsion forces between the polymer chains dominate its solution behavior. The hydrophilic/hydrophobic transition controls the solubilisation/precipitation status of the polymer chains, swelling/de-swelling of hydrogels, or hydrophilic/hydrophobic nature of surfaces.

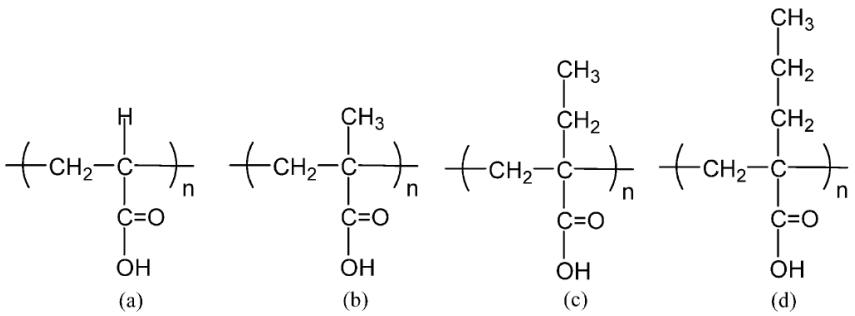

Figure 2.10. Structure of poly(acrylic acid) and its analog polymers. (a) poly(acrylic acid) (PAAc), (b) poly(methacrylic acid) (PMAAc), (c) poly(2-ethyl acrylic acid) (PEAAc), (d) poly(2-propyl acrylic acid) (PPAAc).

Loosely crosslinked PAAc hydrogel networks can absorb many times their weight in water. This kind of polymers is called superabsorbent and finds applications in various fields such as diapers, ion exchange resins, hemodialysis and ultrafiltration membranes, and controlled release devices. The degree of crosslinking is of primary importance because it determines the molecular weight between crosslink points. Consequently, the mechanical strength and swelling ratio can be affected. Bowman used both experimental data and theoretical analysis to investigate how the monomer concentration, pH, ionic strength of the solution during the polymerization affect the degree of crosslinking and primary cyclization during the network formation of multifunctional monomers [59]. The increasing amount of water during the polymerization was found to accelerate primary cyclization, which created a less crosslinked network. The effect of ionic strength and pH were found to be interrelated on the ionic network structure as demonstrated by the swelling results of PAAc. The degree of primary cyclization can be decreased when pH increases. On the other hand, the cyclization is increased with increasing ionic strength.

2.2.2 Other pH responsive polymers

pH sensitive polymers have been designed that mimic biological functions through their graft polymerization onto nanoporous membranes. Masaru grafted poly(methacrylic acid) (PMAA) onto a composite membrane that consisted of a porous substrate [60]. The nano-sized channels can open and close in response to different pH, ionic strength or addition of metal ions to induce water permeability changes of as much as 1000 times.

Peptide copolymers have many advantages over synthetic polymers because they have the ability to hierarchically assemble into stable ordered conformation. They can adopt secondary structures such as α-helix, β-sheet or coil in response to pH or other stimuli. Yukio grafted a pH sensitive polypeptide brush on a gold-coated porous membrane. At low pH the poly(L-glutamic acid) chains form a folded α-helical structure, while an extended random structure is formed at high pH, resulting in a permeation adjustable pH sensitive porous membrane [61].

Poly(4-vinylpyridine) (P4VP) and poly(2-vinylpyridine) (P2VP) is another series of widely studied pH responsive polymers. Malmstrom and *et al.* utilized surface initiated ATRP to prepare thermal and pH dual responsive cellulose surfaces with PNIPAm and P4VP block copolymer brushes. The changes in wettability from highly hydrophilic to hydrophobic indicated the dual response character [62]. Zhu and *et al.* prepared PNIPAm-P4VP via ATRP and investigated its micellization behavior in response to pH and temperature. The polymer was in unimer state at pH 2.8 and 25 ℃. However, when the temperature was 50 ℃, spherical core-shell micelles with PNIPAm as the core and P4VP as the shell layer were observed. By contrast, in response to the pH increment to 6.5, the polymer formed spherical core-shell micelles with P4VP as the core and PNIPAm as the shell layer[63]. Zhang and *et al.* prepared PNIPAm-P2VP block copolymers by RAFT and studied its micellization behavior in response to pH and temperature. A dual responsive behavior similar to that of PNIPAm-P4VP was observed [64].

2.2.3 Applications of pH responsive polymers

Hydrogels of pH responsive polymer are widely used in controlled drug release for their different solubilities or swelling states in various pH environments.

Ghandehari prepared PAAc with azo-aromatic crosslinkers for colon drug delivery [65]. The swelling of the hydrogel was minimal in stomach due to PAAc's hydrophobic aggregation. As a result, the drug release rate was also minimal in the stomach. On the other hand, the swelling rate increased in intestine, as a result of the increased pH value, resulting in the ionization of the carboxylic groups. However, it was only in the colon that the azo-aromatic crosslinks are degraded by azoreductase, which is produced by microbial flora in the colon (Figure 2.11). By varying the crosslinking density, the degradation kinetics and degradation pattern can be controlled.

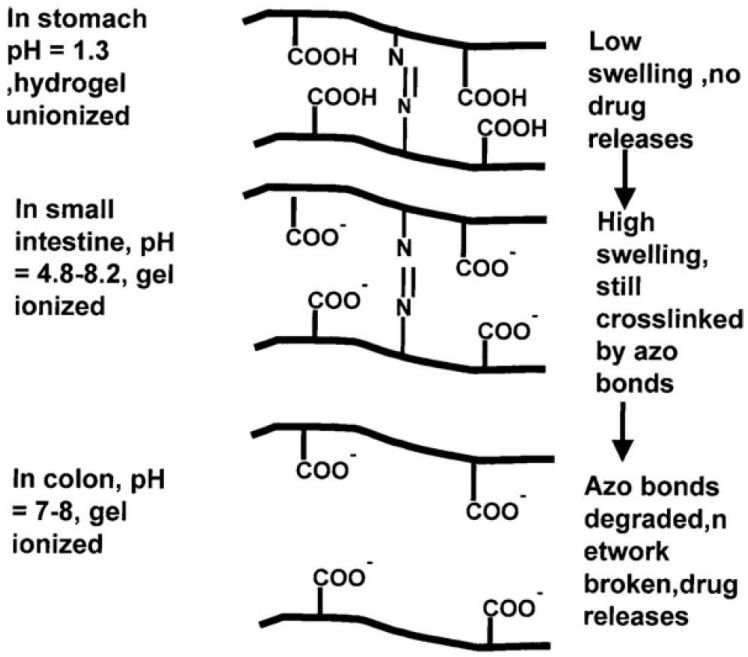

Figure 2.11. Illustration of biodegradable and pH sensitive PAAc in different pH environments [65].

Hoffman and *et al.* prepared poly(2-ethyl acrylic acid) (PEAAc, Figure 2.10c) and poly(2-propylacrylic acid) (PPAAc, Figure 2.10d) that can mimic the membrane-disruptive peptides of viruses. It was found that the polymers have high hemolytic

activities at pH similar to those in endosomes [66]. PEAAc was found to be as effective as mellitin, which was a well-known membrane disruptive peptide, in disrupting red blood cells. The disrupting efficiency could be further increased via tuning the hydrophobicity of the polymer with pH values.

2.3 Thermal and pH dual responsive polymers and hydrogels

In recent years there is much interest in obtaining polymer and hydrogel that is responsive to temperature and pH changes, thus the solution property or swelling behavior can be abruptly and reversibly altered. Temperature and pH have been the solution variables of immense scientific and technological concern because they can be tuned in biological and chemical systems. Polymer responding to both temperature and pH provide the possibility to precise control of the phase behavior of the polymer solution.

Generally, thermal and pH dual responsive polymers can be categorized into three types: (1) random copolymers and copolymer hydrogels, (2) block and graft copolymers, (3) homo-polymers containing groups with dual sensitivity.

2.3.1 Random copolymers and hydrogels

The solution behaviors of thermal responsive polymers are depending on their amphiphilic character and hydrogen bond changes. On the other hand, the pH sensitivity of polymers is determined by the behavior of ionizable moieties. Consequently the vast majority of polymers responding to both temperature and pH are prepared by the the most straightforward method: random copolymerization of different moieties which are responsive to temperature and pH.

Copolymers containing NIPAm and varied monomers, especially those containing carboxylic acid or tertiary amine group, have been widely reported to manipulate the

phase transition temperature as well as the sensitivity of the transition. The hydrophobicity/hydrophilicity of carboxylic acids or tertiary amines can be modified by changing pH of the solution. Hydrophobicity will shift the polymer's LCST to lower temperature and hydrophilicity will modify the LCST to higher temperature. Copolymerization of PNIPAm with these pH sensitive polymers attracts research interest because the thermo-sensitivity can be adjusted to close to physiologic temperature and allow various biomedical applications.

To reveal the influence of hydrogen bonding upon the LCST behavior, Salgado-Rodriguez prepared random PNIPAm copolymers having similar composition and grouped the series into two study systems [67]. One system had a free acid group with controlled number of units, while in the other system the free acid group was protected by methoxyl group. By comparing the two systems the influence of possible hydrogen bonds on LCST could be clarified. The carboxylic acid groups in AAc block can establish hydrogen bonds with the PNIPAm's amide groups (Figure 2.12). It was found that the phase transition was less endothermic than in pure PNIPAm because the hydrogen bond interaction causes fewer sites available for the water to bind to the PNIPAm units.

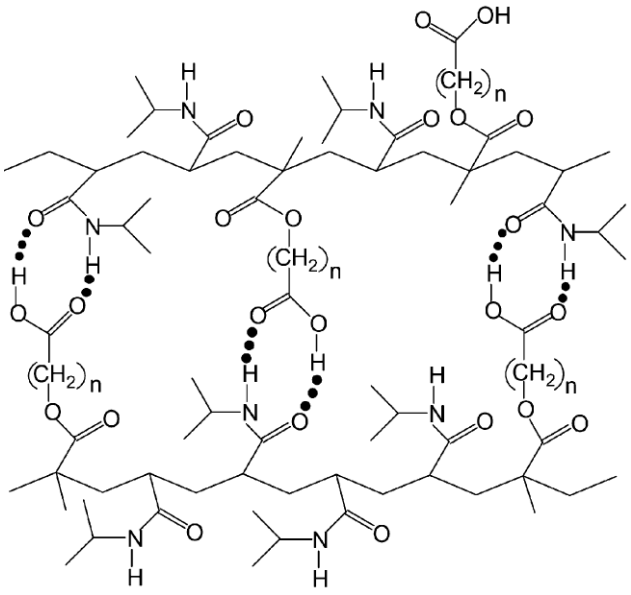

Figure 2.12. Illustration of the hydrogen bondings in PNIPAm-PAAc random copolymers [67].

Poly(lactic acid) (PLA) is well known biodegradable polymer having good biocompatibility and mechanical properties. Kim prepared a ter-polymer by attaching a hydrophobic PLA block to a random PNIPAm-*co*-PAAc [68]. The ter-polymer exhibited properties including thermosensitivity, biodegradability and good mechanical strength. As a result, the biomaterial can control the release of therapeutic agents during the degradation and foster the mechanical functionality of the cells. Fabrication of the material into two- or three- dimensional shapes to support cell adhesion, proliferation and differentiation are applicable. These can also be used for rapid two- and three-dimensional non-invasive cell sheet harvesting due to their thermo responsive behavior

2.3.2 Block and graft copolymers

During the studies of random copolymer, researchers found that when hydrophilic blocks, such as AAc, is much longer than the other blocks, the sensitivity to temperature may disappear. This is because the enhanced hydrophilicity imparts solubility to offset the aggregation of the hydrophobic temperature sensitive components. Although physical mixtures are possible for some applications, the different blocks tend to separate physically and release the drug, ultimately decreasing the strength or other properties rapidly. Thus, the block or graft thermal and pH responsive copolymers attract more attention in recent years due to their more intelligent behavior and controllable properties resulting from their regular structures.

Hoffman prepared graft PNIPAm-PAAc copolymers by grafting PNIPAm side chains onto PAAc backbones and compared the LCST behavior of graft copolymers with random copolymers [5]. At pH 4.0, the high cloud point of random copolymers with high PAAc content is due to the hydrophilic character of the AAc moieties along the backbone, while the graft copolymers show much lower cloud point than homo-PNIPAm at the same

pH (Figure 2.13). This is probably due to (1) the efficient formation of hydrogen bonds between relatively long sequences of PNIPAm and PAAc in the graft copolymer (Figure 2.14), and (2) possible acrylamide and PAAc interpenetrating networks which could not be formed in random copolymers. The hydrogen bonds interfere with the access of water molecules to PNIPAm amide groups. Consequently, the graft chains of PNIPAm were rendered more hydrophobic and their phase separation temperature was lowered. Based on this mechanism the cloud point should be insensitive to PAAc content in graft copolymer, as shown in Figure 2.13. At pH 7.4, the ionization of carboxyl groups disrupted the hydrogen bonds, resulting in the same cloud point as homo-PNIPAm.

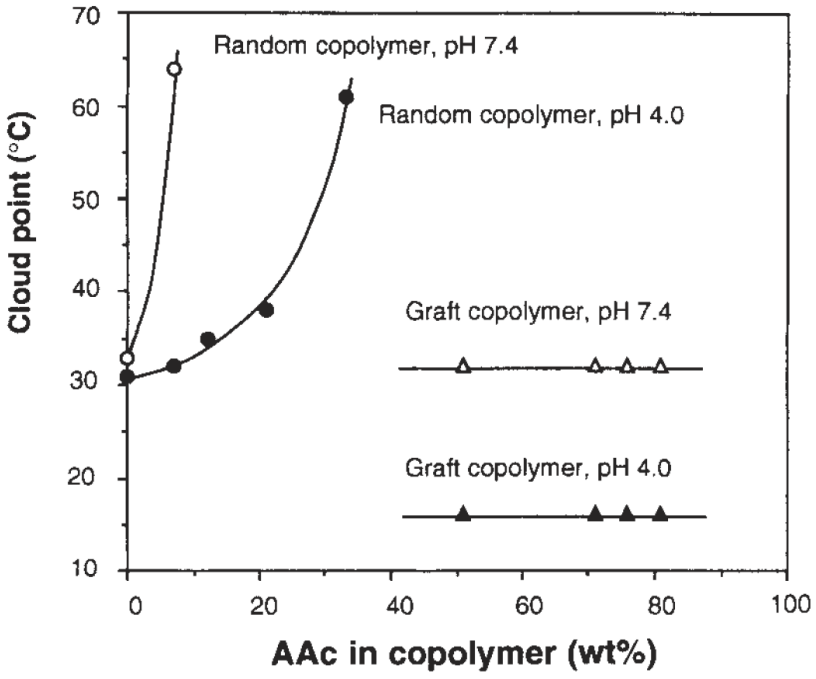

Figure 2.13. Cloud points of random PNIPAm-PAAc and graft PNIPAm-*g*-PAAc plotted against the copolymer PAAc content at pH 4.0 and 7.4 [5].

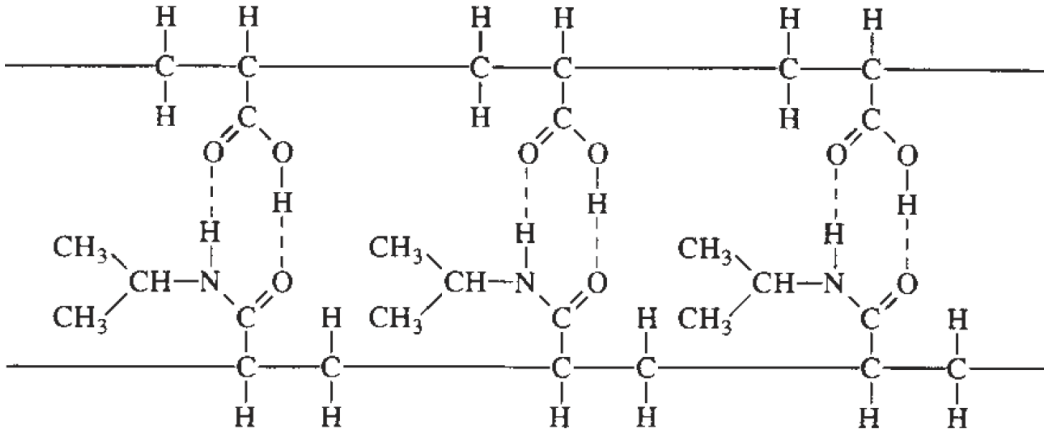

Figure 2.14. Proposed hydrogen bonding between PNIPAm graft chain and PAAc backbone [5].

Müller firstly reported the synthesis of poly(PNIPAm-*b*-AAc) by RAFT polymerization in methanol [9]. PAAc was used as macromolecular chain transfer agent (CTA) in the reaction. The copolymer's solubility in aqueous solution was dependent on the solution's pH. This is because the carboxylate groups are protonated at low pH and render the copolymer less soluble. Hence, the LCST of PNIPAm blocks is modified through the copolymerization of PAAc blocks. Figure 2.15 illustrates the turbidimetric curve of the copolymer at different pH. When the temperature is higher than the T_c of PNIPAm, the transition decreases only slightly from pH 5.0 to 7.0, suggesting the existence of micelles with PNIPAm core and PAAc corona. The transmission drops to zero when the temperature is raised above the critical point at a lower pH of 4.5. This indicates that the formation of larger aggregates is due to increased insolubility of the protonated PAAc blocks. Possible modes of the polymer's aggregate formation in aqueous solution are shown in Figure 2.16.

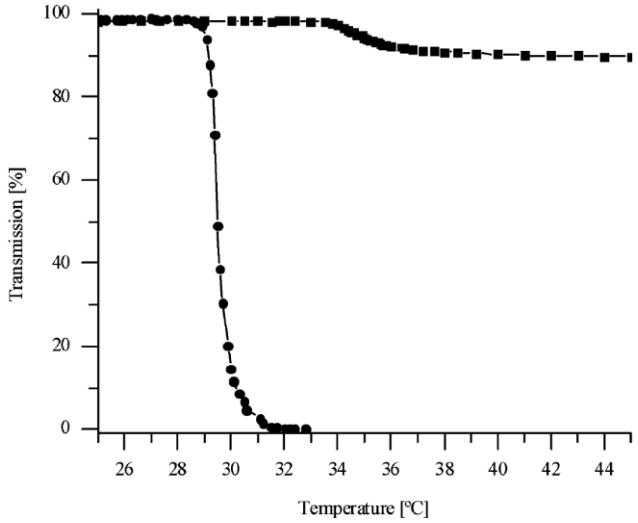

Figure 2.15. The phase transition of poly(NIPAm$_{50}$-*b*-AAc$_{110}$) at (●) pH4.5; (■) pH5-7 [9].

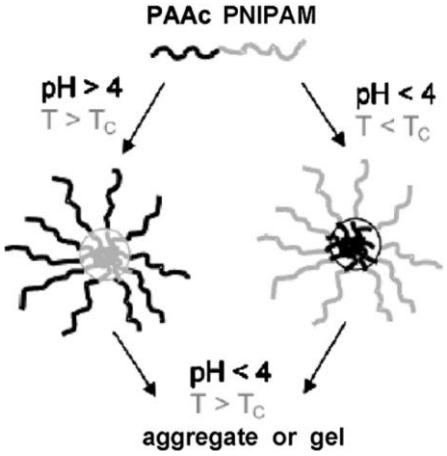

Figure 2.16. Possible aggregate formation of poly(PNIPAm-*b*-PAAc) in aqueous solution in different temperature and pH [9].

An amphiphilic tri-block copolymer poly(*N*,*N*-diethylacrylamide)-poly(acrylic acid)-poly(*N*,*N*-diethylacrylamide) (PDEAAm-*b*-PAAc-*b*-PDEAAm) was prepared by sequential anionic polymerization and selective hydrolysis and neutralization of the middle block poly(*t*-butyl acrylate) (P*t*BA) to its ionic functions[69]. The polymer exhibited thermal sensitivity due to the PDEAAm end blocks, and pH sensitivity due to central PAAc blocks. It was found that the polymeric chains exist as unimers at low temperature and high pH. When the temperature increased to higher than the T_c of PDEAAm, a sol-gel transition occured due to the formation of a three dimensional

transient network, which comprised of physical PDEAAm crosslinks bridged by negatively ionized PAAc blocks. The gelation temperature was around 60 ℃ and about 20 ℃ higher than the T_c of PDEAAm. It was also found that the presence of salt can strongly influence the sol-gel transition and the the physical gel's rheological properties and reduce the LCST of PDEAAm and screen the negatively charged PAAc chains.

2.3.3 Homopolymers

The majority of thermal and pH responsive polymers are prepared via copolymerization of monomers which are responsive to temperature and pH. However, there are homo-polymers that can response to both temperature and pH.

González reported that a kind of homopolymer poly(*N*-ethylpyrrolidine methacrylate) (PEPyM) can exhibit both thermal and pH sensitivity [70]. PEPyM has a phase separation transition temperature at around 15 ℃. At pH 1 to 4, PEPyM behaves as a superabsorbent hydrogel and is barely sensitive to temperature when it was crosslinked with dimethylacrylamide (DMA). At pH 5 to 7.4, the thermal sensitivity can be clearly observed. Whereas under basic conditions, PEPyM hydrogel is in a collapsed state as its phase transition temperature is below 10 ℃. Pulsatile behavior was also observed during swelling-deswelling with reversed stimuli.

Poly(2-hydroxyethyl methacrylate) (PHEMA) is widely applied as soft contact and intraocular lenses, and used in biomedical applications due to its good biocompatibility and low toxicity [71, 72]. PHEMA was initially considered only swellable in water and was often prepared as hydrogel matrix in enzyme immobilization [73]. Even when PHEMA was copolymerized with thermal responsive polymer such as PNIPAm, it was only used as the hydrophobic moiety to adjust the micellization behavior [74-76].

Armes first found that linear PHEMA having low molecular weight can be dissolved in water [77]. The homo-polymer having DP between 20 and 45 exhibited inverse temperature solubility and its T_c was greatly affected by DP (Figure 2.17). PHEMA was only partially soluble when DP was larger than 40 (Figure 2.18). Moreover, the solubility of low molecular weight PHEMA was also pH dependent. The solubility of PHEMA showed no difference between pH 6.5 and 10.0, but its solubility exhibit an increase at pH 2.2, which was attributed to increased hydrogen bonding between polymer chains and water molecules under acidic conditions.

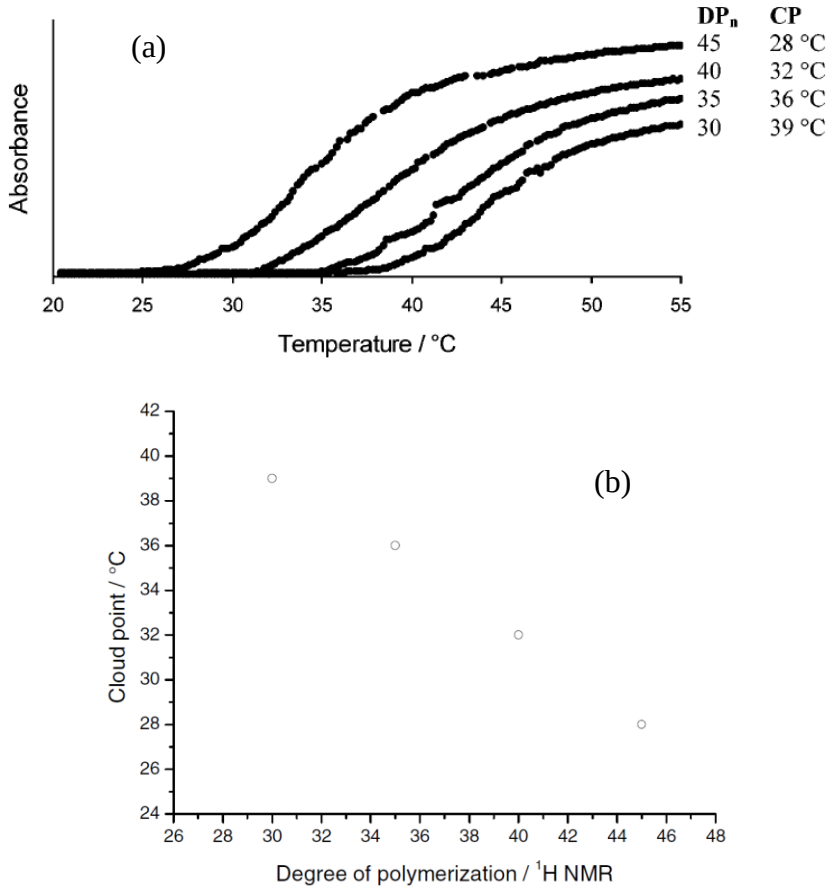

Fig 2.17. (a) Turbidity data of PHEMA homopolymer of different DP. (b) Relationship between DP and T_c for water soluble PHEMA [77].

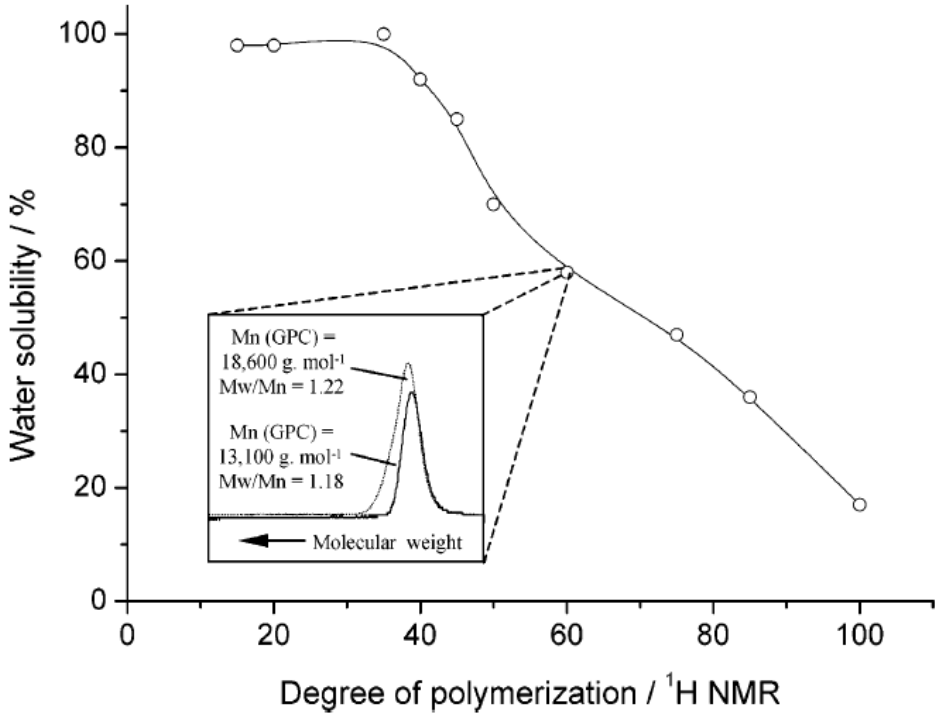

Fig 2.18. Solubility of PHEMA homopolymer having different DP. The insets shows GPC curves for $HEMA_{60}$ homopolymer before and after fractionation [77].

2.4 Polyhedral oligomeric silsesquioxane (POSS)

2.4.1 Structure and Property

In 1946, Scott isolated a series of completely condensed methyl-polysiloxanes from a thermal re-arrangement product of branched-chain methylpolysiloxanes [78]. These low molecular weight methyl-polysiloxanes were named silsesquioxanes by Baney [79] in 1995. According to Baney's definition, silsesquioxane generally refers to all structures having the empirical formula of $RSiO_{3/2}$, where R could be hydrogen, alkyl, aryl groups, or derivatives of them. Silsesquioxanes have different structural forms, such as random, ladder, cage and partial cage structures.

Due to the unique cage-like structures (Figure 2.19) in nanoscale dimensions, POSS are of particular research interest in recent years. In this report, silsesquioxane refers to the T8 structure (Figure 2.19b). The cube-like cage contains eight silicon atoms at the vertexes and each connected to one organic group. Twelve oxygen atoms are located at

the edges of the cube to connect silicon atoms. These compounds have formula unit that is between that of the inorganic ceramic materials SiO_2 and organic silicone polymers R_2SiO. Thus, they are often described as hybrid materials, comprising both the chemically inert and thermally stable inorganic Si-O-Si fragments, and potentially reactive and readily modified Si-R fragments.

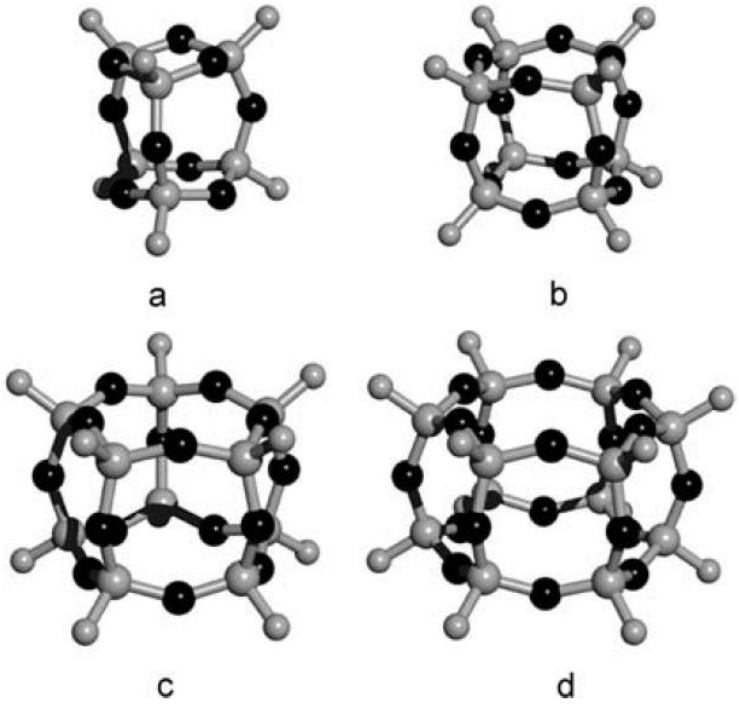

Figure 2.19. The structure of four typical POSS cages. (a) Si_6O_9 trigonal prismatic cage, (b) Si_8O_{12} cubane cage, (c) $Si_{10}O_{15}$ double five ring cage, (d) $Si_{12}O_{18}$ double six ring cage.

It is observed in almost all the organic and polymeric materials that the aliphatic components strongly influence T_g, limit the thermal stability and decrease mechanical property potentials. However, POSS is more rigid and thermal stable. Thus, POSS containing polymers display the advantages including increased temperature of decomposition, increased temperature of glass transition, reduced flammability, lower density, low toxicity [80], increased oxygen permeability [81], lower thermal conductivity [82], oxidation resistance, etc [83-87].

With POSS's well-defined dimension, POSS containing composites may obtain controlled porosities with high surface areas [88], novel mechanical properties [89-91], or high thermal stabilities [86]. POSS materials can even be potentially used as robust thermoplastics with properties that includes resistance to atomic oxygen [92] and be applied as space-survivable material [93].

2.4.2 POSS chemistry

POSS chemistry is versatile for its multi-functionality and the possibility to connect various kinds of functional organic groups onto the silicon atoms on the cage vertex. POSS molecules whereby none of the groups are functionally active can be simply blended into elastomer by usual mixing or compounding techniques [94]. POSS molecules having only one reactive functional group can be attached as polymer pendents [95-99]. Those with two reactive functional groups can be incorporated into polymer backbones by copolymerization [100], while those having more than two reactive functional groups can be used to form crosslinks and yield star-like [84, 101-103] or network structures [104-112].

The most common process to obtain fully condensed POSS is hydrolytic condensation of trifunctional monomers $RSiX_3$, where R is a stable organic group or hydrogen, and X is a highly reactive substituent such as halogen or alkoxy group (Scheme 2.1). The process is difficult and complex because it may involve undesirable side reactions to produce non-cubic silsesquioxane. Factors such as temperature, catalyst, type and ratio of solvent, concentration of monomers, solubility of the polyhedral oligomers, character of R and X groups, even water quantity and its addition rate may affect the reaction [113].

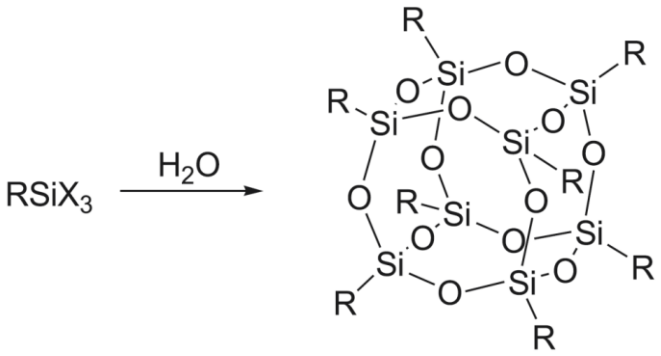

Scheme 2.1. Condensed POSS prepared by hydrolytic condensation.

2.4.3 POSS as star polymer platform

Many stoichiometrically well-defined POSS compounds have been reported since POSS was discovered in the 1940s. However, functional POSS suitable for chemical, physical or biological applications emerged only in recent years. A wide variety of multi-functional POSS derivatives has been prepared for highly crosslinked thermoset nanocomposite [114-118], organic light emitting materials [119-124], thermal responsive materials [106, 125-127], *etc*. Multifunctional POSS are normally prepared via functionalization of POSS cages, which formed in favor of the relatively mature synthesis of simple POSS cages. Among the widely used functional groups such as vinyl, dimethylsilyl, dimethyl-vinyl-silyl and etc, benzene group attracted most interest due to its tailorability and rigidity.

Laine first reported the synthesis of octa(aminophenyl)silsesquioxane (OAPS) as a nano-construction site [105]. The rigid arylamine moieties surrounding POSS core are thermally more stable than aliphatic branches. At the same time, they expand the types of functionality available for polyimide derivatives, nanocomposites or Schiff base derivatives. OAPS was further reacted with 2-bromoisobutyryl bromide to produce an multi-functional ATRP initiator by Hussain [128, 129]. The multi-functional cage initiator can be used to utilize core-first polymerization of various monomers.

Polymers having star or dendritic molecular architecture have attracted much scientific and technical interest in recent years. Star-like and dendritic polymers can provide unique rheological properties [130, 131] and decorated with various functionalized groups to satisfy specific applications [132, 133]. There are two widely used methods for preparation of star-like polymers. They are known as convergent or "arm first" and divergent or "core first" methods. In the "arm first" method, polymer arms are synthesized which are bounded together with multi-functional linking agents afterwards, or the block copolymerization of di-vinyl reagents to the arms followed by formation of a microgel core or core-core coupling. The "core first" method uses multi-functional initiators or transfer agents to induce the polymerization. Regardless of using either method, POSS is a promising material for constructing the star architecture due to its precise cage structure.

Well-defined amphiphilic POSS-PEO was prepared from octa-kis(dimethylsiloxy) POSS and alkyl-PEO through a hydrosilylation reaction by He and *et al*.[134]. The polymer exhibited large R_g/R_h value (1.46) and extremely small average chain density (4×10^{-4}g/cm^3). This indicates that the small hydrophobic POSS core was surrounded by an extended PEO corona.

Lu reported the synthesis of POSS-aniline via emulsion polymerization using OAPS and aniline in the presence of poly(4-styrene sulfonic acid) (PSS) and dodecylbenzene sulphonic acid (DBSA) [135]. The star-like architecture of POSS-aniline decreased its crystallinity. This resulted in an increased ionic conductivity and cation diffusion speed. The electrochromic contrast was hence enhanced by 40% due to the more accessible doping sites in POSS-aniline.

POSS has also been used as cores to prepare dendrimers. Richardson reported a hexadecamer G1 dendrimer having POSS as the core [136]. It was discovered that the mesogenic substrate displayed only a chiral nematic phase, whereas the hexadecamer

dendrimer exhibited enantiotropic chiral nematic, disordered hexagonal columnar and disordered rectangular columnar phases. The formation of mesophases was resulted from the lateral or side-on attachment of the mesogen to the POSS core. Yoshiki prepared poly(amidoamine) (PAMAM) dendrimers with POSS as the core [137]. In comparison to G2 PAMAM dendrimer, the G2 POSS-PAMAM dendrimer can entrap larger amount of guest molecules without loss of affinity.

2.4.4 POSS containing PNIPAm

In recent years, research has been carried out on POSS-containing PNIPAm polymers or hydrogels. Different synthesis methods and architectures have been utilized to construct these organic-inorganic hybrids. The presence of POSS has been reported to have an impact on the mechanical and thermal behavior in solid state and phase transition behavior in aqueous solutions of PNIPAm.

The problem with organic hydrogels is that they often display morphological in-homogeneity, poor mechanical strength, low swelling ratio at equilibrium and slow swelling rates. In the case of PNIPAm hydrogels, the slow de-swelling and re-swelling rates are due to the collective diffusion of water molecules in the crosslinked networks. Organic-inorganic hybrid is an efficient method to overcome these drawbacks. Zheng and his colleagues investigated several kinds of POSS-PNIPAm hydrogels. In 2007 they used octa-(propylglycidyl ether)POSS (OpePOSS) as nanocrosslinking agent to prepare crosslinked PNIPAm networks [106]. When weight percentage of POSS content increased from 0 to 20 percent, the hydrogel displayed a decreasing LCST. This is believed to be the weakening in miscibility of PNIPAm with water due to structural incorporation of hydrophobic POSS moiety. In another work of Zheng *et al.*, 3-acryloxypropylhepta(3,3,3-trifluoropropyl) POSS was used as a modifier in PNIPAm

hydrogel [138]. The crosslinked network was prepared via radical copolymerization of NIPAm, POSS macromer and N,N'-methylenebisacrylamide. The hydrogel displayed enhanced T_g and thermal stability in comparison to plain PNIPAm networks. The swelling, de-swelling and re-swelling response rates of POSS-PNIPAm hydrogel were found to be much faster than plain PNIPAm. This was due to the formation of highly hydrophobic nano-domains self-assembled by POSS content. These domains behave as the microporogens and promote the contact of PNIPAm chains and water. In 2011, Zheng reported POSS capped PNIPAm telechelics and studied its hydrogel and LCST behavior [139]. RAFT polymerization was used to prepare the polymer using hepta(3,3,3-trifluoropropyl) POSS capped di-functional CTA (Scheme 2.2). As a result of the hydrophobicity of POSS, the telechelic polymer formed separated nano-domains 10-30 nm in diameter. The POSS end groups were self-assembled into the domains and dispersed in the PNIPAm matrices. These domains behave similar to physical crosslinking sites and help form a physical hydrogel. Alike to other POSS-PNIPAm hydrogel systems, the telechelic POSS-PNIPAm displayed rapid re-swelling and de-swelling thermoresponsive behavior. In the LCST investigation, the onsets of transmission reduction were taken as LCST. The transmission of POSS-PNIPAm telechelics at low temperature was found lower than that of plain PNIPAm (Figure 2.20a), which was attributed to the formation of aggregates of self-organized nano-objects of the polymer. In addition, when the molecular weight is relatively low, the polymer exhibited lower LCST because of the relatively high content of hydrophobic POSS end groups (Figure 2.20b).

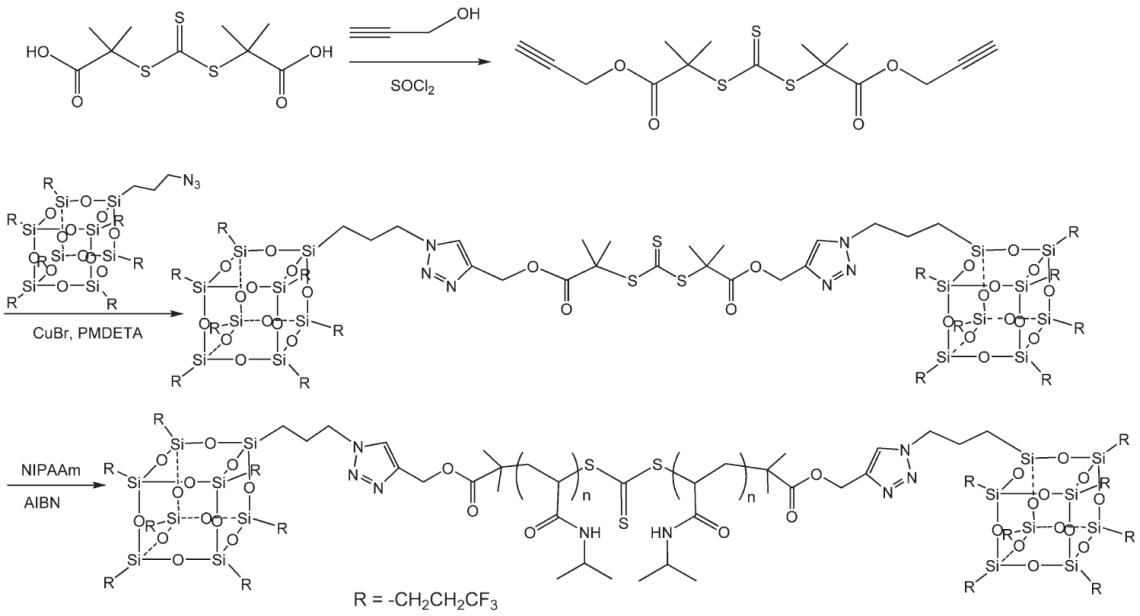

Scheme 2.2. Synthesis of POSS-PNIPAm telechelics [139].

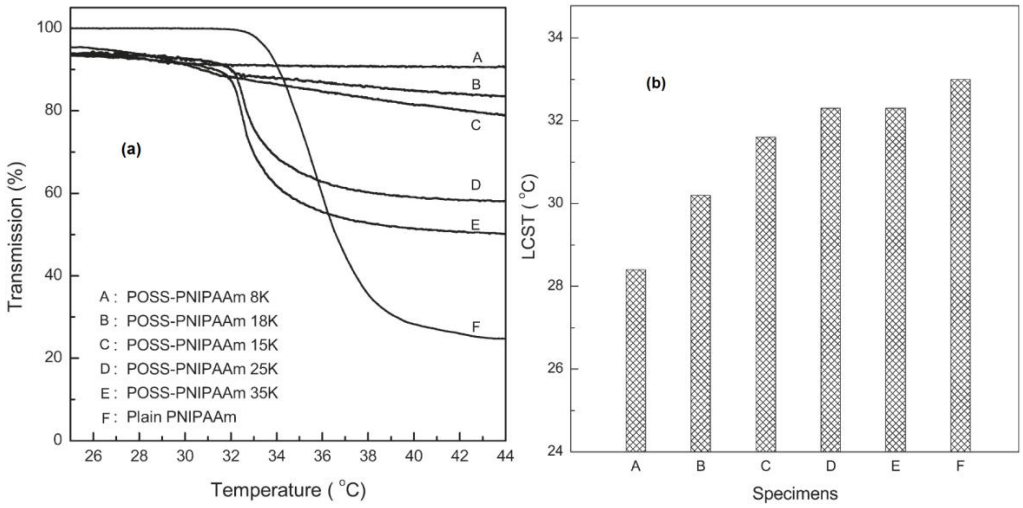

Figure 2.20. (a) Transmission at 550nm as a function of temperature for POSS-PNIPAm telechelics and plain PNIPAm 0.02% solutions for cloud point determination. The numbers in each sample name indicate the molecular weight M_n. (b) Cloud points of POSS-PNIPAm telechelics and plain PNIPAm [139].

Lin and *et al*. used electrospinning techniques to prepare POSS-PNIPAm hydrogel nanofibres [140]. Commercial PNIPAm was electrospinned with octa-glycidyl-POSS (OpePOSS) and 2-ethyl-4-methylimidazole (EMI) together in 10% DMF and THF (1:1) solution, followed by a heat curing treatment. Different from unstable linear PNIPAm

nanofibres in aqueous solution, the POSS crosslinked PNIPAm was dimensionally stable in both aqueous and organic solutions (Figure 2.21) and exhibited fast swelling and de-swelling response triggered by temperature changes. The LCST of the hydrogel was also found to be lower than linear PNIPAm and slightly dependent on the POSS composition.

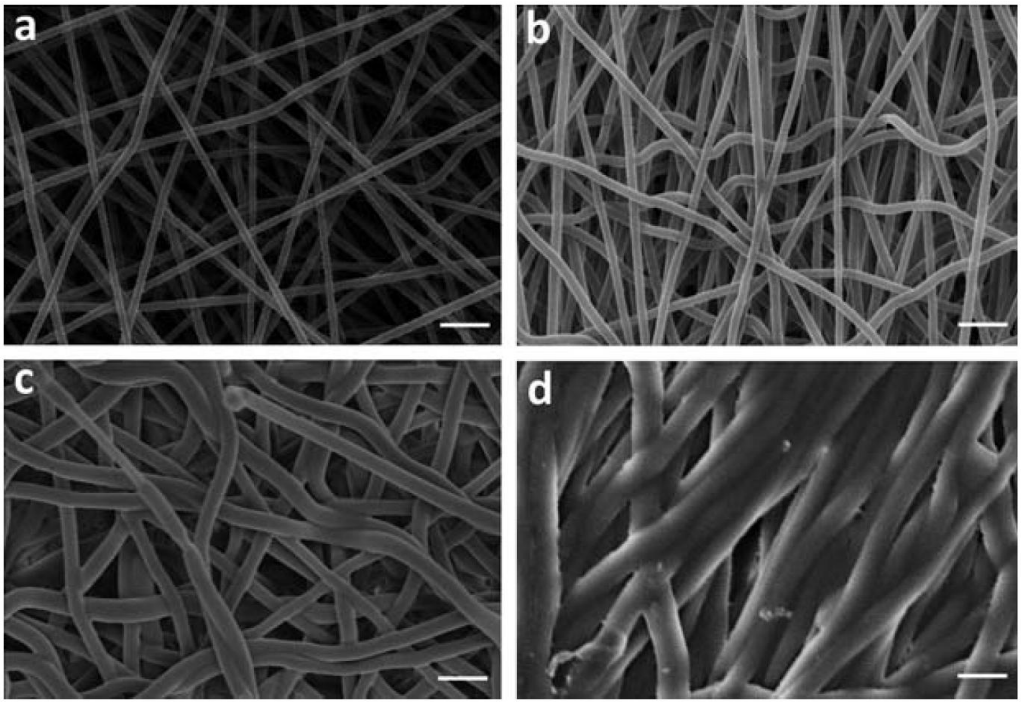

Figure 2.21. SEM images of electrospinned PNIPAm, OpePOSS and EMI solutions (PNIPAm:OpePOSS:EMI = 100:15:0.3, w/w; scale bar = 5 μm): (a) non-cured nanofibres, (b) cured nanofibres, (c) cured nanofibres after swelling in 25 ℃ and deswelling at 40 ℃, (d) cured nanofibres after swelling in 25 ℃ and drying in vacuum at 25 ℃ for 4h [140].

Besides crosslinked PNIPAm hydrogels, POSS has also been used in constructing linear or star-like PNIPAm. Chen *et al*.[141] constructed tad-pole shaped POSS-PNIPAm by RAFT process. Aminopropylisobutyl POSS was used to prepare the CTA and had been confirmed as an effective CTA in RAFT. As in many other polymer systems, POSS content produced enhanced thermal properties and increased glass transition temperatures of the polymer. This was observed until sufficient molecular weight was achieved to weaken the POSS effect. The authors investigated the polymer's self-assembly behavior using AFM and DLS. The polymer was found to behave as core-shell nano-structured

micelles having a uniform size, which increases with increasing molecular weight. Surprisingly, low molecular weight polymers have a much larger and more compact core than those with high molecular weight.

Recently, POSS was used to construct amphiphilic star-shape block copolymer of poly(ε-caprolactone-PNIPAm) by Yao [142]. The hydroxyl functionalized POSS-$(OH)_{32}$ core was synthesized via hydrolytic condensation (Scheme 2.3). After ring-opening polymerization of ε-caprolactone (CL), ATRP was used to polymerize NIPAm as the shell block. The sizes of the core and shell layer could be controlled through adjusting feed ratios of the reagents. Narrowly distributed nano-size micelles were formed by addition of water to a solution of the polymer in DMF. The drug release behavior was found to be affected by temperature due to the thermal sensitivity of the NIPAm block.

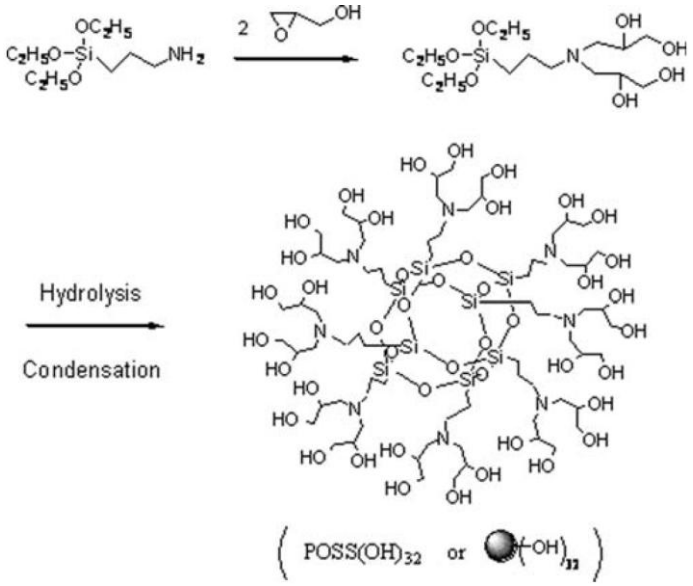

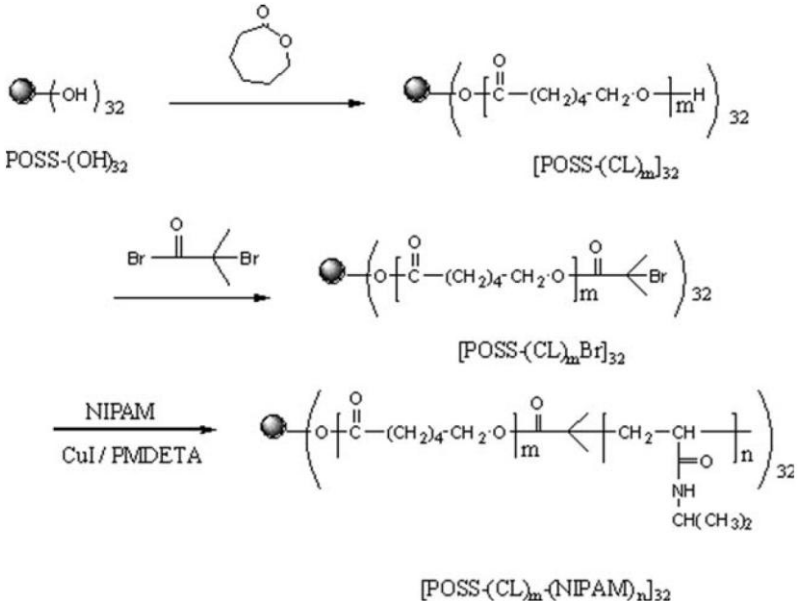

Scheme 2.3. Synthetic of multi-functionalized POSS-$(OH)_{32}$ and POSS-(PCL-*b*-PNIPAm)$_{32}$ [143].

2.5 Atom transfer radical polymerization (ATRP)

2.5.1 Mechanism

In recent years, living controlled radical polymerization (CRP) has attracted much interest because it provides simple and robust routes to the preparation of well defined and narrowly distributed polymers and the fabrication of novel functional materials. Mechanistically, CRP is distinguished from conventional free radical polymerization by the existence of a reversible activation process (Scheme 2.4). The polymer radical $P^{\bullet}$ can be yielded by activation of the dormant (end-capped) chain P–X by thermal, photochemical, or chemical stimuli. $P^{\bullet}$ will then undergo propagation in the presence of monomer M until it is deactivated back to P–X.

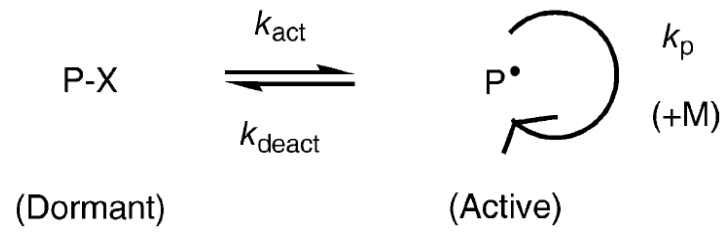

Scheme 2.4. General reversible activation of living radical polymerization.

Atom transfer radical polymerization (ATRP) [144, 145] is one of the most successful CRP. Numerous novel and previously inaccessible materials have been prepared by using ATRP, including not only macromolecules with precisely controlled composition and architecture but also many new hybrids in which well-defined organic polymers are covalently attached to inorganic materials or to natural products. A general mechanism of ATRP is shown in Scheme 2.5 [144]. The radicals, or the active propagating species $R^{\bullet}$, are generated by a reversible redox process catalyzed by a transition metal complex (activator, M_t^n-Y/ligand, where Y may be another ligand or a counterion) which undergoes a one-electron oxidation with concomitant abstraction of a pseudo-halogen atom, X, from a dormant species, R-X. This process occurs with a rate constant, k_{act}, and deactivation constant, k_{deact}.

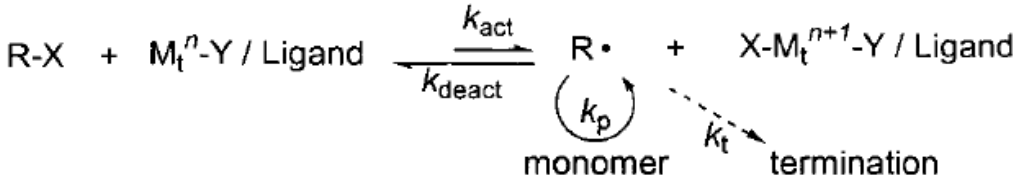

Scheme 2.5. General scheme of ATRP catalyzed by transition metal [144].

ATRP can be operated in bulk, solution or a heterogeneous system such as suspension or emulsion and mini-emulsion. Various organic solvents [146-148] including toluene, acetone, DMSO and DMF have been used for different monomers. ATRP has even been successful in aqueous solution, which is the most environmentally friendly and inexpensive solvent. However, the relatively large amount of catalyst used, typically 0.1 to 1 mol% to monomer amount, is one drawback of the traditional ATRP. The residual metal catalyst may be hazardous in specific applications so that catalyst removal is of primary importance.

ATRP in protic media such as water are usually fast even at ambient temperature. The polymerization speed is accelerated with the increased water concentration in the solvent.

However, several side reactions still make well-controlled ATRP challenging. Tsarevsky and Matyjaszewski reviewed some side reactions in copper mediated aqueous ATRP including dissociation of the deactivator in protic media, disproportionation of Cu based activating complexes, *etc*. (Scheme 2.6) [145].

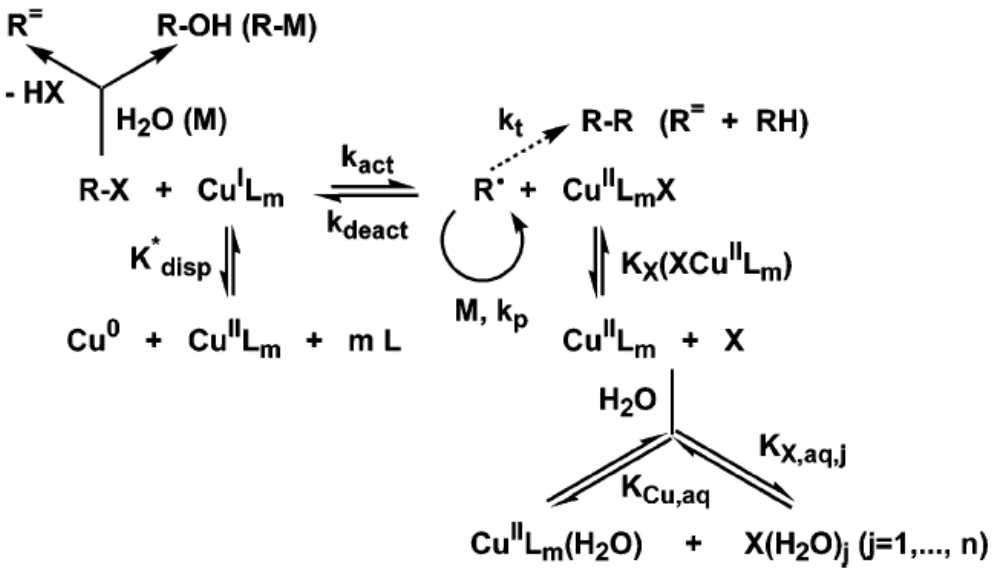

Scheme 2.6. Side reactions in copper mediated aqueous ATRP [145].

2.5.2 ATRP of PNIPAm

Although significant progress has been made in controlled living radical polymerization in recent years, ATRP of NIPAm could not be easily achieved under conventional conditions using linear amines or bipyridine (bpy) based ligands [149, 150]. Additionally, even though there are some reports of surface initiated ATRP of PNIPAm, control of molecular weight and polydispersity could not be achieved. Wang reported the hybrid silica particles coated with PNIPAm shells by surface initiated ATRP in aqueous solution using CuCl/bpy as catalyst [151]. A similar reaction was also investigated by Zhang and *et al*.[152]. However, the polymerization kinetics and molecular weight distributions of PNIPAm chains were not mentioned. In addition, Kim *et al*. reported

surface initiated ATRP of PNIPAm from a dextran surface in aqueous solution, but the living nature was illustrated only by the controlled thickness of PNIPAm film versus polymerization time [153, 154].

The polymerization was not controlled or had very low conversion until Masci reported the first successful ATRP of PNIPAm in DMF/H_2O mixed solvent using ethyl-2-chloropropionate(ECP)/CuCl/Me_6TREN as initiator/ligand at room temperature [155]. In this system linear first order kinetics could be observed up to very high conversions with low polydispersity (Figure 2.22).

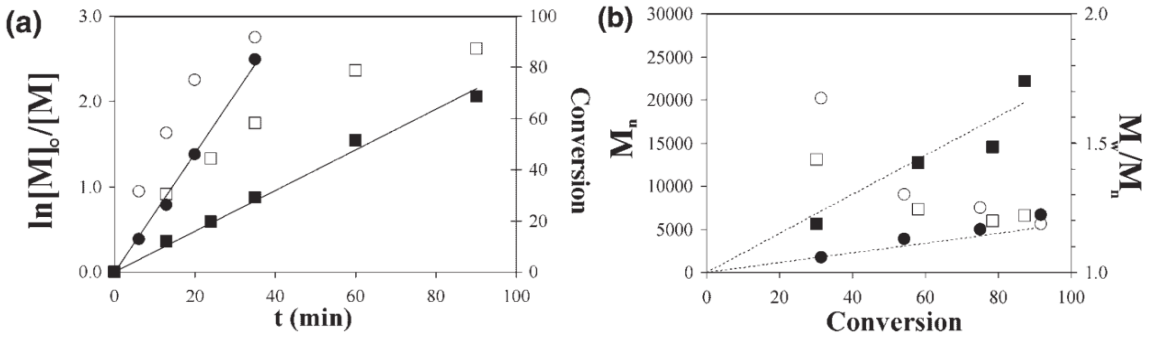

Figure 2.22. Kinetics plots for ATRP of PNIPAm in DMF/H2O = 50:50 at room temperature. Circle = [NIPAm]:[ECP]:[CuCl]:[Me_6TREN] = 50:1:1:1; square = [NIPAm]:[ECP]:[CuCl]:[Me_6TREN] = 200:1:2:2. (a) First order kinetics plot (full symbols) and conversion (open synbols). (b) Dependence of molecular weight (full symbols) and polydispersity (open symbols) on conversion. The dashed lines represent the theoretical molecular weights expected on basis of monomer to initiator ratio [155].

Using the CuCl/Me_6TREN system, Stöver later studied the solvent effect on ATRP of PNIPAm[46]. Methanol, ethanol, iso-propyl alcohol and t-butyl alcohol were investigated. It was found that the branched alcohols led to narrowly dispersed polymers with high conversion and better molecular weight control. It is believed that the branched alcohols could form hydrogen bonds to both monomers and polymer, reducing the deactivation of the catalyst.

In 2008, Liu reported one successful surface initiated ATRP of NIPAm on silica nanoparticles catalyzed by CuCl and Me_6TREN in 2-propanol [156]. The surface grafted PNIPAm exhibited two stage collapses upon heating. The first phase transition that occurred in the range of 20-30 ℃ was attributed to the n-cluster induced collapse of PNIPAm brushes located at inner region close to the silica core. On the other hand, the second transition above 30 ℃ was attributed to the outer region of PNIPAm brushes, which have much lower chain density compared to the inner part.

2.5.3 ATRP of P*t*BA

As the precursor of PAAc, poly(*t*-butylacrylate) (P*t*BA) has been widely studied and successfully polymerized using several different methods including anionic[157, 158], nitroxide mediated and metallocene mediated[159] polymerizations.

Early ATRP studies on P*t*BA mostly utilized bipyridine as ligands, while Davis and Matyjaszewski[160] systematically studied the ATRP using PMDETA as ligand using different initiator and solvent. The addition of a small amount of Cu(II) can decrease the polymerization rate and lower the polydispersity. The increment of solvent polarity was also believed to lower the polydispersity by increasing the concentration of deactivator in solution.

With the development of more multi-dentate amine ligands, Tenhu studied the influence of different ligand on the synthesis of star-like P*t*BA in 2005 [161]. PMDETA, HMTETA and Me_6TREN were compared to 2,2'-bipyridine in his work. These multi-dentate amine ligands are less sterically hindered and thus have higher activities. Polymerizations using these multi-dentate ligands were faster and better controlled than using bpy. However, they also increased the chance of bimolecular coupling especially when Me_6TREN was used in a polar medium.

2.5.4 ATRP of PHEMA

HEMA can be easily polymerized to obtain PHEMA by radical polymerization or by various methods including UV, plasma and γ-rays. However, HEMA is not suitable for anionic or group transfer polymerization because of its reactive pendant hydroxyl groups. Matyjaszewski reported the first successful ATRP of PHEMA in 1999 [162]. The conditions to conduct PHEMA ATRP were investigated and optimized. The best conditions included mixed solvent of methyl ethyl ketone and 1-propanol at a reaction temperature of 50 or 70 °C with a halogen initiator and Cu(I)$[bpy]_2$ catalyst system. However, the polydispersity of 1.30 or even higher was also achieved, suggesting ineffective suppression of termination reactions. Significant differences were found between the GPC data and the target molecular weight. This was due to calibration errors in GPC analysis as polystyrene standards are not reliable for analysis of PHEMA homopolymers. In a later report, Matyjaszewski used PMMA as calibration standards for GPC and the error was reduced to *ca*. two times larger than expected values [163]. The discrepancy was ascribed to the difference in the hydrodynamic volume of PHEMA and PMMA in DMF.

Armes has reported on a more efficient and well-controlled ATRP of PHEMA [77, 164]. The reaction was conducted in methanol/water or pure methanol at room temperature. Much faster polymerization rates, higher conversions, lower polydispersity and good blocking efficiencies were achieved compared to Matyjaszewski's previous results.

2.6 Click reaction

2.6.1 Introduction to click reaction

Click reaction or click chemistry has received much research interest since the concept of "click" was first introduced by Sharpless in 2001 [165]. It generally refers to a kind of reaction that is fast, simple to operate, easy to purify, stereospecsific, versatile and that which has high yields. Click chemistry has four major classes of reactions, i.e. (1) cycloaddition, (2) nucleophilic ring opening, (3) non-aldol carbonyl chemistry and (4) carbon multiple bond addition (Scheme 2.7).

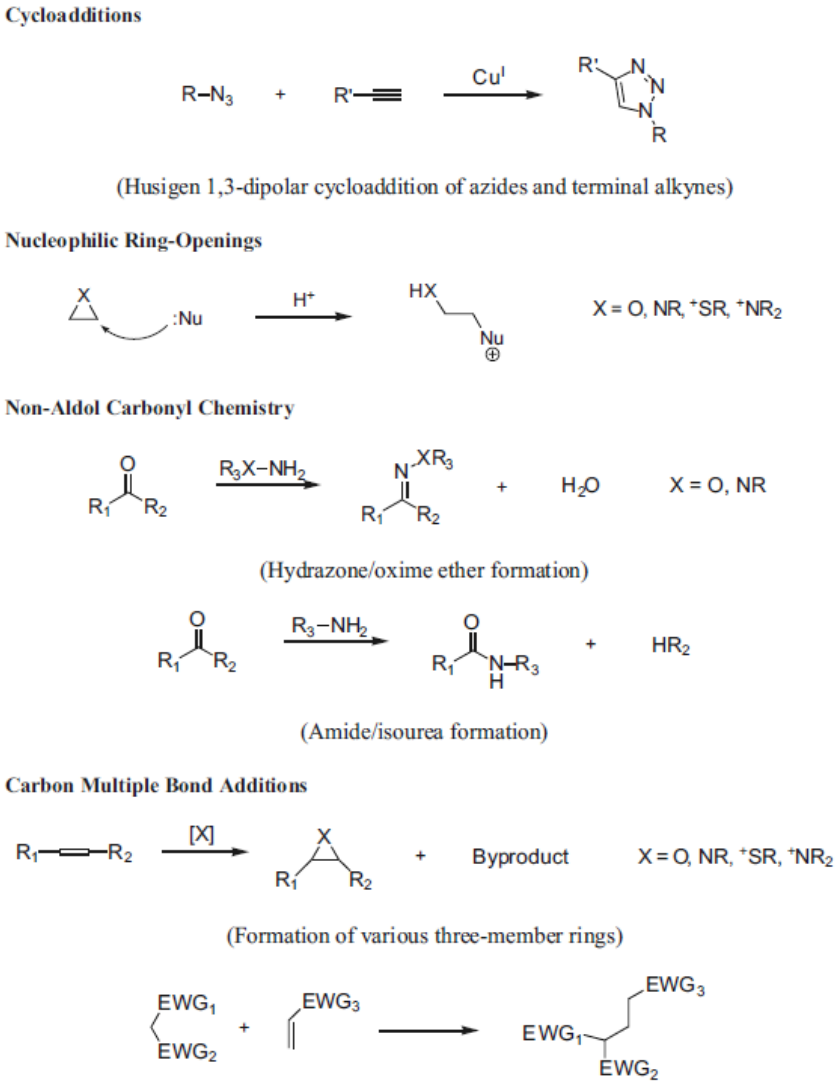

Scheme 2.7. Four classes of click chemistry reactions. Nu: nucleophile, EWG: electro withdraw group [166].

Click reaction has been used together with living radical polymerizations, including ATRP, RAFT and NMP, to produce novel copolymers. The combination of ATRP and click reaction has been used most extensively since first reported by Matyjaszewski [167]. This is because both click reaction and ATRP can be carried out using the same copper-halogen catalytic system, and the halogen end groups of polymer prepared by ATRP can be easily converted to azide group to conduct another click reaction.

2.6.2 Click reaction in star polymers and dendrimers

Star polymers and dendrimers have branched architectures and specific physical and chemical properties compared to linear or random polymers. They have received much research and technical interest nowadays because of their obvious advantages, such as high selectivity and yield. There are a number of reports where click chemistry been used in star polymer and dendrimer synthesis and functionalization.

Liu had prepared well-defined 7 and 21 arm PNIPAm star polymer having β-cyclodextrin as core by ATRP and click reaction [34]. Linear PNIPAm with an alkyne group was synthesized firstly by ATRP and clicked with functionalized β-cyclodextrin with 7 or 21 azide groups. In his another work Liu prepared a PNIPAm dendritic polymer using “arm first” method by a combination of ATRP and click reactions [168]. Short linear PNIPAm was polymerized with an azide containing initiator and clicked with tripropargyl amine to obtain the three armed first generation dendritic polymer. The second generation dendritic polymer was prepared after further steps of azidation and clicking (Scheme 2.8).

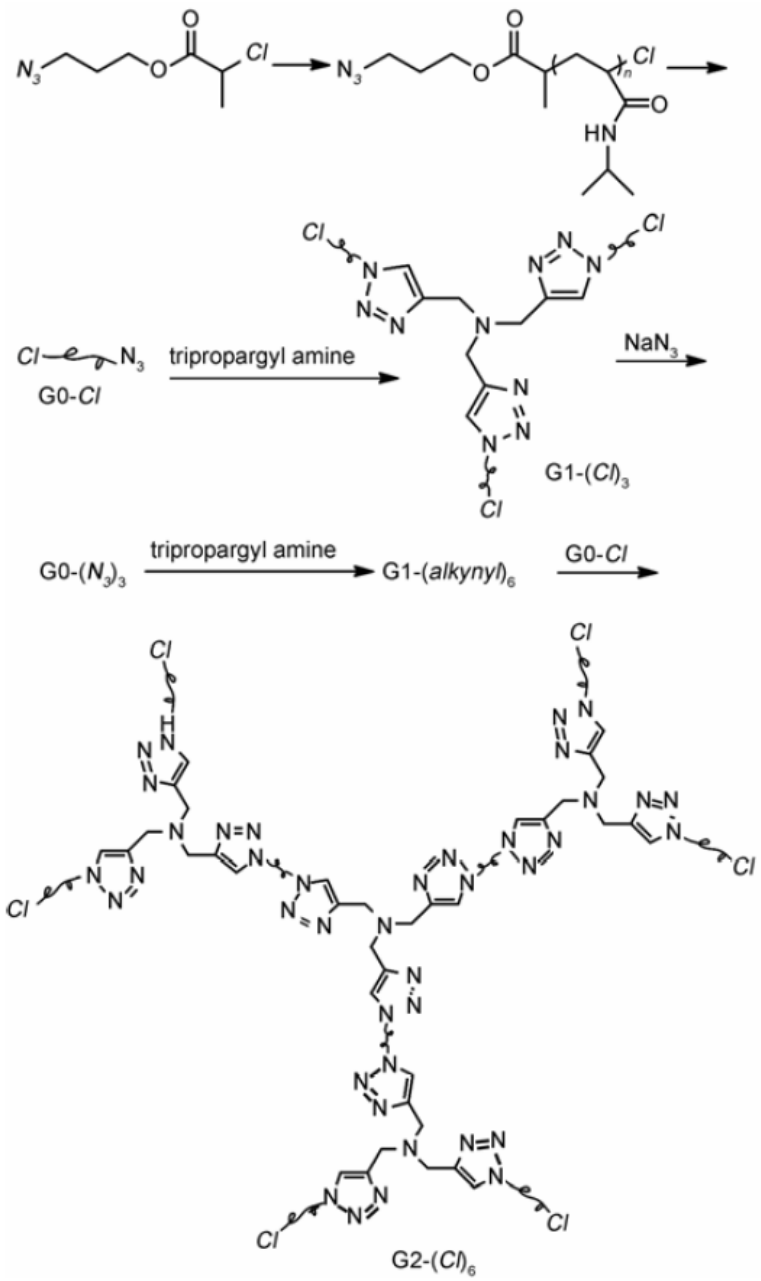

Scheme 2.8. Synthesis of G0-Cl, G1-Cl_3 and G2-Cl_6 dendritic star PNIPAm [168].

Tunca also prepared dendritic miktoarm terpolymer using the combination of ATRP, ring opening polymerization (ROP) and click reaction [169]. Three arms P*t*BA or PS were synthesized by ATRP and used as core after the end groups were modified to azide groups. PS-PCL and P*t*BA-PEG block copolymer having alkyne groups were prepared by NMP and ROP and clicked with star P*t*BA or PS to obtain $(PtBA)_3$-$(PS\text{-}PCL)_3$ and $(PS)_3$-$(PEG\text{-}PtBA)_3$ miktoarm terpolymer (Scheme 2.9).

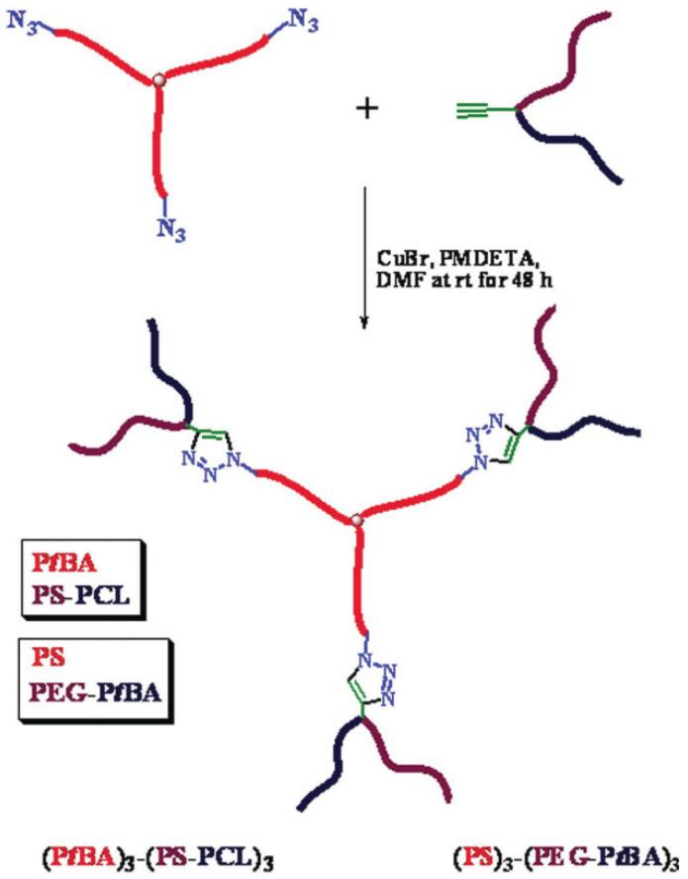

Scheme 2.9. Preparation of miktoarm star terpolymers (P*t*BA)$_3$-(PS-PCL)$_3$ and (PS)$_3$-(PEG-P*t*BA)$_3$ [169].

2.7 Summary

Thermal responsive polymers, pH responsive polymers and some related materials and techniques have been reviewed above. The factors including molecular weight, architecture and end groups are shown to have significant influence on the thermal responsive behavior of PNIPAm. However, the molecular weight effect has been only investigated with linear PNIPAm and not with star architecture. Although there have been a few reports on star-shaped PNIPAm, they have relatively large molecular weight and hydrophobic end groups, which also influence T_c significantly. In next chapters, core first ATRP of PNIPAm using a multi-functional POSS initiator would allow us to construct

the star architecture precisely. The effect of star architecture can be intensively studied in the low molecular weight range without hydrophobic end groups' disturbance.

3. SYNTHESIS AND CHARACTERIZATION OF POSS-TETHERED PNIPAM

3.1 Introduction

In the literature review chapter it has been introduced that the T_c of PNIPAm is affected by many factors including surfactant, ionic strength, and chemical structures such as molecular architecture, end groups and molecular weight.

Although star architecture was reported to decrease T_c of PNIPAm, in previous work RAFT were used for synthesis of the star PNIPAm, which inevitably endowed the polymer with hydrophobic chain transfer agent end groups [7, 30]. It was thus difficult to distinguish the effect of tethering chains and hydrophobic end groups as both would cause a lower T_c. In this work, ATRP is used instead of RAFT to build the star architecture with only halogen end groups. Thus the influence of hydrophobic end groups could be weakened and the effect of star architecture on T_c confirmed.

Regarding the molecular weight effect, previously reported star PNIPAms were in a relatively high molecular weight range (DP > 20) where the polymer chains behave significantly different from short chains [6, 30]. As introduced in the literature review chapter, when DP is low, the T_c of linear PNIPAm increases or even disappears because polymer chains tend to behave like rigid rods rather than random coils and hence the intra-molecular hydrophobic interactions are reduced. It would be interesting to investigate the relationship of T_c with different arm lengths in a star PNIPAm. On the one hand linear PNIPAm chains tend to exhibit rigid rod like chain conformations to reduce intra-chain interactions. On the other hand, the star architecture brings the arms together around a small core and hence produces high local chain density to enhance intra-

molecular (inter-chain) interaction. The competition between the two effects would affect T_c in a synergistic way that may help in better understanding the phase transition behavior of PNIPAm.

In this part of the work, multi-functional POSS is used as the ATRP initiator to prepare star PNIPAm by a divergent way. The PNIPAm arm length and end groups can be well controlled via ATRP. Multifunctional POSS has also been a good platform for preparing hybrid molecules or macromolecules in many reports [105, 128, 129]. Polymer chains tethered at the eight vertexes will induce high local chain density in the near-core region, which provide a precise architecture for us to investigate the effect of molecular weight. Moreover, the halogen end groups of POSS-PNIPAm can be functionalized for further copolymerization, providing a platform for investigation of more complicated star-block and dendritic systems.

3.2 Experimental

3.2.1 Materials

Octa-aminophenyl-silsesquioxane (OAPS) was purchased from Hybrid Plastics™ and used as received. NIPAm (97%, Sigma-Aldrich) was purified by recrystallization from hexane and toluene (v/v= 4/1) and thoroughly dried in vacuum and stored at 4 ℃. Tris[2-(dimethylamino)ethyl] amine (Me_6TREN) was synthesized according to a previous reported method from tris(2-aminoethyl)amine (96%, Sigma-Aldrich)[170]. Copper(I) bromide (CuBr) was washed with acetic acid followed by methanol and dried in vacuum before use. Acetone, 2-propanol, n-hexane, dimethyl formamide (DMF), hydrofluoric acid (40%, HF), trifluoroacetic acid (TFA), lithium bromide (LiBr), 2-bromoisobutyryl bromide (99%), ethyl 2-bromo-isobutyrate, basic aluminium oxide for chromatography were purchased from Sigma-Aldrich and used as received. Regenerated cellulose dialysis

membrane Spectra/Por® MWCO 1000 was purchased from Spectrum Laboratories, Inc. and is thoroughly washed by de-ionized water before use.

3.2.2 Characterization

^{1}H and ^{13}C NMR spectra were recorded on a 400 MHz Bruker Avance-DRX-400 NMR spectrometer. Polymer's molecular weights and polydispersities were measured via absolute size-exclusion chromatography (ASEC) using a Waters 2690 separation module with size-exclusion column coupled with multi-angle light scattering detector from Wyatt technology and differential refractive index detector Waters 410. The eluent was DMF containing 0.1% LiBr. The data were collected and processed by ASTRA software.

Elemental analysis was conducted via the following methods: for bromine analysis, ion chromatography instrumentation includes 818 IC Pump, 820 Separation Center, 830 Interface, 833 Liquid handling Unit, 732 Detector and 813 Compact Autosampler were used. Samples were combusted, and then collected in an absorbing liquid that was fed to ion chromatography. For carbon, hydrogen, nitrogen and sulphur (CHNS) analysis, instrumentation includes Elementar Vario Micro Cube was used and the samples were directly analyzed.

Cloud points (T_c) were characterized using the turbidity method with a Shimazu 2501PC UV-vis spectrometer. The concentrations of sample solutions were 2 mg/mL. The transmittance at the wavelength of 500 nm was recorded as a function of temperature. At each temperature, the samples were equilibrated for sufficient time to ensure the transmittance had a stable value. T_c was defined as the temperature corresponding to 50% of total transmittance change.

3.2.3 Synthesis of POSS based ATRP initiator

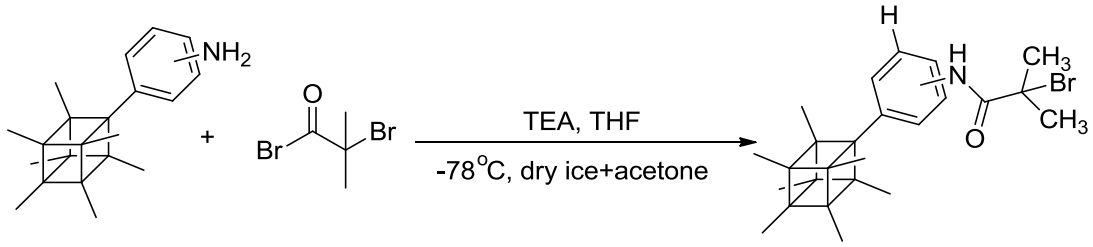

Scheme 3.1. Synthesis of multi-functional POSS ATRP initiator.

The multi-functional POSS-based ATRP initiator was prepared from OAPS and 2-bromoisobutyl bromide according to the method reported by Hussain [129]. The reaction was carried out in a dry-ice-acetone bath under protection of N_2 (Scheme 3.1). OAPS (4.0 g) was dissolved in anhydrous THF (150 ml) in a round bottom flask equipped with magnetic stirring. TEA (8.0 ml) was added via syringe before the reaction flask was dipped into a dry-ice-acetone bath. After the internal temperature was stable, 2-bromoisobutyryl bromide (10.0 ml) was injected by syringe at once. After the addition of 2-bromoisobutyryl bromide, the solution turned from tea to pink-red color. The reaction was stirred in dry-ice-acetone bath for 5 hours then at room temperature for another 2 hours. The precipitation was removed by filtration to obtain a brown solution. After the solvent was removed by rotary evaporation, a dark brown oil residue was obtained. The oil was dissolved in dichloromethane (30 ml) and then washed with de-ionized water 6 times. The brown dichloromethane solution was dropped into an excess amount of n-hexane to give a gray precipitate. The gray precipitate was purified by a dissolution-precipitation process again and dried in vacuum to yield the final product 4.43 g. ^{1}H NMR (Figure 3.1a, d-DMSO, ppm): 7.0-9.0 (br, Ar-*H* and N-*H*), 2.02 (s, –C*H*$_3$). ^{13}C NMR (Figure 3.1b, d-DMSO, ppm): 170.5 (–*C*=O), 123.7, 126.2, 129.3, 130. 9, 137.3 (aromatic carbon), 32.8 (-*C*H_3), 62.1 (–*C*-$(CH_3)_2$Br).

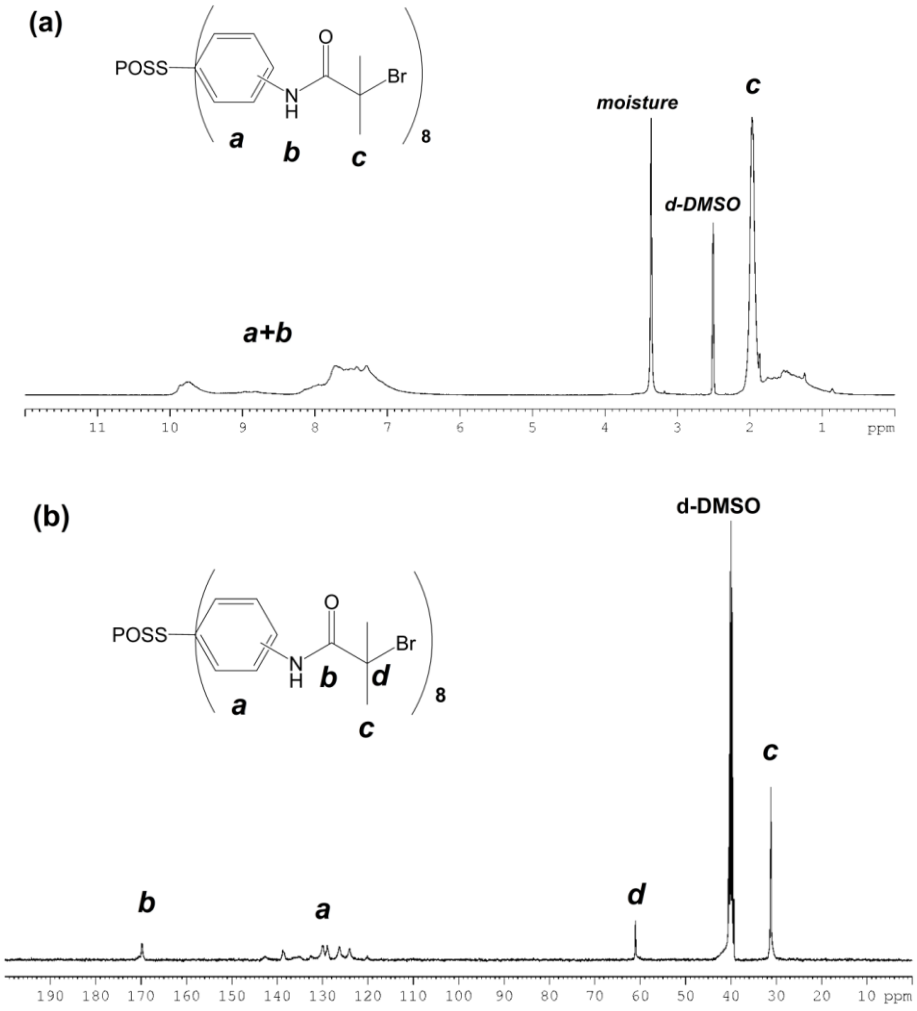

Figure 3.1. (a) ^{1}H NMR and (b) ^{13}C NMR of multifunctionial POSS ATRP initiator in d-DMSO.

3.2.4 Polymerization of POSS-PNIPAm

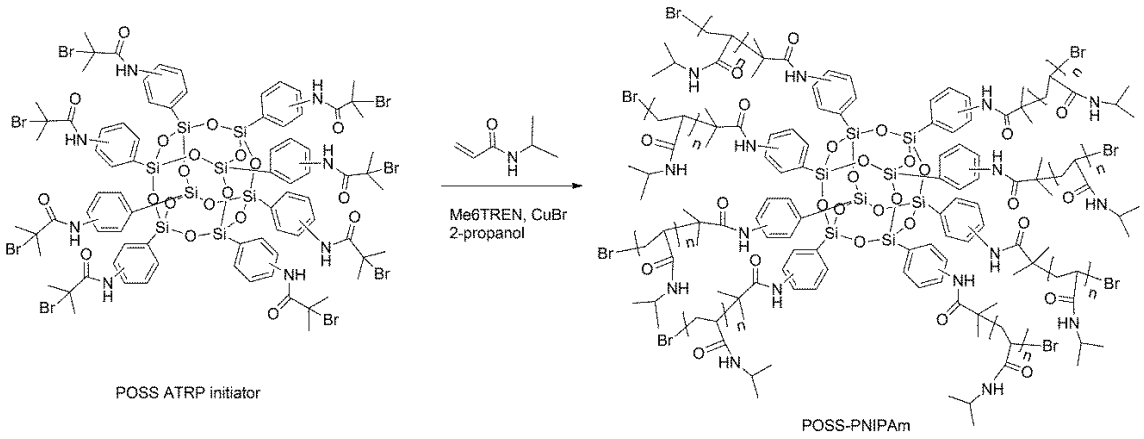

Scheme 3.2. ATRP of PNIPAm with multi-functional POSS initiator.

As illustrated in Scheme 3.2, in a typical ATRP polymerization to obtain POSS-PNIPAm, the multi-functional POSS initiator, NIPAm monomer and Me_6TREN were

dissolved in 2-propanol and charged in a Schlenk tube. After degassing three times via a freeze-pump-thaw process, CuBr was added into the Schlenk tube quickly when the solution was in a frozen state. After two more freeze-pump-thaw cycles, the solution was allowed to stir at room temperature under protection of N_2. A typical molar ratio of [initiator Br group]:[NIPAm]:[Me_6TREN]:[CuBr] was 1:50:2.2:2. Polymers having different molecular weights were obtained by varying the monomer to initiator ratio and the reaction time. At certain time intervals, samples were drawn by syringe for NMR characterization to confirm the living nature of and to investigate the kinetics of the polymerization. The polymerization was terminated by dipping the Schlenk tube into liquid nitrogen. A few drops of THF were also dropped in the flask during exposure to air. The greenish solution was passed through a short column filled with basic aluminium oxide to remove the copper catalyst. Freeze drying was used to obtain the product as a white powder after dialysis in water. ^{1}H NMR (Figure 3.2, D_2O, ppm): 6.6-8.0 (br, 4H, aromatic *H*), 3.80 (s, -C*H*-$(CH_3)_2$), 1.92 (br, >C*H*-CH_2-), 1.49 (br, >CH-CH_2-), 1.17 (s, 6H, >C-(CH_3)$_2$), 1.05 (s, -CH-(CH_3)$_2$). ^{13}C NMR (D_2O, ppm): 175.2, 175.4 (NH-*C*O), 125.4, 126.8, 128.8, 130.3 (aromatic *C*), 41.8 (-*C*H-$(CH_3)_2$), 33.8 to 37.0 (>*C*H-*C*H_2-), 21.6 (-CH-(*C*H_3)$_2$).

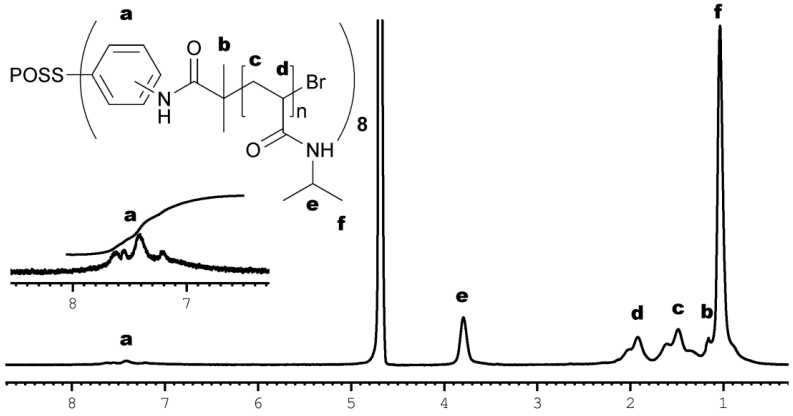

Figure 3.2. A typical ^{1}H NMR of POSS-PNIPAm in D_2O. DP estimated by integration ratio of peak e to a.

3.2.5 Hydrolysis of POSS-PNIPAm

POSS-PNIPAm was dissolved in acetone in a round bottom flask equipped with a magnetic stirrer. An excess amount of aqueous HF was added and the solution was stirred at room temperature overnight. After reaction the solution was diluted with an excess amount of acetone and the solvent was removed by rotary evaporation. The product was purified by dialysis against water. A white product was obtained by freeze drying.

3.2.6 Polymerization of linear PNIPAm

In a typical ATRP reaction the initiator ethyl 2-bromo-isobutyrate, NIPAm monomer and Me_6TREN and 2-propanol were charged in a Schlenk tube and degassed three times via a freeze-pump-thaw process. CuBr was added in quickly when the solution was in a frozen state. After two more freeze-pump-thaw cycles to degas, the solution was allowed to stir at room temperature under protection of N_2. A typical molar ratio of [initiator]:[NIPAm]:[Me_6TREN]:[CuBr] was 1:25:2.2:2 and the molecular weight was controlled via monomer to initiator ratio and reaction time. The polymerization was terminated by dipping the Schlenk tube into liquid nitrogen and addition of a few drops of THF during exposure to air. The copper catalyst was removed by passing the solution though a short basic aluminium oxide column using acetone as eluent. White product was obtained by freeze drying after dialysis in water. ^{1}H NMR (Figure 3.3a, D_2O, ppm): 4.01 (t, end group C*H*$_2$), 3.80 (s, -C*H*-$(CH_3)_2$), 1.93 (br, >C*H*-CH_2-), 1.50 (br, -CH-C*H*$_2$-), 1.15 (s, 6H, >C-(C*H*$_3$)$_2$), 1.05 (s, -CH-(C*H*$_3$)$_2$ and end group C*H*$_3$). ^{13}C NMR (Figure 3.3b, D_2O, ppm): 175.3 (NH-*C*O), 61.8 (end group -*C*H_2-), 43.0 (-*C*$(CH_3)_2$-), 41.8 (-*C*H-$(CH_3)_2$), 33.0 to 38.0 (backbone >*C*H-*C*H_2-), 21.5 (-CH-(*C*H_3)$_2$ and -C(*C*H_3)$_2$-), 13.3 (end group -*C*H_3).

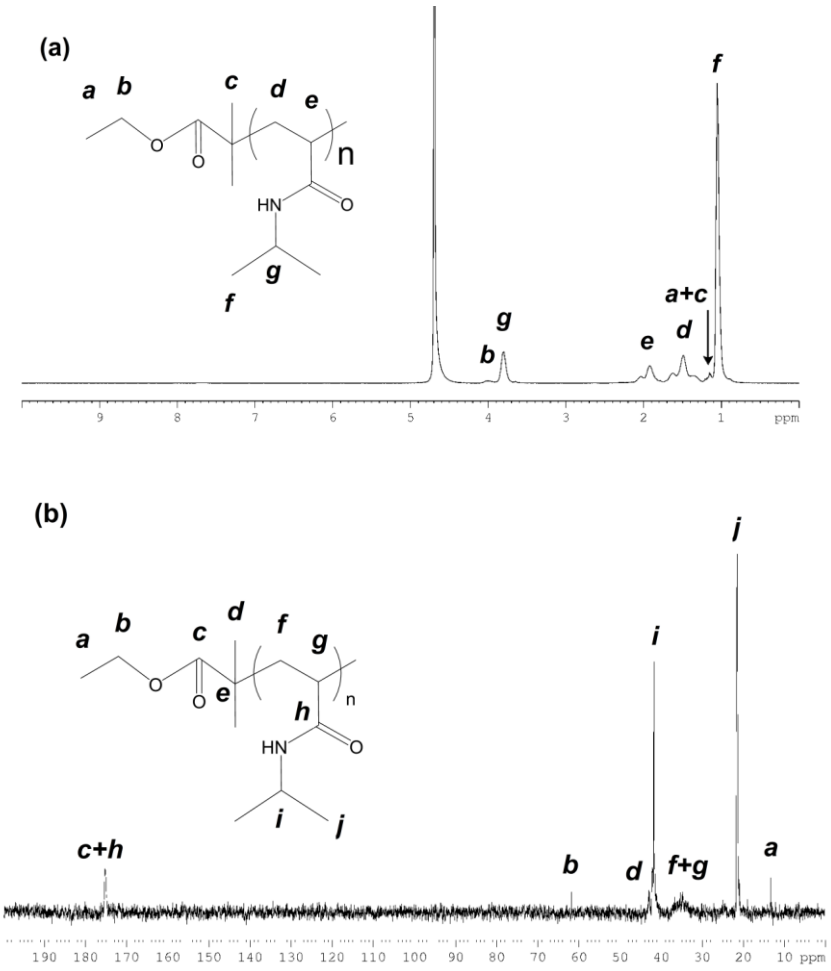

Figure 3.3. (a) ^{1}H NMR and (b) ^{13}C NMR of linear PNIPAm in D_2O.

3.3 Results and Discussion

3.3.1 Initiator structure

The structure of ATRP initiator POSS-Ph-CO-C$(CH_3)_2$Br was confirmed by ^{1}H and ^{13}C NMR (Figure 3.1). The weight averaged molecular weight (M_w) obtained by SEC was 2133 with polydispersity 1.10. However, the M_w given by SEC is not the real molecular weight because this molecule has a spherical shape while the SEC instrument was calibrated using linear polystyrene standards. On the other hand, the starting material OAPS was not pure octa-aminophenyl para-substituted but containing a mixture of isomers. The amino groups may be connected to the phenyl rings at ortho-, meta- or para-positions.

Elemental analysis (EA) was used to analyze the ratio of Br to N to verify the conversion of the reaction between OAPS and 2-bromoisobutyl bromide. The results are listed in Table 3.1. The ratio of calculated value to EA result indicates the complete conversion of NH_2 groups to 2-bromoisobutyl amide groups.

Table 3.1. Elemental analysis of POSS ATRP initiator.

	Calculated value (%)	EA result (%)	Ratio of cal./EA
C	40.96	39.78	1.03
H	3.75	3.91	0.96
N	4.78	4.44	1.08
Br	27.30	25.22	1.08

3.3.2 Structural verification of POSS-PNIPAm

Molecular weights of POSS-PNIPAm and linear PNIPAm are listed in Table 3.2. Since the peaks corresponding to Ar-H and N-H overlap in the range from 7 to 8 ppm, the ^{1}H NMR measurements were carried out in D_2O to obtain accurate integration of phenyl protons without the influence of N-H to prove the successfully polymerization of NIPAm with the functional POSS (Figure 3.2). From the integration ratios of PNIPAm's methine proton to phenyl proton peaks the molecular weights of POSS-PNIPAm can also be estimated. By assuming that there are 8 arms on each cage, the molecular weights of the polymer are estimated using the following equation:

$$M_{n,NMR} = \frac{I_{methine}}{I_{phenyl}/4} \times 8 \times M_{NIPAm} + M_{initiator}$$

where $M_{n,NMR}$ is the number average molecular weight, $I_{methine}$ and I_{phenyl} are the integration of methine protons and phenyl protons, respectively and M_{NIPAm} and $M_{initiator}$ are molar mass of NIPAm unit and POSS ATRP initiator, respectively. The estimated M_ns are listed in Table 3.2. The numbers in the sample names indicate the DP of the PNIPAm arms estimated from the integration ratios. The molecular weights of linear PNIPAm were

also estimated by ^{1}H NMR using a similar method, i.e. determination by integration ratio of PNIPAm's methine group (Figure 3.3a, peak g) to methylene end group (Figure 3.3a, peak b).

Table 3.2. Number average molecular weights (M_n) and polydispersities (PDI) of linear PNIPAm, POSS-PNIPAm and degraded POSS-PNIPAm arms.

	$M_{n,\ NMR}$	$M_{n,\ ASEC}$	PDI by ASEC	No. of arms [c]
Linear $PNIPAm_{11}$ [a]	1427	3122	1.09	-
Linear $PNIPAm_{18}$ [a]	2186	3806	1.09	-
Linear $PNIPAm_{27}$ [a]	3289	4830	1.15	-
Linear $PNIPAm_{44}$ [a]	5120	7172	1.20	-
POSS-$PNIPAm_{13}$ [b]	14385	24950	1.15	6.6
POSS-$PNIPAm_{13}$ arm	-	3775	1.33	
POSS-$PNIPAm_{18}$ [b]	18544	28160	1.15	7.4
POSS-$PNIPAm_{18}$ arm	-	3824	1.67	
POSS-$PNIPAm_{21}$ [b]	21733	36370	1.11	7.2
POSS-$PNIPAm_{21}$ arm	-	5035	1.18	
POSS-$PNIPAm_{37}$ [b]	35512	48700	1.07	6.9
POSS-$PNIPAm_{37}$ arm	-	7062	1.11	
POSS-$PNIPAm_{57}$ [b]	54156	72790	1.10	8.7
POSS-$PNIPAm_{57}$ arm	-	8337	1.12	

DP indicated in the sample names were determined from ^{1}H NMR integration ratios of (a) PNIPAm's methine group to methylene end group; (b) PNIPAm's methine group to phenyl proton. (c) Number of arms of POSS-PNIPAm was determined by dividing $M_{n,ASEC}$ of POSS-PNIPAm by that of PNIPAm arm obtained from cleavage of POSS.

The molecular weights of POSS-PNIPAm determined by ASEC have consistent trends to $M_{n,\ NMR}$. As ^{1}H NMR could not provide information about the average number of arms, $M_{n,ASEC}$ were used to estimate the arm numbers on each POSS cage. HF was used

to hydrolyze POSS cage to obtain cleaved PNIPAm arms. The typical molecular weight changes were traced by ASEC as illustrated in Figure 3.4 and the results are listed in Table 3.2. It is evident that the peak in ASEC is unimodal after hydrolysis. This implies that during the hydrolysis POSS cages are completely degraded to release the arms of the star polymer. The number of arms is estimated via dividing $M_{n,ASEC}$ of POSS-PNIPAm by $M_{n,ASEC}$ of its cleaved arms. The values obtained are listed in Table 3.2 and are reasonably close to the assumed number of active sites in each POSS initiator molecule.

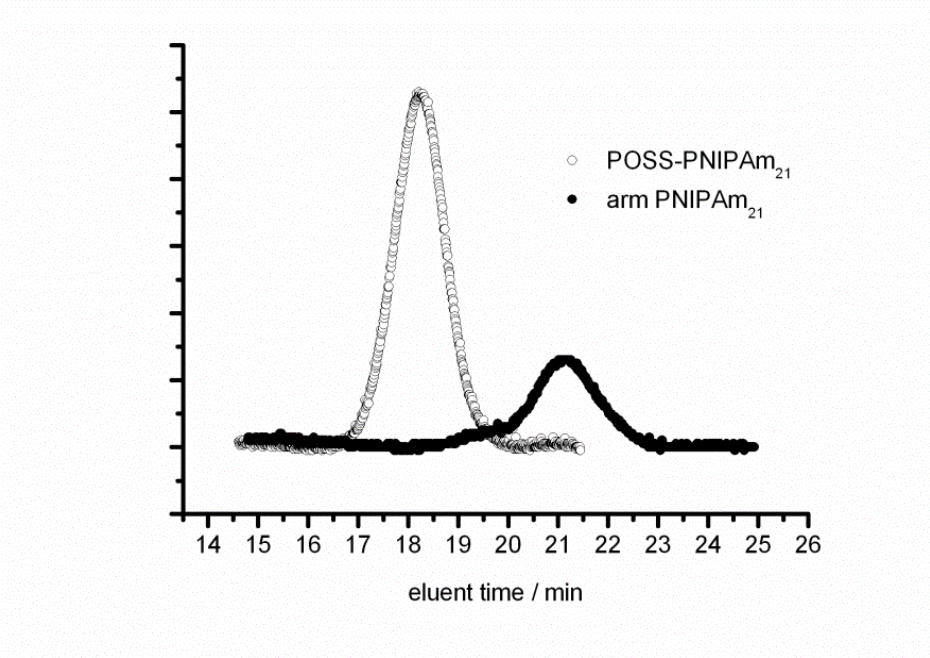

Figure 3.4. ASEC of POSS-PNIPAm$_{21}$ and its cleaved arm.

3.3.3 Kinetics

Figure 3.5 shows a semilogarithmic kinetic plot of monomer conversion (M_0/M_t) vs. reaction time for a typical POSS-PNIPAm ATRP polymerization, where M_0 and M_t are monomer concentration at initial and at time t, respectively. The linearity of the initial part of the curve indicates a stable radical concentration in the system when the monomer conversion is low. After five hours, the monomer conversion does not increase much further, which is likely to be caused by undesirable coupling termination, which is often

observed when a multi-functional ATRP initiator is used. Based on this result, all ATRP reactions were terminated within five hours to achieve narrow molecular weight distributions.

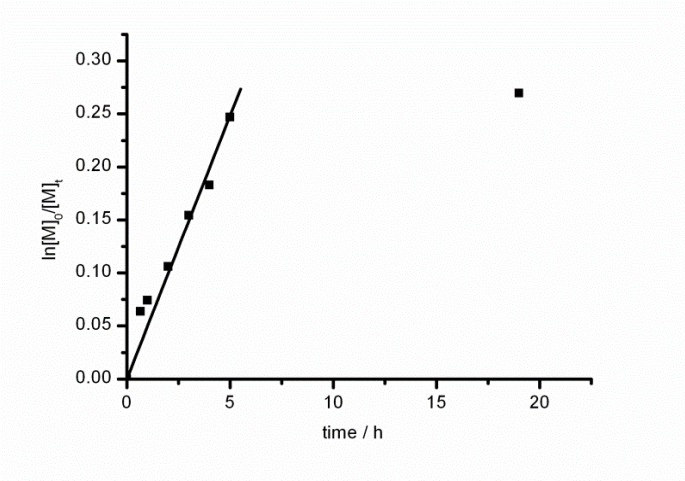

Figure 3.5. First order kinetic plot for ATRP of POSS-PNIPAm in the initial 5 h.

3.3.4 Phase transition behavior

The phase transition behaviors of the linear PNIPAm, POSS-PNIPAm and its cleaved arms obtained from hydrolysis are shown in Figure 3.6. The T_c of the linear PNIPAm is decreasing with increasing molecular weight (Figure 3.6a), and is approximately proportional to reciprocal square root of the DP (inset of Figure 3.6d). This shows that the scaling law is still applicable in such low molecular weight range. When DP is 13 which is slightly larger than the persistence length predicted by Asher [25], the T_c occurs at 57 ℃, indicating that short linear PNIPAm chains with lengths close to persistence length do behave like flexible rods at relatively low temperatures, and this suppresses intra-molecular hydrophobic interactions and increases T_c.

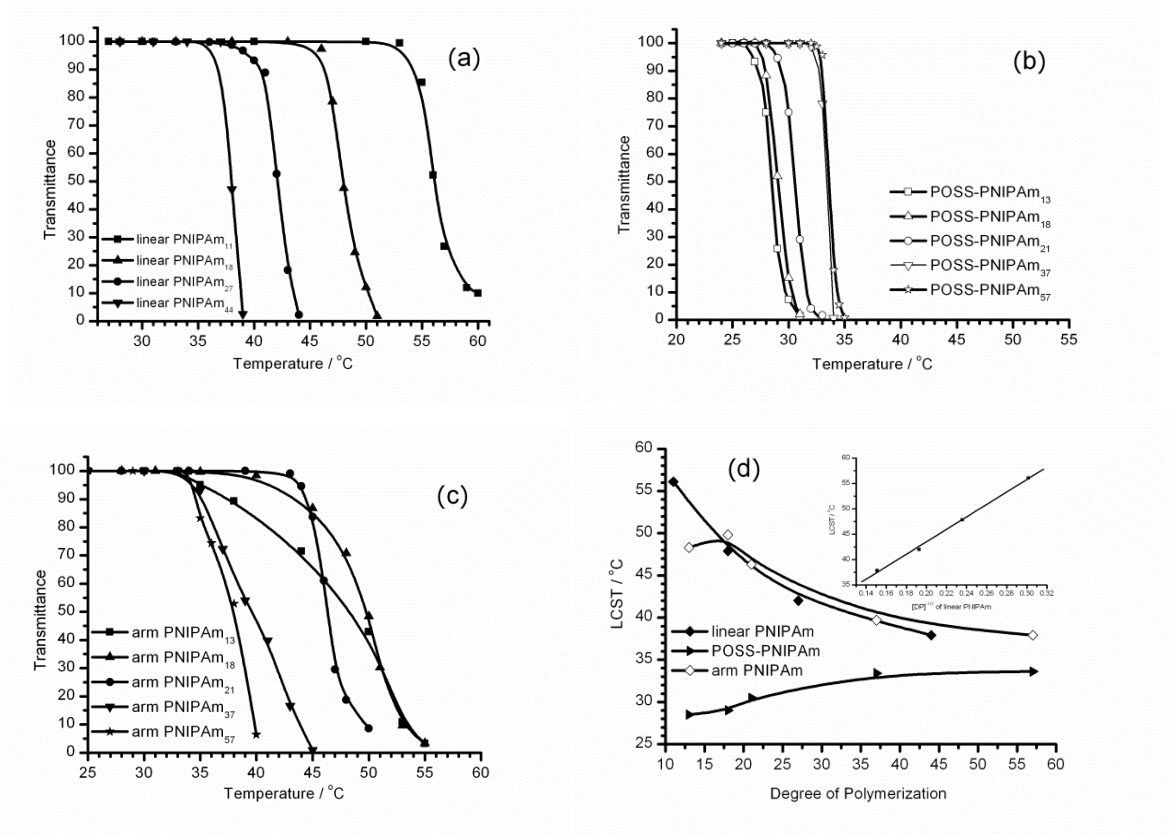

Figure 3.6. The effect of molecular weight on T_c of (a) linear PNIPAm, (b) POSS-PNIPAm, (c) hydrolyzed arm PNIPAm, (d) T_c as a function of DP, the inset is T_c of linear PNIPAm as a function of reciprocal of square root of DP.

Comparing to linear PNIPAm, the T_c of POSS-PNIPAm exhibits a contrary trend that it decreases with decreasing molecular weight (Figure 3.6b). This is because the chain density in the near-core region is higher. Consequently the intra-molecular interaction between PNIPAm arms is more prominent with shorter arms. When the chains are long enough, both linear PNIPAm and PNIPAm arms on POSS behave like random coils and tend to exhibit T_c close to the well-known value of *ca*. 34 ℃. Comparing with previously reported star PNIPAm ended with CTA groups [6, 26] or long alkyl chains [171] which were prepared by RAFT, POSS-PNIPAm synthesized by the "core first" ATRP has bromine end groups, which have limited hydrophobic influence. The T_c of cleaved PNIPAm arms is similar to that of linear PNIPAm (Figure 3.6d), indicating a well defined

star architecture. It is also worth noting that for both linear PNIPAm and POSS-PNIPAm, the transition becomes sharper with increasing molecular weight, indicating that intra-molecular interaction dominates the sharpness of the transition. This is supported by the fact that POSS-PNIPAm exhibits sharper transitions than the linear PNIPAm having similar chain length because in POSS-PNIPAm intra-molecular interactions may also occur between neighbouring arms.

3.4 Summary

A series of star polymers having POSS as the core and narrow distributed short PNIPAm arms has been successfully prepared via "core first" ATRP. The star architecture has been confirmed by molecular weight analysis of the star polymers and their corresponding cleaved arms using ASEC. Comparing to previously reported star PNIPAm synthesized by RAFT, the straightforward and easy-to-operate "core first" ATRP provides good control over the chain length and molecular weight distribution. Moreover, polymers prepared by ATRP do not have hydrophobic end groups as the CTA groups by RAFT, thus the impact of star architecture to T_c has been investigated without the influence of hydrophobic end groups. The T_c of POSS-PNIPAm is much lower than linear counterparts having similar chain lengths especially in low molecular weight range, which is ascribed to the high local chain density in the near-core region where the intra-molecular hydrophobic interactions between the PNIPAm arms are significantly increased. The star effect is weakened when the molecular weight increases thus the obvious T_c difference exists only in low molecular weight range. However, the halogen end groups of POSS-PNIPAm provide the possibility for further functionalization and copolymerization to investigate more complicated star copolymers or dendritic polymers.

4. SYNTHESIS AND CHARACTERIZATION OF TEMPERATURE AND PH DUAL RESPONSIVE POSS-TETHERED STAR-BLOCK COPOLYMERS

4.1 Introduction

In last chapter, the synthesis and structural verification of POSS-tethered PNIPAm have been reported. The effects of molecular weight and star architecture on T_c of POSS-PNIPAm have been clarified. In comparison with linear PNIPAm, the star architecture increases intra-molecular interaction that induces phase transition at a lower temperature, especially in the low molecular weight range.

As the most widely studied pH responsive polymer, PAAc has been reported to copolymerize with PNIPAm forming various copolymer structures, including linear, graft, interpenetrating network and random copolymers. Molecular architecture has been found to have a crucial effect on the thermal and pH responsive behaviors of these copolymers. However, star-block PNIPAm-PAAc has not yet been studied and it is not clear whether local chain density will also play an important role in influencing their dual-responsive behaviors. In this part of work, PAAc blocks are introduced into star polymers as the pH sensitive segment near the core. The structure is realized by using two steps of ATRP with POSS as the multi-functional initiator. The pH responsive PAAc blocks are able to exhibit different ionized or protonated state at different pH and affect the phase transition. Moreover, inserting a short block of PAAc between POSS core and PNIPAm arms may facilitate the possible hydrogen bonding between the arms located in the high density region. Systematic investigation of the solution behaviors of these star-block copolymers with that of the POSS-PNIPAm polymer as reference would allow us to probe into the

influence of star architecture and block length of each segments on temperature and pH dual responsive behaviors of the copolymers.

4.2 Experimental

4.2.1 Materials

Tert-butyl acrylate (*t*BA, 98%, Sigma-Aldrich) and N,N,N',N',N''-pentamethyl-diethylenetriamine (PMDETA) (99%, Sigma-Aldrich) was dried and distilled from CaH_2 before use. Trifluoro acetic acid (TFA), buffer solutions with pH = 5.0 (citric acid and sodium hydroxide), 6.0 (citric acid and sodium hydroxide), 7.4 (sodium phosphate dibasic and potassium phosphate monobasic) and 10.0 (boric acid, potassium chloride and sodium hydroxide) were purchased from Sigma-Aldrich and used as received. For other chemicals and materials, please refer to Chapter 3.2.1.

4.2.2 Characterizations

For ^{1}H and ^{13}C NMR, ASEC and T_c measurement conditions, please refer to Chapter 3.2.2.

4.2.3 Synthesis of POSS-P*t*BA macroinitiator

Star-shaped POSS-P*t*BA was synthesized via ATRP of *t*BA using the same multi-functional ATRP initiator as in Chapter 3 (Scheme 4.1). In a typical reaction, the multi-functional POSS initiator, *t*BA monomer, PMDETA and 2-propanol were charged in a Schlenk tube. After three times' degassing via freeze-pump-thaw process, CuBr was then added into the tube quickly when the mixture was in a frozen state. After two more freeze-pump-thaw cycles, the solution was allowed to stir at room temperature under

protection of N_2 gas. A typical molar ratio of [initiator Br groups]:[*t*BA]:[PMDETA]:[CuBr] was 1:10:2.2:2. Polymers having different molecular weight were obtained by varying the monomer to initiator ratio and reaction time. The polymerization was terminated by dipping the Schlenk tube into liquid nitrogen and addition of a few drops of THF during exposure to air. After the catalyst was removed by passing the solution though a short column filled with basic aluminium oxide, the solution was dialyzed in THF. Finally the solvent was removed by rotary evaporation and vacuum dried to obtain the yellowish wax-like product. ^{1}H NMR (Figure 4.1, acetone-d6, ppm): 6.8-7.8 (br, aromatic *H*), 2.30 (br, >C*H*-CH_2-), 1.88 (br, >CH-CH_2-), 1.52 (s, -C(CH_3)$_3$), 1.30 (s, -C(CH_3)$_2$-).

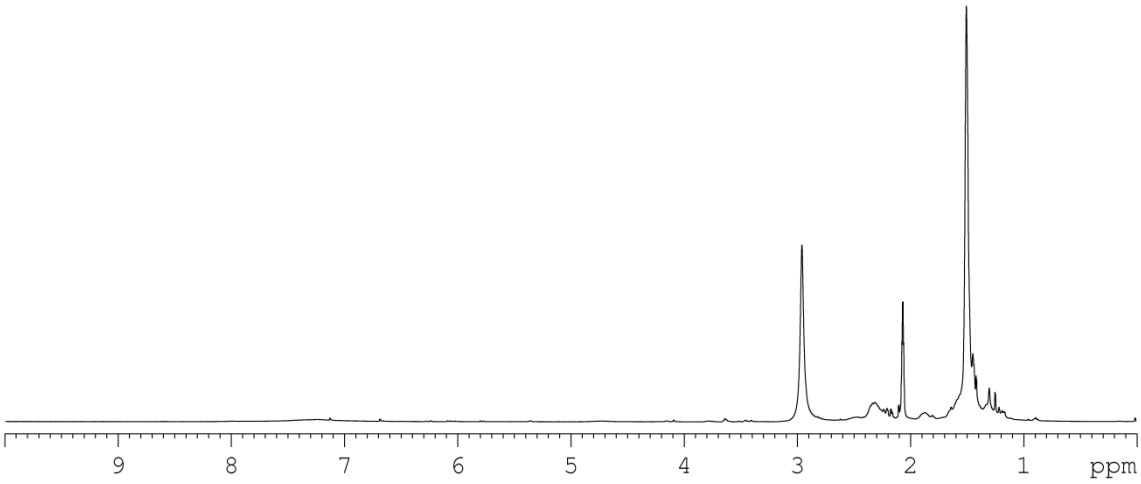

Figure 4.1. ^{1}H NMR of POSS-P*t*BA$_8$ in acetone-d6.

4.2.4 Synthesis of POSS-P*t*BA-*b*-PNIPAm

POSS-P*t*BA was used as a macro-initiator to prepare star block POSS-P*t*BA-PNIPAm via sequential ATRP (Scheme 4.1). A polymerization method similar to POSS-PNIPAm, as well as the purification procedure, was used to achieve POSS-P*t*BA-*b*-PNIPAm as white or yellowish powder. ^{1}H NMR (Figure 4.2a, acetone-d6, ppm): 6.8-7.8 (br, N-*H*

and aromatic *H*), 4.02 (s, -C*H*-$(CH_3)_2$), 2.31 (br, >C*H*-CH_2-), 1.64 (br, >CH-CH_2-), 1.50 (s, -C(CH_3)$_3$),1.30 (s, >C-(CH_3)$_2$),1.16 (s, -CH-(CH_3)$_2$).

4.2.5 Synthesis of POSS-PAAc-*b*-PNIPAm

POSS-PAAc-*b*-PNIPAm was prepared via hydrolysis of POSS-P*t*BA-*b*-PNIPAm in presence of TFA (Scheme 4.1). In a typical reaction, a round bottom flask containing POSS-P*t*BA-*b*-PNIPAm was put in ice bath under protection of N_2 gas while an excess amount of TFA was injected into the flask. The ice bath was removed after one hour and the solution was allowed to stir at room temperature overnight. After removal of the solvent by rotary evaporation, acetone was added to dissolve the sample. The product was obtained by freeze-drying after dialysis of the acetone solution in water. ^{1}H NMR (Figure 4.2b, acetone-d6, ppm): 6.8-7.8 (br, N-*H* and aromatic *H*), 4.02 (s, -C*H*-$(CH_3)_2$), 2.22 (br, >C*H*-CH_2-), 1.65 (br, >CH-CH_2-), 1.30 (s, >C-(CH_3)$_2$),1.16 (s, -CH-(CH_3)$_2$).

4.2.6 Cleavage of of POSS-P*t*BA-*b*-PNIPAm

The arms of the star block copolymer were cleaved for molecular weight analysis by ASEC to verify the average arm number. A typical POSS-P*t*BA-*b*-PNIPAm sample was dissolved in acetone and THF (v/v=1/1) in presence of HF and stirred at room temperature overnight. After the hydrolysis, an excess amount of acetone was added in the solution for dilution. The solvent was removed by rotary evaporation and drying in vacuum to obtain yellowish product.

4.3 Results and discussion

4.3.1 Synthesis and structural verification of star-block copolymers

Sequential ATRP of *t*BA and NIPAm were used to prepare POSS-P*t*BA-*b*-PNIPAm as shown in Scheme 4.1. Because of the reported different reactivity of *t*BA [161] and NIPAm [155] in ATRP, PMDETA and Me_6TREN were used as the ligand in the sequential ATRP, respectively,. The successful two step reaction proved the livingness of the polymerization. The molecular weights were controlled via varying the monomer to initiator ratio and reaction time.

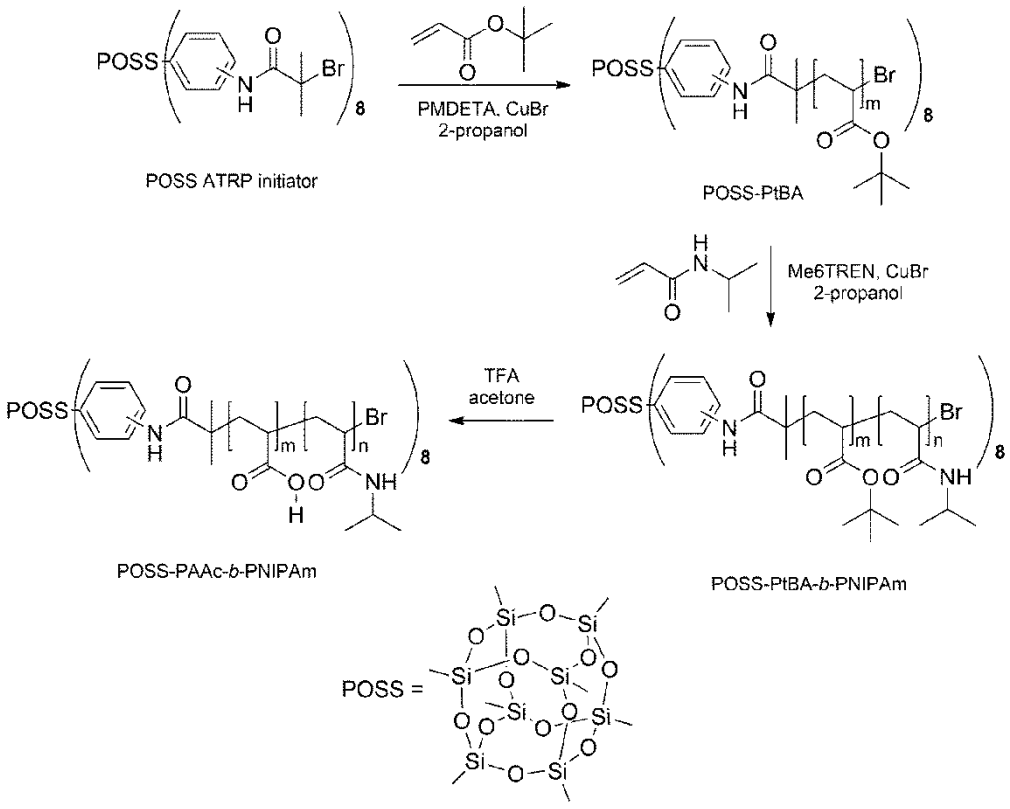

Scheme 4.1. Synthesis of POSS-P*t*BA-*b*-PNIPAm and POSS-PAAc-*b*-PNIPAm.

As shown in the ^{1}H NMR spectra in Figure 4.2a, the lengths of the P*t*BA and PNIPAm blocks in the copolymer can be calculated from the integration ratio of the characteristic peaks of P*t*BA, PNIPAm and POSS-based initiator. The $M_{n,NMR}$ and DP of

POSS-P*t*BA-*b*-PNIPAm were estimated from integration ratio of methine proton (s, 4.02) and methyl proton (s, 1.50) to aromatic and secondary amino proton (br, 6.7-8.0), which belong to PNIPAm segment, P*t*BA segment and the POSS initiator respectively. Due to the overlapping of NH from PNIPAm with the POSS initiator, the equivalent of ^{1}H integration of PNIPAm should be subtracted from total integration of the broad peak 6.7-9.0. A similar method was used to estimate M_n and DP of other POSS-P*t*BA-PNIPAm copolymers. The $M_{n,NMR}$ is estimated based on the assumption that eight arms are attached to each POSS cage and is listed in Table 4.1.

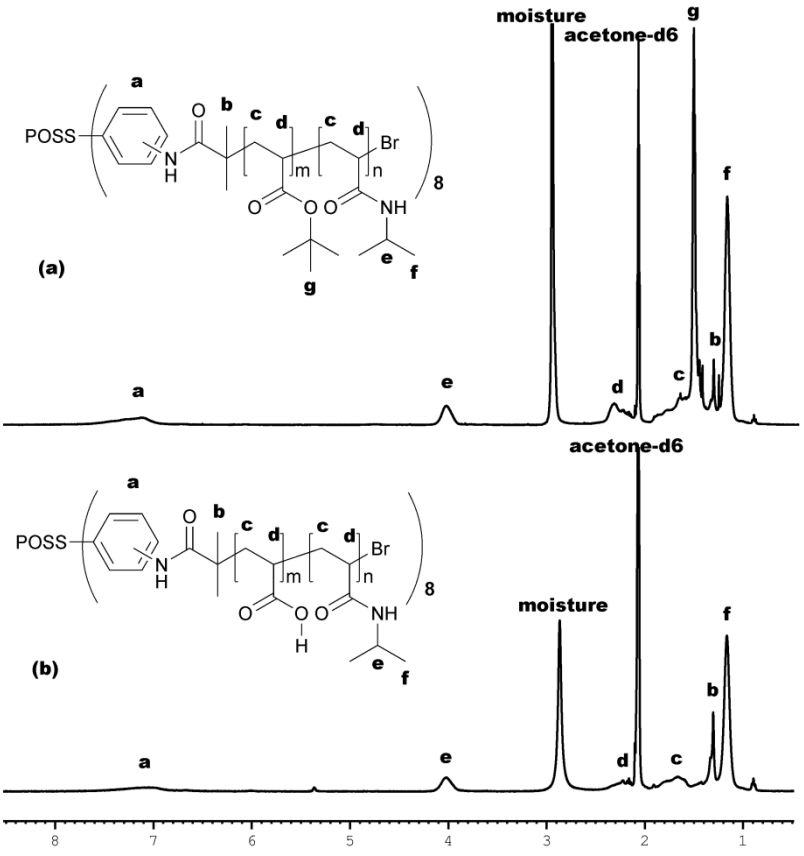

Figure 4.2. ^{1}H NMR of (a) POSS-P*t*BA$_8$-*b*-PNIPAm$_{11}$ and (b) POSS-PAAc$_8$-*b*-PNIPAm$_{11}$ in acetone-d6.

The molecular weights determined by ASEC are also listed in Table 4.1. The polydispersities of the star-block copolymers are found to be significantly larger than POSS-PNIPAm. This is because the two-step polymerizations would inevitably broaden

the distribution of the copolymer. On the other hand, the polymerization to prepare POSS-P*t*BA macro-initiator was terminated after a very short time and low conversion to obtain short P*t*BA block. This made the distribution even broader because polydispersity is relatively higher at the early stage of polymerization, and decreases with increasing reaction time in typical ATRP reactions [9].

POSS-PAAc-*b*-PNIPAm was hydrolyzed from POSS-P*t*BA-*b*-PNIPAm in the presence of TFA. The TFA treatment has been reported to allow effective removal of *t*-butyl groups without breaking the Si-O bonds of the POSS cage [172]. In the ^{1}H NMR spectrum, the *t*-butyl signal at δ=1.50 (Figure 4.2a) disappears after hydrolysis (Figure 4.2b), implying the complete conversion of P*t*BA to PAAc. Star POSS-PNIPAm and linear PNIPAm with similar arm/chain lengths prepared in last chapter were used as reference samples. Their molecular weights are listed in Table 4.1.

Table 4.1. Number average molecular weights (M_n) and polydispersities (PDI) of linear $PNIPAm_{11}$, $POSS\text{-}PNIPAm_{13}$ and star-block POSS-P*t*BA-*b*-PNIPAm determined by ^{1}H NMR and ASEC.

Polymer *	$M_{n,NMR}$	$M_{n,ASEC}$	PDI by ASEC
Linear $PNIPAm_{11}$	1427	3122	1.09
$POSS\text{-}PNIPAm_{13}$	14385	24950	1.15
$POSS\text{-}PtBA_2\text{-}b\text{-}PNIPAm_{11}$	13270	18170	1.62
$POSS\text{-}PtBA_8\text{-}b\text{-}PNIPAm_{11}$	18820	24410	1.51

* DP indicated in sample names are estimated from ^{1}H NMR.

POSS has been reported to be a good platform to construct star polymers due to its cage-like structure and multi-functionality [79, 105]. However, as indicated in last chapter that OAPS is a mixture of isomers [128, 129], the POSS-PNIPAm and the star-block copolymers synthesized in this research inevitably have varied arm numbers and lengths. In order to investigate the star architecture, HF was used to hydrolyze the POSS cages of POSS-P*t*BA-*b*-PNIPAm star-block copolymer to obtain its cleaved P*t*BA-*b*-PNIPAm arms. The molecular weight changes were traced by ASEC as shown in Figure 4.3. The

single peak after hydrolysis indicates that POSS cages are completely hydrolyzed. The average arm numbers are estimated by dividing $M_{n,ASEC}$ of the star copolymer by that of its hydrolyzed counterpart. The resulting value 7.9 is fairly close to the expected number of active sites in POSS initiator molecule and our assumption, indicating the well-defined architecture of the star-block copolymers.

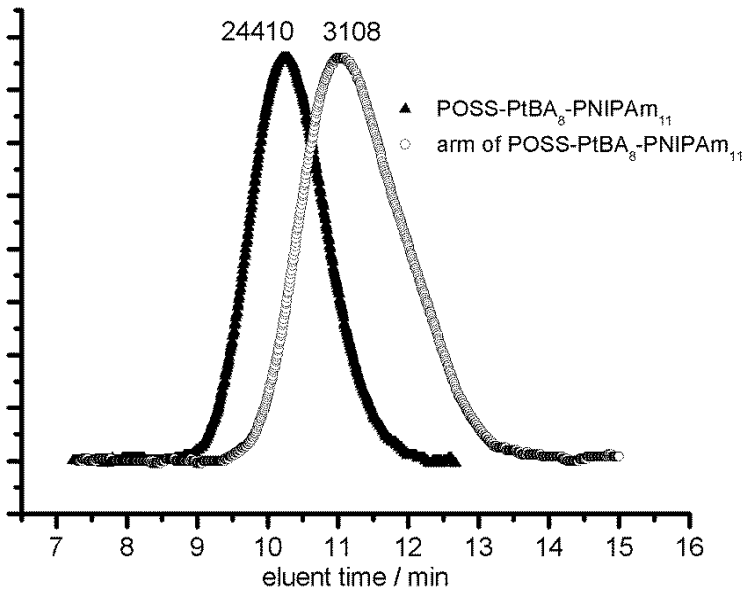

Figure 4.3. Molecular weights of POSS-P*t*BA-*b*-PNIPAm and the corresponding hydrolyzed product traced by ASEC with their $M_{n,\ ASEC}$ indicated.

4.3.2 Dual responsive behavior and mechanism

In last chapter, the high local chain density in the near-core region brought by the star architecture has been found to lower the T_c significantly especially in the low molecular weight range. To study the local chain density effects on the dual-responsive behavior of the star-block copolymers, short segments of PAAc were inserted between POSS and PNIPAm blocks. By varying the length of the PAAc blocks and pH value, it is possible to manipulate the hydrophilicity of the molecules and intra-molecular interactions.

The P*t*BA segments in POSS-P*t*BA-*b*-PNIPAm copolymers are hydrophobic. Consequently, star-block POSS-P*t*BA-*b*-PNIPAm is not soluble in aqueous solution and

can only form a translucent micellar solution. Unlike P*t*BA, the pH responsive PAAc is hydrophilic at high pH values owing to ionization and becomes more hydrophobic in lower pH environment due to protonation of the carboxylic groups. The thermal response behaviors of POSS-PAAc$_2$-*b*-PNIPAm$_{11}$ at different pH are shown in Figure 4.4a. The T_c increases from *ca*. 26.2 to 48.7 °C when pH increases from 5.0 to 10.0. The temperature variation range is wide and fairly different from the previously reported dual responsive behaviors of PNIPAm-PAAc block copolymers [9] and graft copolymers [10].

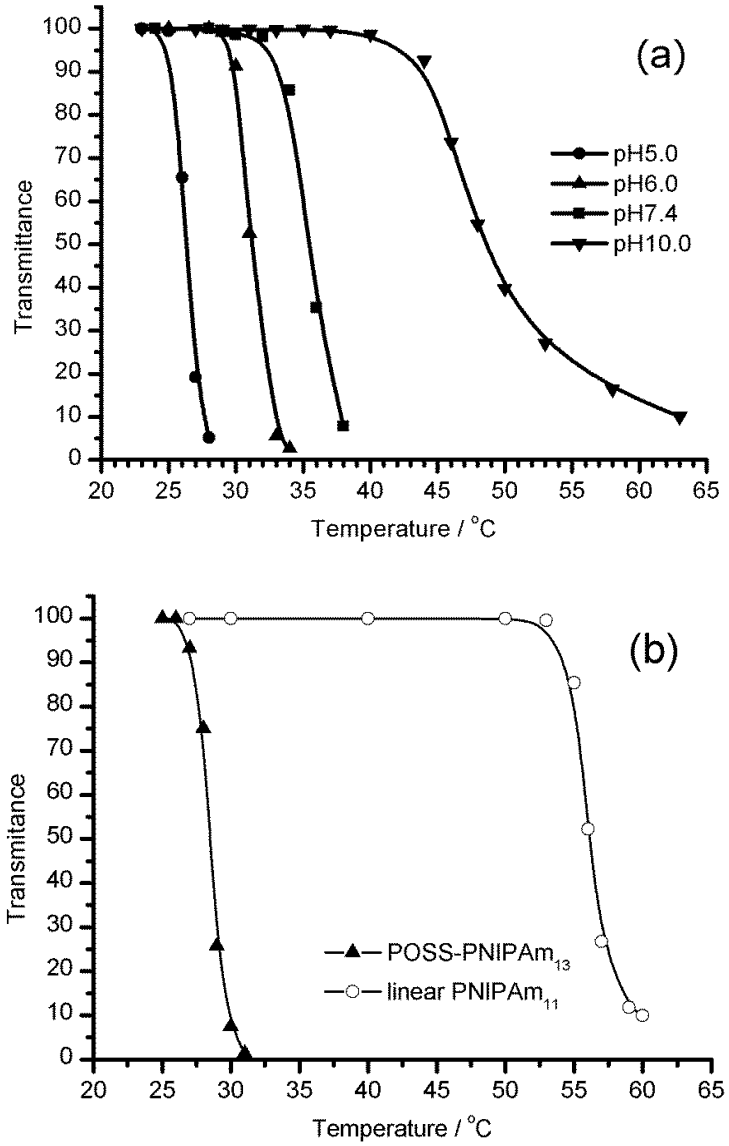

Figure 4.4. (a) Thermal response behavior of POSS-PAAc$_2$-*b*-PNIPAm$_{11}$ at different pH. (b) Thermal response behavior of POSS-PNIPAm$_{13}$ and linear PNIPAm$_{11}$.

The thermal response behavior comparison between linear PNIPAm, POSS-PNIPAm and POSS-PAAc$_2$-*b*-PNIPAm$_{11}$ can help us understand the mechanism of the dual-responsive behavior of star-block PAAc-PNIPAm. The preparation and thermal responsive behaviors of linear PNIPAm$_{11}$ and POSS-PNIPAm$_{13}$ were discussed in Chapter 3. As shown in Figures 4.4b, the T_c of linear PNIPAm$_{11}$ is high due to the rod-like behavior that suppresses intra-molecular hydrophobic interactions, and the lower T_c of POSS-PNIPAm$_{13}$ is due to the high local chain density in the near-core region that promotes intra-molecular interaction between the adjacent PNIPAm arms.

Based on the above analysis on linear PNIPAm and star POSS-PNIPAm, it can be deduced that at high pH values, the ionized carboxylic groups in POSS-PAAc-PNIPAm push the arms away from each other owing to the electrostatic repulsion between the charged carboxylic groups. As a result, the short PNIPAm blocks in POSS-PAAc$_2$-*b*-PNIPAm$_{11}$ are isolated like linear short PNIPAm rods, leading to much higher T_c. Indeed, the T_c of POSS-PAAc$_2$-*b*-PNIPAm$_{11}$ in pH 10 solutions is at 48.7 ℃ and closer to the T_c of linear PNIPAm$_{13}$ rather than POSS-PNIPAm$_{11}$. At low pH values, the PAAc blocks are protonated and more hydrophobic to enhance the intra-molecular interactions. As a result, the thermal responsive behavior of POSS-PAAc$_2$-*b*-PNIPAm$_{11}$ more resembles that of POSS-PNIPAm$_{13}$. When pH is 5.0, POSS-PAAc$_2$-*b*-PNIPAm$_{11}$ even shows slightly lower T_c (26.2 ℃) than POSS-PNIPAm$_{13}$ (28.5 ℃). As previously reported, hydrogen bonds can be formed between PAAc and PNIPAm segments under acidic conditions [9, 10]. As for the star-block POSS-PAAc$_2$-*b*-PNIPAm$_{11}$, the lower T_c at pH 5.0 also implies that there is a synergistic effect between high local chain density and inter-chain hydrogen bonding (Figure 4.5a). In the region near the core, there is a high tendency that the PAAc blocks interfere with PNIPAm blocks, facilitating the intra-molecular hydrophobic interactions. The molecular model in Figure 4.5b illustrates that such inter-arm hydrogen bonds are allowed with the molecular geometry of POSS-PAAc$_2$-*b*-PNIPAm$_{11}$.

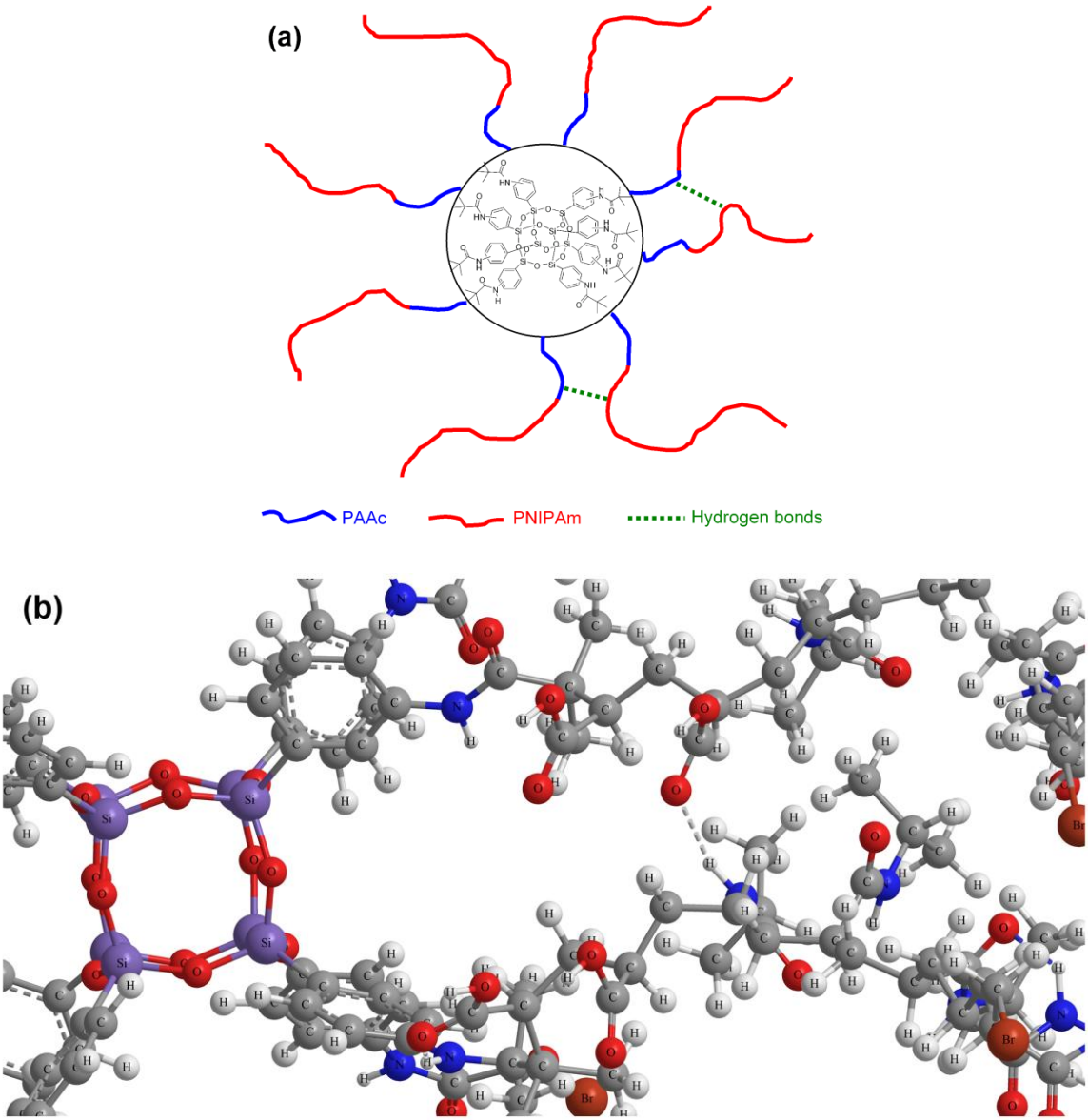

Figure 4.5. (a) Structure illustration of star-block POSS-PAAc-*b*-PNIPAm with possible hydrogen bonds between adjacent arms indicated. (b) A molecular model of two adjacent arms of POSS-$PAAc_2$-*b*-$PNIPAm_{11}$ in the near core region showing a hydrogen bond between AAc and NIPAm.

It is striking to see that unlike POSS-$PAAc_2$-*b*-$PNIPAm_{11}$, the dual responsive behaviors are very different when the star-block copolymer has slightly longer PAAc or PNIPAm block.

With slightly longer PAAc block, POSS-$PAAc_8$-*b*-$PNIPAm_{11}$ exhibits much broader but similar T_c at about 42 ℃ under both acidic and basic conditions (Figure 4.6a). This is because that the interaction between PAAc and PNIPAm segments dominates the phase

transition of the star-block copolymers. The anchoring of longer PAAc blocks next to the core increases the distance between PAAc and PNIPAm blocks on neighbouring arms. As a result, the probability of formation of inter-chain hydrogen bonds is reduced. On the other hand, the chain rigidity in such low molecular weight range also suppresses the interactions between the PAAc and PNIPAm blocks on the same arm. Thus POSS-$PAAc_8$-*b*-$PNIPAm_{11}$ exhibits T_c which is not very sensitive to pH changes. Furthermore, the lower local PNIPAm chain density also suppresses the intra-molecular hydrophobic interaction between PNIPAm blocks. Consequently, the T_c of $PAAc_8$-*b*-$PNIPAm_{11}$ in the whole pH range studied is much higher and broader than that of POSS-$PNIPAm_{13}$, but still lower than linear $PNIPAm_{11}$. Another implication is that although the POSS core may be considered to reduce T_c to some extent due to its hydrophobicity, the fairly high T_c of POSS-$PAAc_8$-*b*-$PNIPAm_{11}$ at low pH, in which condition an even larger hydrophobic core comprising POSS and protonated PAAc segments should be formed, indicates that the hydrophobicity of the core is not the major factor affecting LCST in this case.

Comparing to POSS-$PAAc_2$-*b*-$PNIPAm_{11}$, POSS-$PAAc_4$-*b*-$PNIPAm_{25}$ has a similar length of PAAc block. However, with a longer PNIPAm block, its T_c is lower than the well-known value of 34 ℃ and varies in a much narrower range at different pH (Figure 4.6b). This is due to the random coil conformation of longer PNIPAm blocks. On the other hand, the comparison clearly verifies that the high T_c of POSS-$PAAc_2$-*b*-$PNIPAm_{11}$ and POSS-$PAAc_8$-*b*-$PNIPAm_{11}$ are indeed due to the rod like behavior of the isolated short PNIPAm blocks.

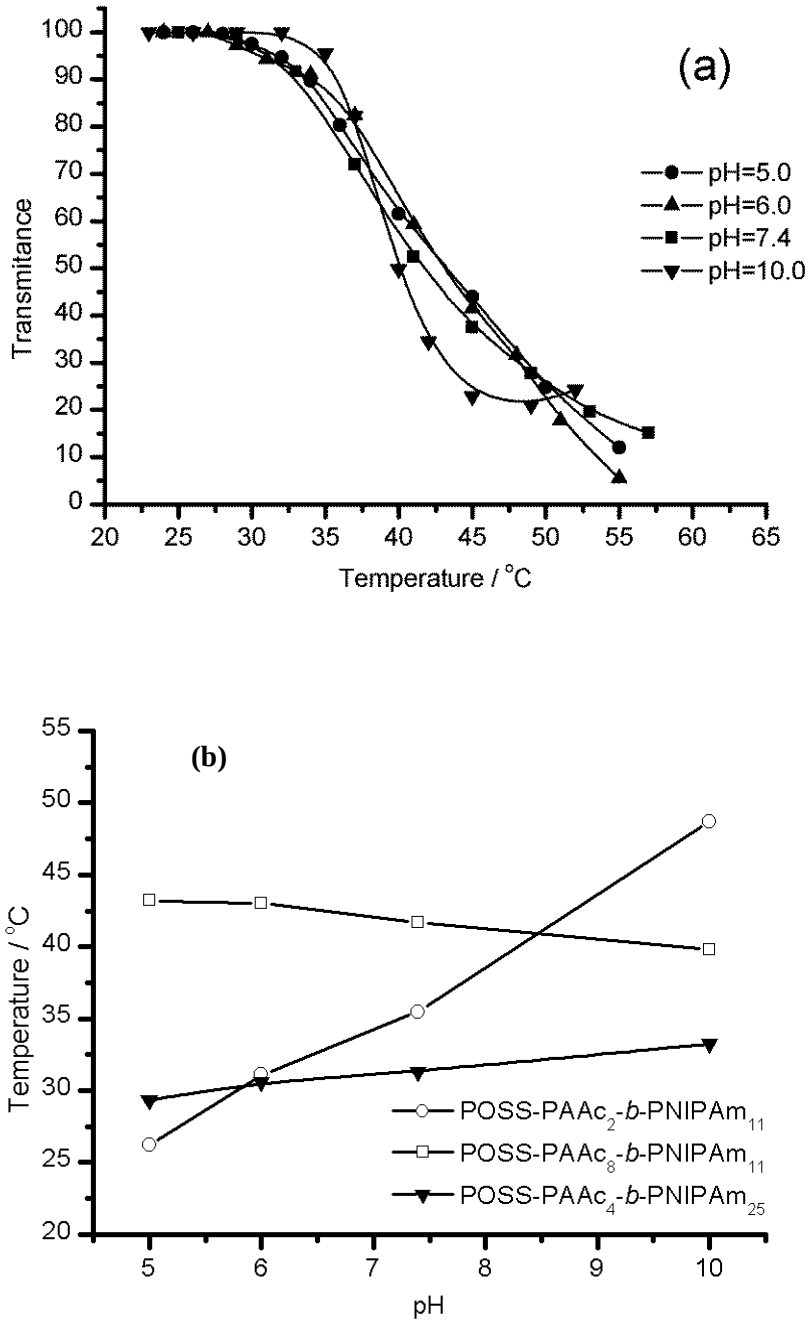

Figure 4.6. (a) Thermal and pH responsive behaviors of POSS-PAAc$_8$-*b*-PNIPAm$_{11}$. (b) The T_c of POSS-PAAc$_2$-*b*-PNIPAm$_{11}$, POSS-PAAc$_8$-*b*-PNIPAm$_{11}$ and POSS-PAAc$_4$-*b*-PNIPAm$_{25}$ as a function of pH.

4.4 Summary

Star-block POSS-PAAc-*b*-PNIPAm copolymers have been successfully synthesized via sequential core-first ATRP of *t*BA and NIPAm followed by removal of *t*-butyl groups by hydrolysis using TFA. The well-defined star architecture has been confirmed by

molecular weight analysis of the star-block copolymer and its cleaved arms using ASEC. The T_c of POSS-PAAc$_2$-*b*-PNIPAm$_{11}$ is found to vary in a wide temperature range with pH changes. Its T_c is even lower than that of POSS-PNIPAm$_{13}$ at pH 5.0, implying a synergic effect between high local chain density and intra-molecular hydrogen bonding. However, its T_c is high and broad at pH 10.0 due to ionization of PAAc that reduces inter-chain interaction and frees the PNIPAm block as isolated rigid rods, which behave similar to linear PNIPAm$_{11}$. With a slightly longer PAAc block, the T_c of POSS-PAAc$_8$-*b*-PNIPAm$_{11}$ is broad and exhibits almost no response to pH. This is because the increased distance between PAAc and PNIPAm blocks may hinder the intra-molecular hydrogen bonding between them.

In last chapter it has been revealed that the high local chain density near the core is crucial to the phase transition behavior of POSS-PNIPAm having the star architecture. The results of this chapter further confirm the importance of the local chain density in the star-block architecture. Moreover, the dual-responsive behaviors of star-block PAAc-PNIPAm demonstrate the feasibility to control the T_c by varying the block size to induce dramatically different response to pH stimuli. The findings may be used to design new thermal and pH responsive polymeric and hybrid systems with controlled block size, such as dendrimer and surface grafted nanoparticles, where the interactions between different blocks can be adjusted via pH or other kind of stimuli.

5. SYNTHESIS AND CHARACTERIZATION OF TEMPERATURE AND PH DUAL RESPONSIVE DENDRITIC PNIPAM WITH PHEMA SHELL

5.1 Introduction

In last chapter the pH dual-responsive behaviors of POSS-PNIPAm-PAAc star-block copolymers have been studied. Besides of the most widely studied PNIPAm- PAAc systems, copolymers of PNIPAm and many other pH-responsive polymers also attract much research interests.

Poly(2-hydroxyethyl methacrylate) (PHEMA) is well known to have very good biocompatibility and widely used in contact lenses, drug delivery and implant materials [71]. PHEMA was once considered only swellable in aqueous solution. Armes *et al.* discovered that linear PHEMA homopolymer having low degree of polymerization (DP) prepared by atom transfer radical polymerization (ATRP) could be dissolved in aqueous solution [77]. Moreover, the solutions of low-molecular-weight PHEMA exhibited cloud points and the T_c varied in a wide range depending on DP and solution pH.

The pH sensitivity of PHEMA provides the possibility to modify PNIPAm with short PHEMA chains to form core-shell nanostructures that may have both dual-responsive properties and improved biocompatibility. Till now, however, only temperature-responsive PNIPAM nanospheres and microspheres with cross-linked PHEMA shell have been reported [173, 174]. Although a few dual-responsive PNIPAm-PHEMA block or graft copolymers have been studied, they do not show core-shell morphology [75, 76, 175]. In this chapter, the synthesis of POSS-cored dendritic PNIPAm with peripheral PHEMA layers is reported. Both POSS-PNIPAm star core and Y-shaped PNIPAm and

PHEMA precursors were prepared via ATRP and the core-shell dendritic architecture was built up via click reaction. The adoption of dendritic instead of star molecular architecture is because that the dendritic structure will provide higher local chain density than star structure, especially for chain segments that are not very close to the core. This would allow effective inter-molecular interactions among PHEMA segments. Herein, the solution behaviors of the POSS-PNIPAm-PHEMA system in response to thermal and pH stimuli are described and discussed in detail. Moreover, the dendritic structure may also act as nanocarriers. The dual-responsive controlled release capability of the dendritic POSS-PANIPAm-PHEMA copolymers is also demonstrated.

5.2 Experimental

5.2.1 Materials

2-Hydroxyethyl methacrylate (HEMA, Sigma-Aldrich, 97%) was dissolved in water and washed with hexane six times and salted out of the aqueous phase by addition of NaCl. After drying in $MgSO_4$, it was distilled under reduced pressure and stored in refrigerator before use. 2,2-Bis(hydroxymethyl)propionic acid (98%), propargyl alcohol (99%), N,N'-dicyclohexylcarbodiimide (DCC), 4-dimethylamino-pyridine (DMAP), sodium azide, Amberlite® IRA-400 azide exchange resin (azide group 3.8 mmol/g), calcein blue, pH buffer solutions with pH = 4.0 (phthalate), were purchased from Sigma-Aldrich and used without further purification. For other chemicals and materials, please refer to Chapter 3.2.1.

5.2.2 Characterizations

FTIR was recorded on a PerkinElmer spectrum GX FTIR system. Dynamic light scattering (DLS) measurements were conducted with a Brookhaven BI-200SM multiangle goniometer equipped with a BI-APD detector. The light source was a Melles Griot 05-LHP-928 He-Ne laser emitting vertically polarized light of wavelength 632.8nm. Measurements were taken at 20 ˚C and the relaxation time (τ) distribution function was calculated using Gendist program. Fluorescence spectroscopy was measured at 437 nm with an irradiation at 322 nm using a Shimadzu RF-5301PC fluorescence spectrophotometer. For ^{1}H and ^{13}C NMR, ASEC and T_c measurements, please refer to Chapter 3.2.2.

5.2.3 Synthesis of PBMP

In the first step, 2,2-bis(hydroxymethyl)-propionic acid 13.41g (0.1mol) and 100mL anhydrous chloroform was charged in a nitrogen protected round bottom flask before adding in 57.3g α-bromoisobutyryl bromide (0.25mol) via dropping funnel. The mixture was refluxed for several hours until no more gas was released and washed with water after reaction. The organic layer was dried by MgSO4 and then precipitated in n-hexane twice to afford white powder product 2,2'-bis(2'-bromo-2'-methylpropionyloxymethyl)-propionic acid (BPA). NMR. ^{1}H NMR: 4.35-4.45(m, -CH_2-OOC-), 1.94 (s, -C(CH_3)$_2$-Br), 1.40 (s, CH_3-C(CH$_2$-)-).

In the second step, BPA 4.32g (0.01mol) and propargyl alcohol 1.15g (0.021mol) was dissolved in anhydrous chloroform and charged in a round bottom flask equipped with magnetic stirrer. DCC 4.54g (0.022mol) and DMAP 0.12g (0.001mol) was dissolved in anhydrous chloroform and dropped into the flask under protection of nitrogen gas. After two hours the reaction mixture was filtered to remove the white DCU precipitate. The

chloroform solution was washed by water before dried with $MgSO_4$. After removing chloroform by rotary evaporation, the product was re-dissolved in ethyl acetate and filtered to remove the remaining small amount of DCU. The solution was then concentrated and purified by column chromatography with dichloromethane and n-hexane (v/v = 2/1) as eluent to afford the product as a white powder (PBMP). ^{1}H NMR ($CDCl_3$, ppm, Figure 5.1a): 4.76 (d, O-C*H*$_2$-CCH), 4.36-4.44 (m, -C*H*$_2$-OOC-), 2.50 (t, -CC*H*), 1.94 (s, -C(C*H*$_3$)$_2$-Br), 1.34 (s, C*H*$_3$-C(CH$_2$-)-). ^{13}C NMR ($CDCl_3$, ppm, Figure 5.1b): 171.64 (-*C*OO-CH$_2$-CCH), 170.96 (Br-(CH$_3$)$_2$-C-*C*OO-CH$_2$-), 75.42 (-*CC*H), 66.20 (C-*C*H$_2$-OOC-), 55.29 (-COO-*C*H$_2$-CCH), 52.82 (-*C*(CH$_3$)$_2$-Br), 46.75 (CH$_3$-*C*(CH$_2$-)-), 30.65 (-C(*C*H$_3$)$_2$-Br), 17.73 (*C*H$_3$-C).

5.2.4 Synthesis of PNIPAm and PHEMA precursors

PNIPAm and PHEMA precursors were synthesized via ATRP using PBMP as initiator (Scheme 5.1). The molecular weights were controlled via monomer to initiator ratio and reaction time. The typical molar ratio of [initiator]:[monomer]:[ligand]:[CuBr] was 1:30:1.8:1.8. Ligand and solvent were Me_6TREN and 2-propanol for PNIPAm synthesis, and PMDETA and methanol/acetone (v/v = 1/1) for PHEMA. In a typical polymerization, the initiator, monomer, ligand and solvent were charged in a Schlenk tube and degassed three times via freeze-pump-thaw process. The solution was kept in a frozen state while CuBr was added in quickly, followed by two more freeze-pump-thaw cycles. The reaction was carried out under protection of nitrogen gas at room temperature and terminated by freezing in liquid nitrogen followed by exposure to air and addition of a few drops of THF. The reaction mixture was passed through a basic aluminium oxide column to remove the copper catalyst. After being dialyzed against water, the mixture

was centrifuged to remove possible undissolved PHEMA and freeze dried to obtain the white product.

5.2.5 Synthesis of POSS-PNIPAm (DN1)

POSS-PNIPAm (DN1) was synthesized using the same procedure as in Chapter 3.2.4.

5.2.6 Azidation reaction

To attach azide group to DN1 to form DN1-N_3, DN1 (840 mg, Br group *ca*. 0.47 mmol) and NaN_3 (310 mg, 4.77 mmol) were dissolved in DMF (10 ml) and stirred at 80˚C for 48 h. The reaction mixture was passed through a neutral aluminium oxide column using DMF as eluent. After the solvent was removed by rotary evaporation, the residue was dissolved in acetone, dialyzed in water and freeze dried to obtain white product. DN2-N_3 was prepared using the same method.

5.2.7 Click reaction

In a typical click reaction to prepare DN2, DN1-N_3 (138 mg, azide group *ca*. 0.08 mmol), PMDETA (17 mg, 0.10 mmol) and PNIPAm precursor (636 mg, *ca*. 0.10 mmol) were dissolved in DMF (5 ml) in a Schlenk tube and degassed by three freeze-pump-thaw cycles. CuBr (14.3 mg, 0.1 mmol) was added in when the solution was at frozen state followed by two more degas cycles. After the solution was heated to 80 ˚C for 24 h under protection of nitrogen gas, it was frozen again by liquid nitrogen and azide resin (10.0 mg, azide group *ca*. 0.038 mmol) was added followed by several freeze-pump-thaw cycles. The solution was then stirred at 80 ˚C for another 24 h before being stopped by freezing in liquid nitrogen and exposure to air. After passing through a neutral aluminium oxide

column to remove catalyst and resin, the solvent was removed by rotary evaporation. The residue was dialyzed in water and freeze dried to obtain white product. Other dendritic polymers (DNH, DN3, DN2H) were prepared using the same procedure.

5.2.8 Release of dyes

20 mg of DN2H and 1 mg of calcein blue were dissolved in 2 mL methanol and ultrasonicated for 30 min. The solvent was put in PBS buffer solution and dialyzed using a MWCO 8000 dialysis tube for 3 h at room temperature to remove unloaded dyes. To measure temperature-responsive release profile, the dialysis tube was put in 100 mL fresh PBS solution at room temperature and the temperature was adjusted to 40 ˚C after 3 h. To measure pH-responsive release profile, the dialysis tube was put in 100 mL fresh PBS solution at room temperature and the pH was adjusted to 5.0 after 3 h. One mL solution was taken out at designed time intervals and the same amount of fresh PBS solution was added in for compensation. All the sample solutions were diluted to 10 mL before fluorescence spectroscopy measurement.

5.3 Results and discussion

5.3.1 Structure verification

The synthesis of initiator propargyl 2,2-bis((2'-bromo-2'-methyl-propionyloxy)-methyl) propionate (PBMP) was illustrated in Scheme 5.1. The structure of PBMP was confirmed by ^{1}H and ^{13}C NMR (Figure 5.1).

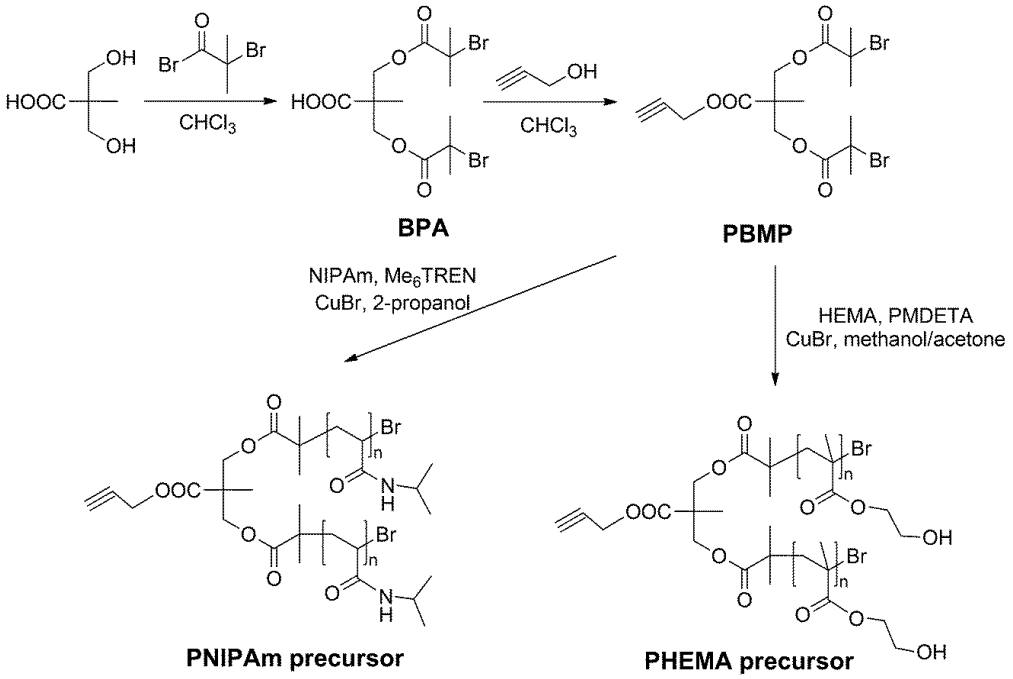

Scheme 5.1. Synthesis of initiator PBMP and ATRP of precursors of PNIPAm and PHEMA.

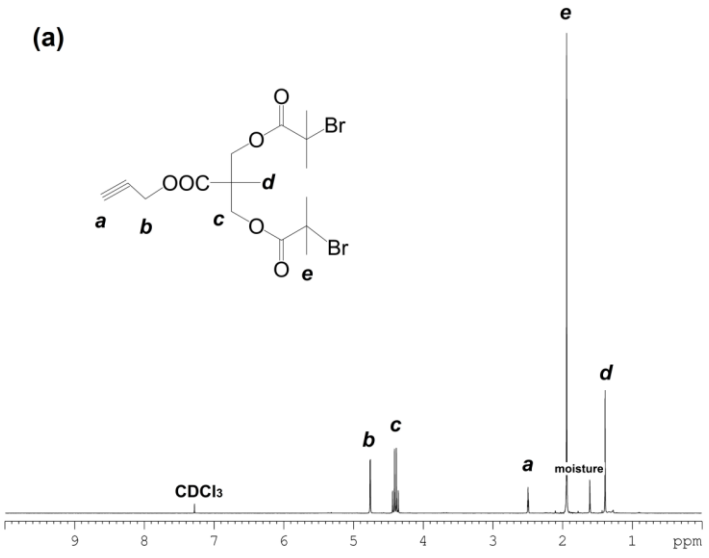

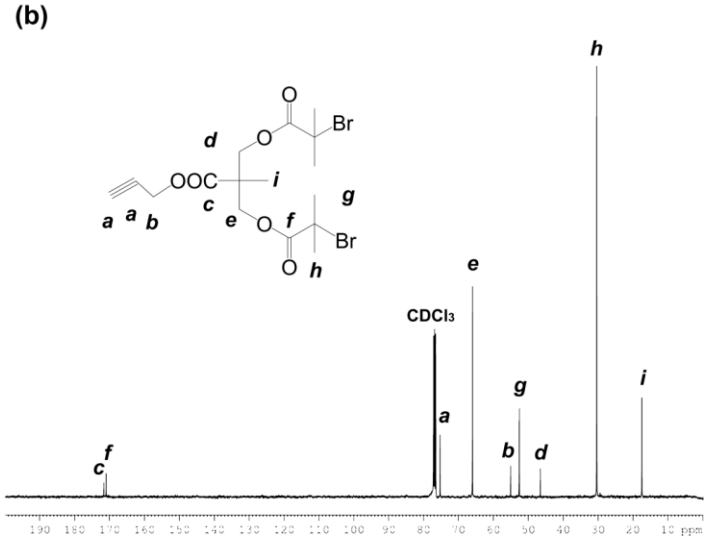

Figure 5.1. (a) ^{1}H NMR and (b) ^{13}C NMR of PBMP.

PNIPAm and PHEMA precursors were synthesized via ATRP using bi-functional initiator and Me_6TREN [155] and PMDETA[176] as ligands, which have been reported to control the distribution in good manner, respectively. The molecular weights of the precursors were measured by ASEC and ^{1}H NMR. Table 5.1 shows that fairly narrow molecular weight distributions have been achieved for both the PNIPAm and PHEMA precursors. However, it has been reported that the molecular weights of PHEMA measured by ASEC are seriously over-estimated because of the difference in the hydrodynamic volumes of the PMMA standards and PHEMA in DMF [163, 164]. Our ASEC data also show that the molecular weights of the PHEMA precursor are much higher than the value from ^{1}H NMR, which is calculated based on the integration ratios of certain peaks from the initiator and HEMA units (Figure 5.2). Thus ^{1}H NMR was used to estimate the DP and then calculate number-average molecular weights (M_n) of the precursors and the results are compared with the ASEC results in Table 5.1. $M_{n,\ NMR}$ of the PNIPAm precursor is reasonably close to that determined by ASEC ($M_{n,\ ASEC}$),

indicating the validity of the NMR method. Hence, for both precursors $M_{n,\,NMR}$ values are used for the estimation of the M_n values of the dendrimers, which will be discussed later.

Table 5.1. Number-average molecular weights (M_n), weight-average molecular weights (M_w) and polydispersities (PDI) of the polymers determined by ASEC and ^{1}H NMR

	$M_{n,\,ASEC}$	$M_{w,\,ASEC}$	PDI, $_{ASEC}$	$M_{n,\,NMR}$
PNIPAm precursor	7449	7740	1.04	6356
PHEMA precursor	14050	14450	1.03	3907
DN1	23870	26770	1.12	14385[a]
DN2	77950	93540	1.20	53188[b]
DNH	116600	153300	1.32	29836[b]
DN3	170800	204800	1.20	154900[b]
DN2H	190600	242600	1.27	108180[b]

[a] Estimated from the ^{1}H NMR integrations of the characteristic peaks of PNIPAm and POSS-based initiator based on the assumption that there are eight arms on each POSS cage (details in Figure 3.2).

[b] Calculated based on the $M_{n,\,NMR}$ of DN1 and the precursors, and the assumption that eight and sixteen precursor molecules are attached onto the core in the first and second click reactions, respectively.

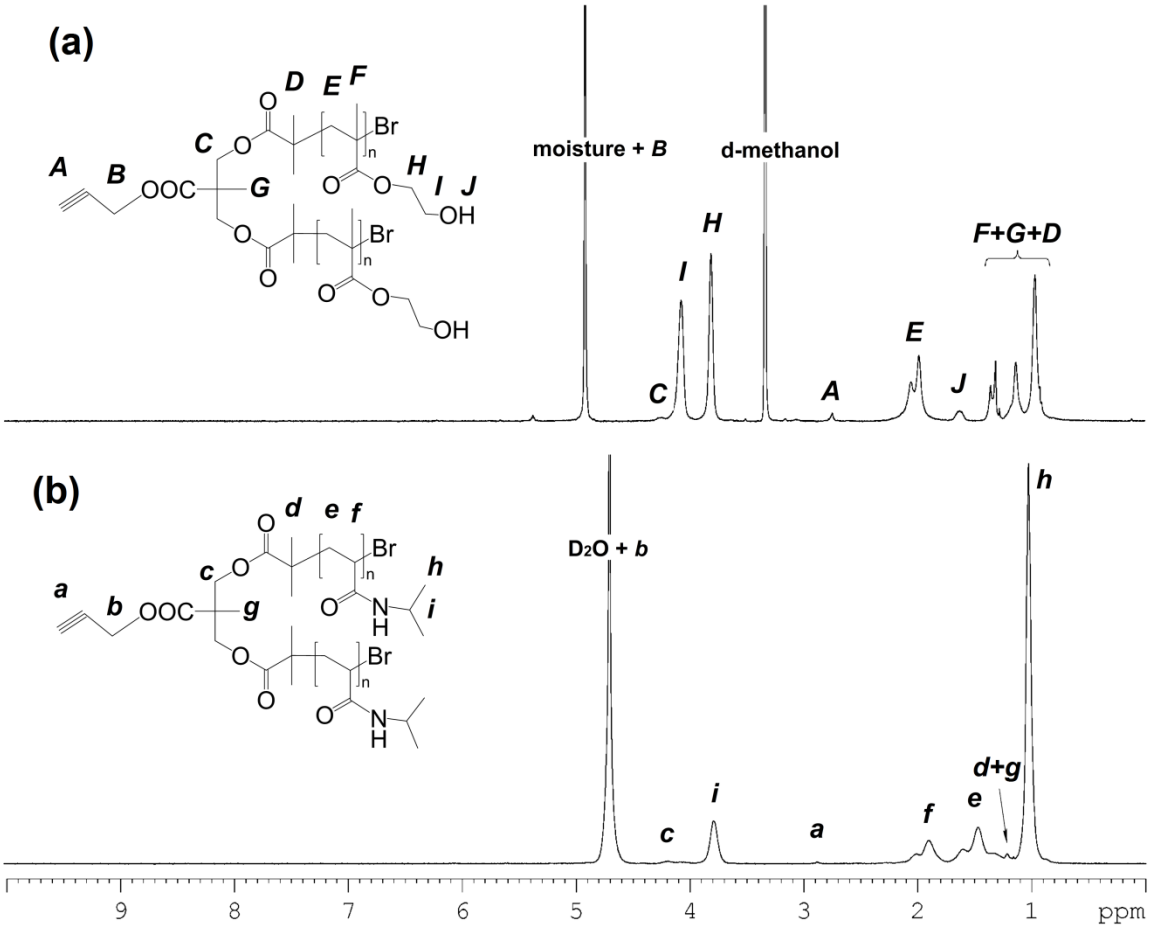

Figure 5.2. ^{1}H NMR of (a) PHEMA precursor and (b) PNIPAm precursor. $M_{n,NMR}$ were calculated by integration ratio of (a) peak H to A; (b) peak i to a.

To enable the click reaction, the Br end groups of DN1 and DN2 were modified with NaN_3 to prepare DN1-N_3 and DN2-N_3, respectively. After the azidation reaction the characteristic infrared band of azide group can be identified at 2030 cm^{-1} (Figure 5.3).

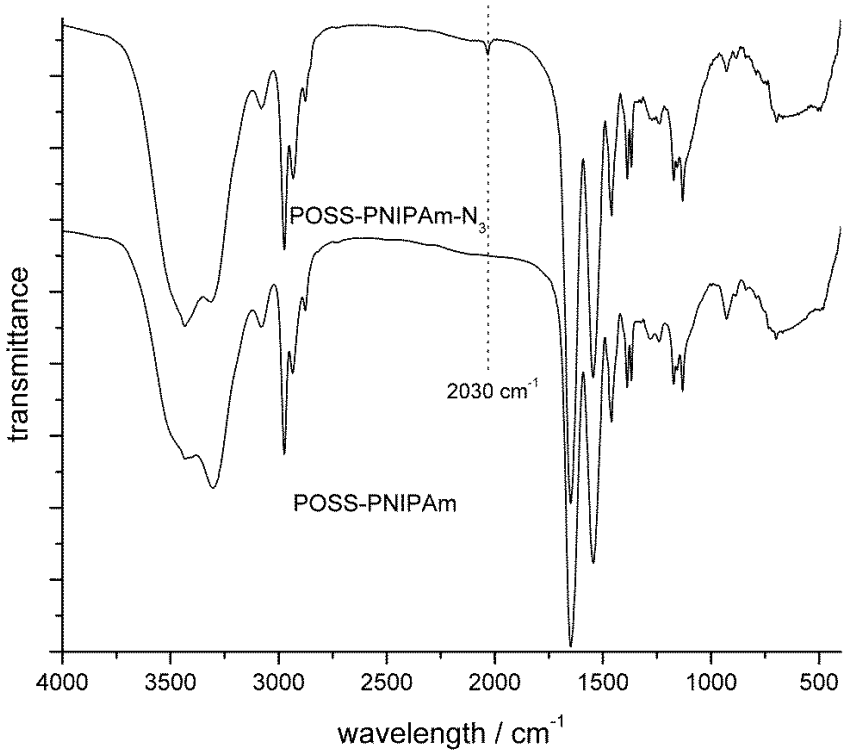

Figure 5.3. FTIR spectra of the star POSS-PNIPAm (DN1) and POSS-PNIPAm-N_3 (DN1-N_3).

The route for the synthesis of the dendrimers is illustrated in Scheme 5.2. The star POSS-PNIPAm (DN1) was prepared as the core of the dendrimer by the ATRP method reported in our previous publication, and its average number of PNIPAm arms has been proven to be close to 8. The second and third generations of dendritic polymers were obtained by reacting PNIPAm or PHEMA precursor with DN1-N_3 and DN2-N_3, respectively. By comparing the 1H NMR spectra of DN2 and DN2H (Figure 5.4), the characteristic peaks of both PNIPAm and PHEMA can be clearly found in the latter. The molecular weights of the dendrimers were measured by ASEC. For the dendrimers, no peak was found in low molecular weight range, indicating the successful removal of the excess amount of the precursors by the azide resin. The narrow distribution and the shifting towards the high molecular weight side with each step of click reaction (Figure 5.5) suggest the successful click reactions. In Table 5.1, the $M_{n,ASEC}$ of the dendrimers are

compared with the values calculated based on the $M_{n,NMR}$ values of DN1 and the precursors and by assuming that 8 and 16 precursor molecules are attached onto the core in the first and second click reactions, respectively. For DN2 and DN3, their $M_{n,\,ASEC}$ and $M_{n,\,NMR}$ are reasonably close to each other, while similar to that of the PHEMA precursor, the $M_{n,\,ASEC}$ values of the dendrimers containing PHEMA moieties are much larger than their $M_{n,\,NMR}$ values.

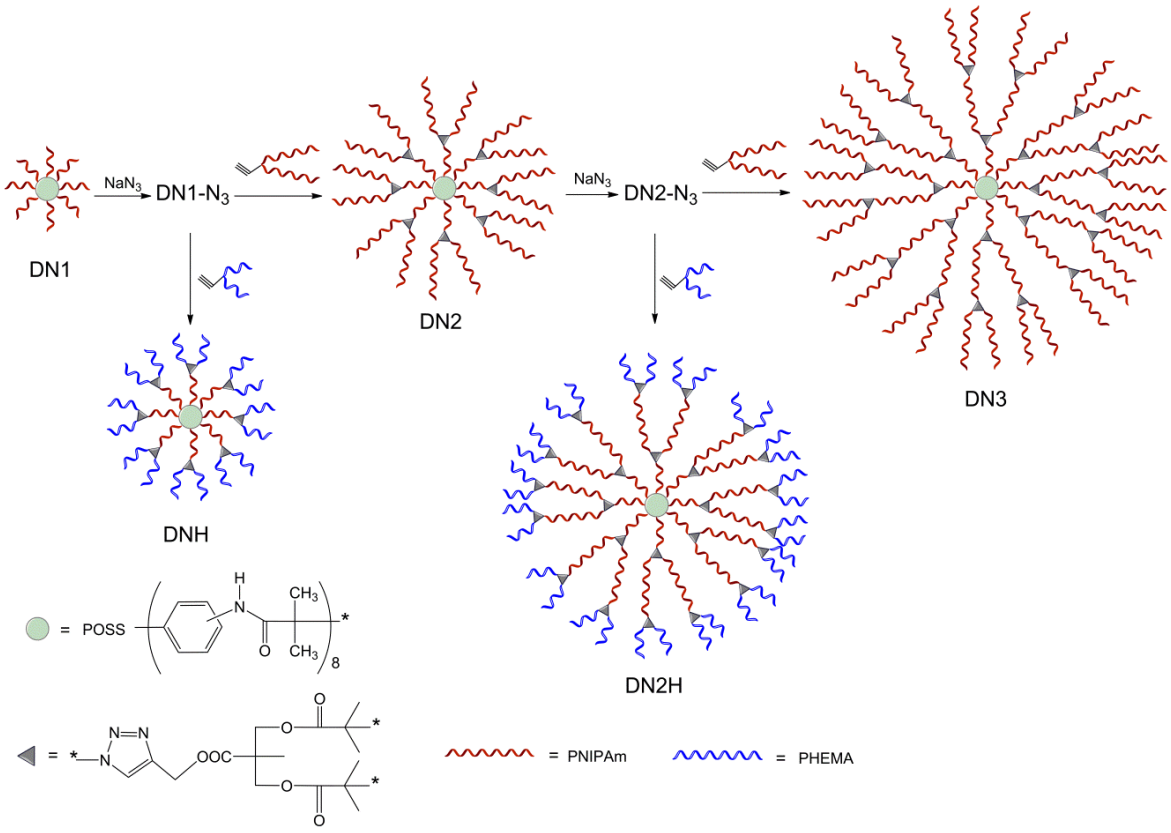

Scheme 5.2. Synthesis of the dendrimers via ATRP and click reaction.

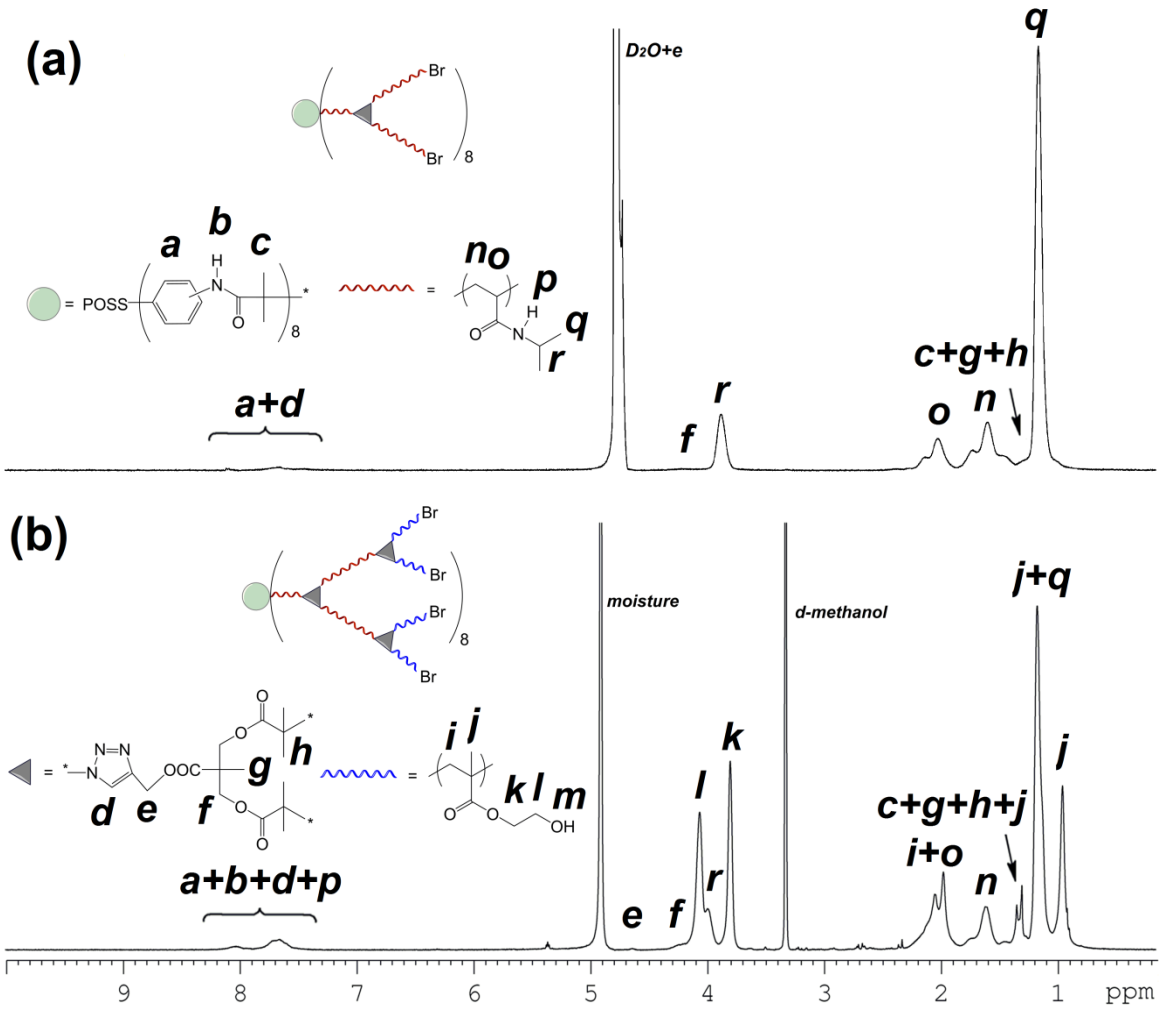

Figure 5.4. ^{1}H NMR of (a) DN2 and (b) DN2H.

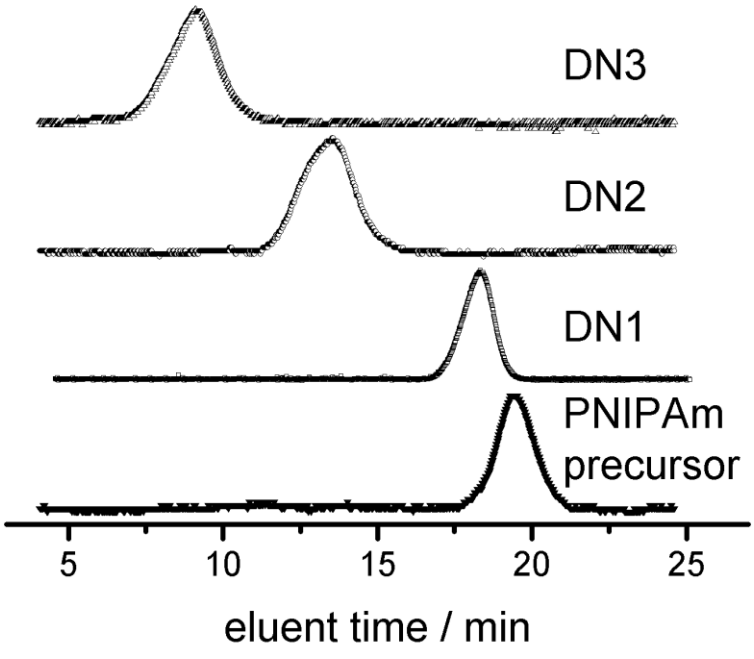

Figure 5.5. ASEC curves of PNIPAm precursor, DN1, DN2 and DN3.

5.3.2 Thermal and pH responsive behavior

The temperature-responsive behaviors of the star POSS-PNIPAm and dendritic PNIPAm with different generations as well as the PNIPAm precursor are shown in Figure 5.6. It can be seen that the T_c of the PNIPAm precursor is about 33.2 ℃, which is consistent with the commonly reported T_c value for high molecular weight linear PNIPAm. By contrast, the T_c of the star POSS-PNIPAm (DN1) is much lower (28.5 ℃) as its high local chain density in the near-core region promotes intra-molecular interactions between the adjacent PNIPAm arms [177]. With the addition of one more generation of PNIPAm branches, the dendritic DN2 exhibits a much higher T_c than that of DN1. This may be attributed to the reduced average local chain density as although the periphery layer of DN2 may have 16 chains, the volume of the periphery layer is much larger as the DP of each branch in this layer is about 26 while the DP of DN1 arms is only about 13. It is worth noting that the T_c of DN2 is still lower than that of the PNIPAm precursor, indicating that the dendritic structure still plays the role of increasing local chain density and hence reducing T_c to some extent in comparison with that of linear PNIPAm. With the third generation of PNIPAm branches, the T_c of DN3 is further increased; it is even slightly higher than that of the PNIPAm precursor, implying that when the diameter of the dendrimer increases further, the PNIPAm chains in the periphery layer might be more difficult to interact with one another owing to the much reduced local chain density.

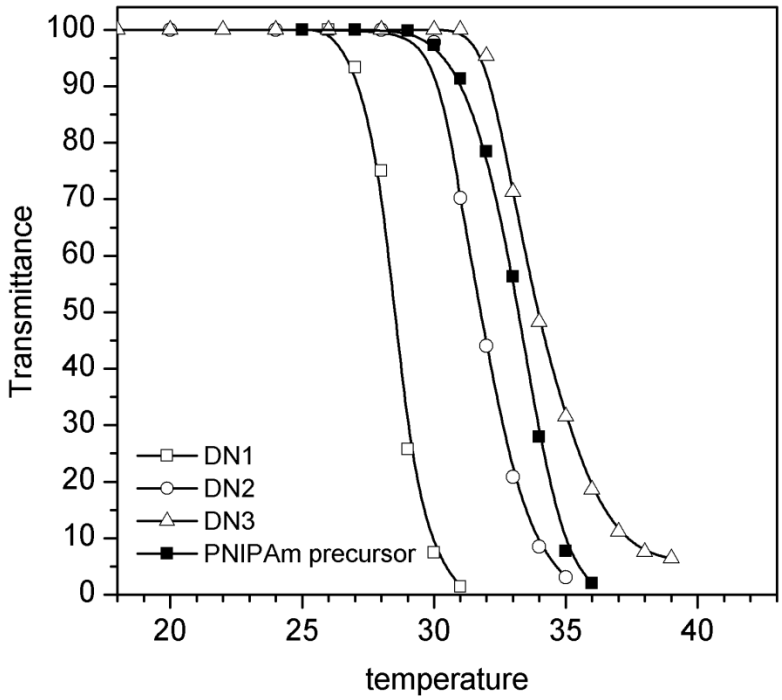

Figure 5.6. Thermal responsive behavior of PNIPAm precursor, DN1, DN2 and DN3.

The temperature-responsive behaviors of DNH, DN2H and the PHEMA precursor are shown in Figure 5.7 Low molecular weight PHEMA has been reported to exhibit reduced solubility in water with increasing temperature [77]. Consistent with the above report, the PHEMA precursor exhibits a broad phase transition from 45 ˚C onward. However, it is striking to see that when PHEMA precursor molecules are clicked onto DN1 and DN2, the resultant DNH and DN2H dendrimers show a single phase transition at a much lower temperature than the T_c of the PHEMA precursor. This implies that when short PHEMA chains are brought close to each other by the dendritic structure, the intra-molecular interactions between the PHEMA chains are enhanced. Such interactions work together with the hydrophobic interactions between PNIPAm chains to give a single T_c dominated by the PNIPAm component.

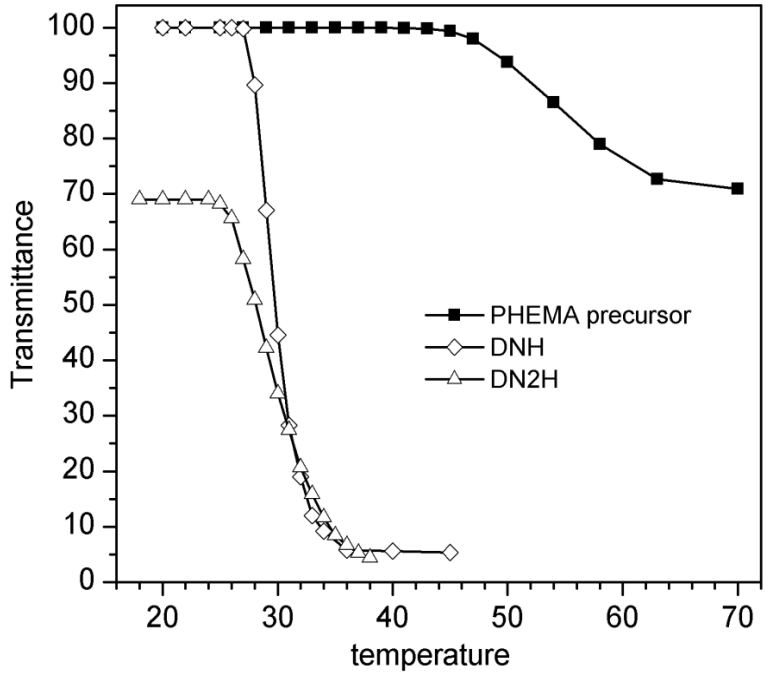

Figure 5.7. Thermal responsive behavior of PHEMA precursor, DNH and DN2H in DI water.

The pH-responsive behaviors of the dendrimers are shown in Figure 5.8. The T_c of DN2H decreases from *ca*. 33.6 ˚C to 23.8 ˚C when pH is reduced from 10.0 to 5.0. However when pH is further reduced to 4.0, the T_c is increased to *ca*. 29.2 ˚C. This is because both intra-molecular hydrogen bonding between PHEMA branches in each dendrimer molecule and inter-molecular hydrogen bonding among the dendrimer molecules play significant roles in the pH range of 10.0 to 5.0. It is believed that the inter-molecular hydrogen bonds may be partially replaced by the intra-molecular hydrogen bonds as the acidity increases from 10.0 to 5.0, and this would promote the intra-molecular hydrophobic interactions between the PNIPAm chains, leading to the reduced T_c with pH. When the pH reaches 4.0, the intra-molecular hydrogen bonds are also diminished and the PHEMA shell mainly form hydrogen bonds with water molecules, enhancing the solubility of the dendrimer in water and hence leading to a higher T_c.

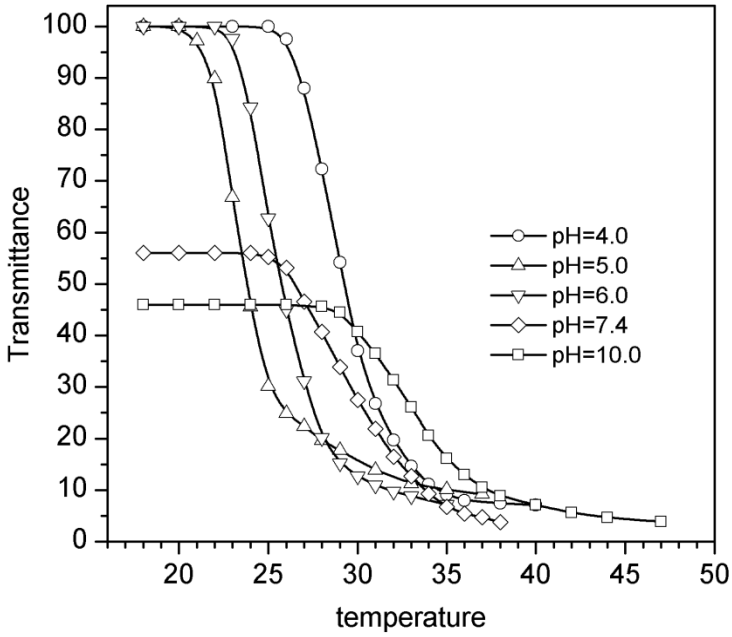

Figure 5.8. Temperature and pH response behaviors of DN2H in different pH buffer solutions.

It is noticeable that the initial transmittances of the DN2H solutions at pH = 7.4 and 10.0 are lower than 100% at temperatures below T_c, indicating the existence of large aggregates. To explain this, the relaxation-time distribution functions of DN2H have been measured at scattering angle 90˚ under different pH conditions (Figure 5.9). The aggregation behaviors of DN2H are indeed greatly influenced by pH. At pH = 4.0, the particle size distribution is unimodal and only the fast mode, which is corresponding to hydrodynamic radius (R_h) of about 5 nm, can be observed. The mono-disperse distribution of the very small particles suggests good solvation of the peripheral PHEMA segments in the highly acidic solution, supporting our hypothesis that the PHEMA shell mainly forms hydrogen bonds with water molecules at pH = 4.0. The fast mode does not disappear until pH reaches 7.4. However, slower modes are also observed in the solutions of pH 5.0 and higher, indicating aggregation of the dendrimers. In the solutions of pH = 7.4 and 10.0, only much slower modes, which corresponds to R_h of *ca*. 120 to 5000 nm,

could be observed, indicating the presence of large aggregates, which agrees well with the observation that the initial transmittances of these solutions are low at temperatures lower than T_c, confirming that at pH = 7.4 and 10.0, inter-molecular interactions among dendrimer molecules are fairly intensive.

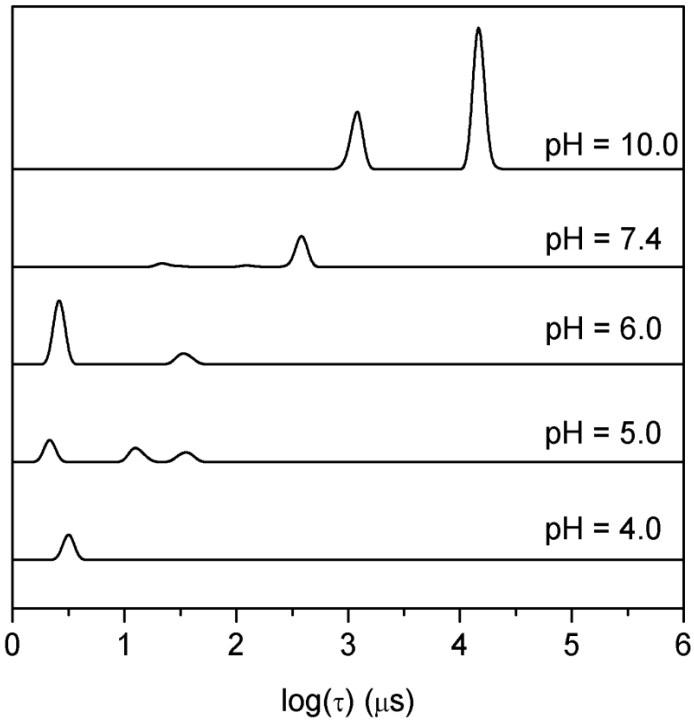

Figure 5.9. Relaxation time (τ) distribution functions of DN2H at different pH.

5.3.3 Controlled release behavior

Till now, most temperature and pH dual-responsive polymeric drug carriers are based on cross-linked hydrogels or self-assembled micelles formed from linear, graft or random block copolymers. Hydrogels are difficult to degrade and be excreted from the body, while block copolymer micelles are relatively instable and easy to be destroyed under dilution, shear forces or some other conditions. The dendritic POSS-PNIPAm-PHEMA could be a good candidate for controlled drug release due to its good solubility in aqueous solution, good biocompatibility of the periphery PHEMA layer and stable micelle

structure. Moreover, its capability of collapsing into compact state upon thermal and pH stimuli would help to deliver the small molecules loaded in the interior cavities to the targets. To further demonstrate the dual responsive behavior of the dendritic copolymer, the release profiles of DN2H in response to temperature or pH changes were examined using a commonly used fluorescent label molecule calcein blue (Figure 5.10) as the loading compound. Figure 5.11a illustrates the fluorescence intensity changes at pH 7.4 when temperature increases from 25 ˚C to 40 ˚C. At the first stage, the temperature is low at 25 ˚C and the fluorescence intensity increases with time slowly. After 3h, when the temperature is raised to 40 ˚C, which is higher than its T_c at pH 7.4, the intensity increases fairly sharply as the hydrophilic to hydrophobic phase transition occurs and hence water molecules and calcein blue molecules are expelled from the cavities among dendritic branches. Figure 5.11b illustrates the response of DN2H to pH changes at constant 25 ˚C. In the first 3 h, DN2H also exhibits a slow release profile at pH 7.4 and a relatively abrupt increase in fluorescence intensity of calcein blue after the pH of the solution is adjusted to 5.0. This is because the T_c of DN2H at pH 5.0 is much lower than at pH 7.4 and is even lower than 25 ˚C (Figure 5.8). Thus the phase transition and release can be triggered when pH decreases from 7.4 to 5.0. It is worth mentioning that although the approach presented in this thesis might be useful for designing new smart drug carriers, such as those used for delivering drugs to tumors that have slightly acidic extracellular pH environment, the major objective of this part of work was to further demonstrate the dual-responsive properties of this novel material system rather than to conduct a quantitative study on its controlled release behavior; the latter would be a subject for future study.

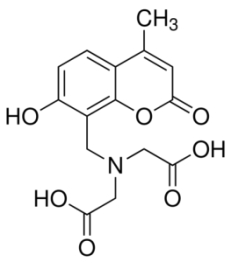

Figure 5.10. Structure of calcein blue.

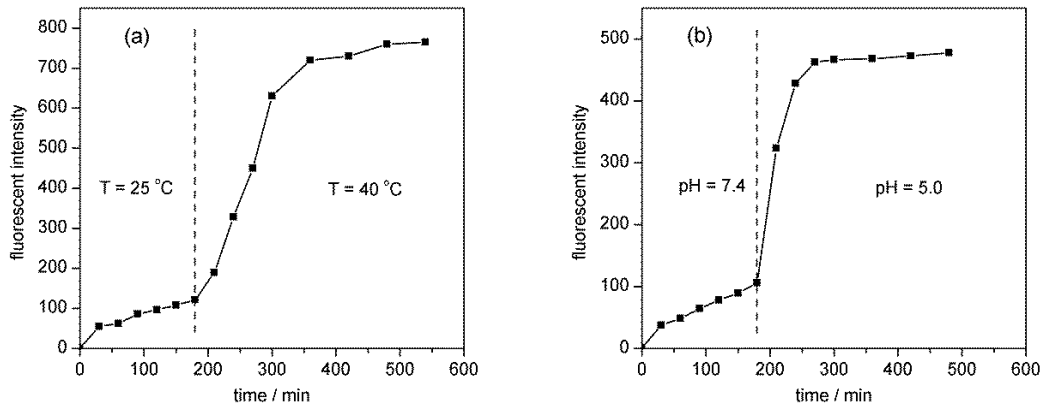

Figure 5.11. Release profile of calcein blue from DN2H at (a) different temperature at pH 7.4; (b) different pH at 25 ℃.

5.4 Summary

Dendritic POSS-PNIPAm-PHEMA copolymers have been successfully prepared via combination of ATRP and click reaction and their structures are verified by ^{1}H NMR, FTIR and ASEC data. The higher generation dendritic PNIPAm exhibits higher T_c, which is due to the relatively long length of PNIPAm segments that increases dendrimer volume significantly after each step of click reaction and hence reduces local chain density, weakening intra-molecular hydrophobic interaction. DN2H is found to be temperature and pH dual-responsive. Its T_c decreases with decreasing pH from 10.0 to 5.0 due probably to the enhanced intra-molecular hydrogen bonds and the weakened inter-molecular interactions. However, the T_c exhibits a small increase from pH 5.0 to 4.0 due to better solvation of PHEMA at highly acidic condition. Particle size measurement reveals that DN2H forms large aggregations at high pH values, whereas at pH 4.0 it has a mono-dispersed distribution with R_h of about 5 nm. The controlled release experiments at different temperature and pH demonstrate that DN2H is a promising candidate for temperature and pH dual-responsive nanocarriers.

6. CONCLUSION AND RECOMMENDATIONS

6.1 Conclusions

The main purpose of this research is to study the effects of star molecular architecture coupled with short chain lengths on solution behaviors of POSS-cored star-block and dendritic PNIPAm copolymers upon pH and thermal stimuli.

Star-shaped PNIPAm polymers have been successfully synthesized by "core first" ATRP using the multi-functional POSS initiator. The well-defined star architecture has been confirmed by molecular weight analysis of the star polymers and their hydrolyzed arms using ASEC. The effect of arm length on thermal responsive behaviors of the star polymers is systematically studied. The T_cs of the star polymers, especially those having short arms, are found to be significantly lower than their linear counterparts having similar chain length. Comparing with the rigid short linear PNIPAm, the star POSS-PNIPAm having short arms exhibits dramatically different solution behaviors due to its high chain density in the near core region that significantly enhanced intra-molecular hydrophobic interactions.

To study the effects of molecular architecture and block length on temperature and pH dual-response of star-shaped copolymer, POSS-PAAc-*b*-PNIPAm star-block copolymers with varied block length have been successfully prepared via sequential ATRP. The structure and architecture have been verified by NMR and ASEC. The dual sensitivity to pH and temperature is found to be closely related to the length of each block. With short PAAc block inserted between POSS core and short PNIPAm block, the T_c varied in a wide range of nearly 20 ℃ from pH 5.0 to 10.0. But when either PNIPAm block or PAAc

block is long, the variation range was much narrower, suggesting a strong synergic effect between high local chain density and the intra-molecular hydrogen bonding.

A series of dendritic thermal and pH responsive POSS-PNIPAm and POSS-PNIPAm-PHEMA copolymers has also been synthesized. The dendritic structures are constructed by click reaction of POSS-PNIPAm and Y-shaped precursors. PNIPAm dendrimers exhibits relatively higher T_c due to their relatively longer length of PNIPAm branches that increases dendrimer volume significantly with increasing generation and at the same time reduces local chain density. When Y-shaped PHEMA precursor is clicked on to form a PHEMA peripheral layer, the short PHEMA chains endow the dendrimer pH responsive solution behavior in a wide range from 10.0 to 4.0. The T_c decreases from 10.0 to 5.0 probably because of the enhanced intra-molecular hydrogen bonding and the weakened inter-molecular interactions. The T_c increases at pH 4.0 due to better solvation of PHEMA at acidic condition. The ability to release small molecules in response to temperature and pH as well as the good biocompatibility of the dendritic PNIPAm-PHEMA make it a promising candidate as a nanocarrier for controlled drug release.

6.2 Recommendations for future studies

PHEMA has already been widely used as soft contact lenses due to its good biocompatibility and low toxicity. However, only in recent years has PHEMA been found to be responsive to pH stimuli and only limited research has been carried out to study the pH responsive behaviors of PHEMA copolymers. In this thesis it has been demonstrated that a short block of PHEMA in the peripheral layer can endow the copolymers with pH sensitivity. As a previously less investigated property, the pH sensitivity of PHEMA should be able to attract more research interest in the future. In addition to PNIPAm, other thermal responsive polymers, such as PVCL, PVP and PVME, can be copolymerized with

short blocks of PHEMA in various architectures to achieve pH-tunable temperature responsive behaviors. The biocompatibility of PHEMA can provide more feasibility of these materials in biomedical related fields.

In this thesis I have simply demonstrated the controlled release ability of dendritic POSS-PNIPAm-PHEMA in response to temperature and pH. Future studies on crosslinking of the peripheral PHEMA layer are recommended to investigate the crosslink density on properties of the material. The dendritic POSS-PNIPAm will form porous nano-sized domains. A higher loading efficiency can be expected with the crosslinked structure with the porous domains. On the other hand, the pH sensitivity could possibly be partly retained when the crosslink density is low.

Another interesting area of research would be using star PNIPAm copolymers as physical crosslinkers to create self-assembled smart hydrogels with other functional materials, such as polydopamine-modified graphene.

REFERENCES

1. I. Y. Galaev and B. Mattiasson, (1999). 'Smart' polymers and what they could do in biotechnology and medicine. *Trends in Biotechnology*, **17**(8),335-340

2. I. Amato, (1990). Smart as a brick. (cover story). *Science News*, **137**(10),152-155

3. C. A. Rogers, (1995). Intelligent materials. *Scientific American*, **273**(3),154

4. H. G. Schild, (1992). Poly (*N*-isopropylacrylamide) - experiment, theory and application. *Progress in Polymer Science*, **17**(2),163-249

5. G. Chen and A. S. Hoffman, (1995). Graft copolymers that exhibit temperature-induced phase transitions over a wide range of pH. *Nature*, **373**(6509),49-52

6. R. Plummer, D. J. T. Hill and A. K. Whittaker, (2006). Solution properties of star and linear poly(*N*-isopropylacrylamide). *Macromolecules*, **39**(24),8379-8388

7. A. P. Vogt, S. R. Gondi and B. S. Sumerlin, (2007). Hyperbranched polymers via RAFT copolymerization of an acryloyl trithiocarbonate. *Australian Journal of Chemistry*, **60**(6),396-399

8. I. Dimitrov, B. Trzebicka, A. H. E. Müller, A. Dworak and C. B. Tsvetanov, (2007). Thermosensitive water-soluble copolymers with doubly responsive reversibly interacting entities. *Progress in Polymer Science (Oxford)*, **32**(11),1275-1343

9. C. M. Schilli, M. F. Zhang, E. Rizzardo, S. H. Thang, Y. K. Chong, K. Edwards, G. Karlsson and A. H. E. Müller, (2004). A new double-responsive block copolymer synthesized via RAFT polymerization: poly(*N*-isopropylacrylamide)-block-poly(acrylic acid). *Macromolecules*, **37**(21),7861-7866

10. S. X. Liu, X. Liu, F. Li, Y. Fang, Y. J. Wang and J. Yu, (2008). Phase behavior of temperature- and pH-sensitive poly(acrylic acid-*g*-*N*-isopropylacrylamide) in dilute aqueous solution. *Journal of Applied Polymer Science*, **109**(6),4036-4042

11. Y. Shen, X. Ma, B. Zhang, Z. Zhou, Q. Sun, E. Jin, M. Sui, J. Tang, J. Wang and M. Fan, (2011). Degradable dual pH- and temperature-responsive photoluminescent dendrimers. *Chemistry – A European Journal*, **17**(19),5319-5326

12. X. D. Ye, Y. W. Ding and J. F. Li, (2010). Scaling of the molecular weight-dependent thermal volume transition of poly(*N*-isopropylacrylamide). *J. Polym. Sci., Part B: Polym. Phys.*, **48**(12),1388-1393

13. I. Idziak, D. Avoce, D. Lessard, D. Gravel and X. X. Zhu, (1999). Thermosensitivity of aqueous solutions of poly(*N*,*N*-diethylacrylamide). *Macromolecules*, **32**(4),1260-1263

14. M. Hahn, E. Gornitz and H. Dautzenberg, (1998). Synthesis and properties of ionically modified polymers with LCST behavior. *Macromolecules*, **31**(17),5616-5623

15. Y. Fang, J. C. Qiang, D. D. Hu, M. Z. Wang and Y. L. Cui, (2001). Effect of urea on the conformational behavior of poly(*N*-isopropylacrylamide). *Colloid and Polymer Science*, **279**(1),14-21

16. N. A. Plate, T. L. Lebedeva and L. I. Valuev, (1999). Lower critical solution temperature in aqueous solutions of *N*-alkyl-substituted polyacrylamides. *Polymer Journal*, **31**(1),21-27

17. M. Meewes, J. Ricka, M. Desilva, R. Nyffenegger and T. Binkert, (1991). Coil globule transition of poly(*N*-isopropylacrylamide) - a study of surfactant effects by light-scattering. *Macromolecules*, **24**(21),5811-5816

18. Y. M. Mohan, T. Premkumar, D. K. Joseph and K. E. Geckeler, (2007). Stimuli-responsive poly(*N*-isopropylacrylamide-co-sodium acrylate) hydrogels: a swelling study in surfactant and polymer solutions. *Reactive & Functional Polymers*, **67**(9),844-858

19. C. Wu and S. Q. Zhou, (1996). Effects of surfactants on the phase transition of poly(*N*-isopropylacrylamide) in water. *Journal of Polymer Science Part B-Polymer Physics*, **34**(9),1597-1604

20. B. Widom, P. Bhimalapuram and K. Koga, (2003). The hydrophobic effect. *Physical Chemistry Chemical Physics*, **5**(15),3085-3093

21. M. Heskins and J. E. Guillet, (1968). Solution properties of poly(*N*-isopropylacrylamide). *J. Macromol. Sci. Chem.*, **A2**(8),1441-1455

22. D. P. K. Dusek, (1968). Transition in swollen polymer networks induced by intramolecular condensation. *Journal of Polymer Science Part A-2: Polymer Physics*, **6**(7),1209-1216

23. C. Wu and S. Q. Zhou, (1996). First observation of the molten globule state of a single homopolymer chain. *Physical Review Letters*, **77**(14),3053-3055

24. Y. Maeda, T. Higuchi and I. Ikeda, (2000). Change in hydration state during the coil-globule transition of aqueous solutions of poly(*N*-isopropylacrylamide) as evidenced by ftir spectroscopy. *Langmuir*, **16**(19),7503-7509

25. Z. Ahmed, E. A. Gooding, K. V. Pimenov, L. Wang and S. A. Asher, (2009). Uv resonance raman determination of molecular mechanism of poly(*N*-isopropylacrylamide) volume phase transition. *Journal of Physical Chemistry B*, **113**(13),4248-4256

26. P. Kujawa, F. Segui, S. Shaban, C. Diab, Y. Okada, F. Tanaka and F. M. Winnik, (2006). Impact of end-group association and main-chain hydration on the thermosensitive properties of hydrophobically modified telechelic poly(*N*-isopropylacrylamides) in water. *Macromolecules*, **39**(1),341-348

27. Y. Xia, N. A. D. Burke and H. D. H. Stöver, (2006). End group effect on the thermal response of narrow-disperse poly(*N*-isopropylacrylamide) prepared by atom transfer radical polymerization. *Macromolecules*, **39**(6),2275-2283

28. S. Furyk, Y. J. Zhang, D. Ortiz-Acosta, P. S. Cremer and D. E. Bergbreiter, (2006). Effects of end group polarity and molecular weight on the lower critical solution temperature of poly(*N*-isopropylacrylamide). *Journal of Polymer Science, Part A: Polymer Chemistry*, **44**(4),1492-1501

29. Y. Xia, X. C. Yin, N. A. D. Burke and H. D. H. Stöver, (2005). Thermal response of narrow-disperse poly(*N*-isopropylacrylamide) prepared by atom transfer radical polymerization. *Macromolecules*, **38**(14),5937-5943

30. K. N. Plunkett, X. Zhu, J. S. Moore and D. E. Leckband, (2006). PNIPAm chain collapse depends on the molecular weight and grafting density. *Langmuir*, **22**(9),4259-4266

31. Y. Katsumoto and N. Kubosaki, (2008). Tacticity effects on the phase diagram for poly(*N*-isopropylacrylamide) in water. *Macromolecules*, **41**(15),5955-5956

32. B. Ray, Y. Okamoto, N. Kamigaito, M. Sawamoto, K. Seno, S. Kanaoka and S. Aoshima, (2005). Effect of tacticity of poly(*N*-isopropylacrylamide) on the phase separation temperature of its aqueous solutions. *Polymer Journal*, **37**(3),234-237

33. T. Kitayama, W. Shibuya and K. Katsukawa, (2002). Synthesis of highly isotactic poly(*N*-isopropylacrylamide) by anionic polymerization of a protected monomer. *Polymer Journal*, **34**(5),405-409

34. J. Xu and S. Y. Liu, (2009). Synthesis of well-defined 7-arm and 21-arm poly(*N*-isopropylacrylamide) star polymers with beta-cyclodextrin cores via click chemistry and their thermal phase transition behavior in aqueous solution. *Journal of Polymer Science, Part A: Polymer Chemistry*, **47**(2),404-419

35. H. Yim, M. S. Kent, D. L. Huber, S. Satija, J. Majewski and G. S. Smith, (2003). Conformation of end-tethered PNIPAm chains in water and in acetone by neutron reflectivity. *Macromolecules*, **36**(14),5244-5251

36. J. Xu, J. Ye and S. Liu, (2007). Synthesis of well-defined cyclic poly(*N*-isopropylacrylamide) via click chemistry and its unique thermal phase transition behavior. *Macromolecules*, **40**(25),9103-9110

37. M. J. Snowden, B. Z. Chowdhry, B. Vincent and G. E. Morris, (1996). Colloidal copolymer microgels of *N*-isopropylacrylamide and acrylic acid: pH, ionic strength and temperature effects. *Journal of the Chemical Society, Faraday Transactions*, **92**(24),5013-5016

38. C. Ramkissoon-Ganorkar, M. Baudyš and S. W. Kim, (2000). Effect of ionic strength on the loading efficiency of model polypeptide/protein drugs in pH-/temperature-sensitive polymers. *Journal of Biomaterials Science - Polymer Edition*, **11**(1),45-54

39. T. Ueki and M. Watanabe, (2007). Lower critical solution temperature behavior of linear polymers in ionic liquids and the corresponding volume phase transition of polymer gels. *Langmuir*, **23**(3),988-990

40. D. Dhara and P. R. Chatterji, (2000). Phase transition in linear and cross-linked poly(*N*-isopropylacrylamide) in water: effect of various types of additives. *Journal of Macromolecular Science-Reviews in Macromolecular Chemistry and Physics*, **C40**(1),51-68

41. P. W. Zhu and D. H. Napper, (1996). Effects of anionic surfactant on the coil-to-globule transition of interfacial poly(*N*-isopropylacrylamide). *Langmuir*, **12**(25),5992-5998

42. H. G. Schild and D. A. Tirrell, (1990). Microcalorimetric detection of lower critical solution temperatures in aqueous polymer solutions. *Journal of Physical Chemistry*, **94**(10),4352-4356

43. K. Otake, H. Inomata, M. Konno and S. Saito, (1990). Thermal-analysis of the volume phase-transition with *N*-isopropylacrylamide gels. *Macromolecules*, **23**(1),283-289

44. E. I. Tiktopulo, V. N. Uversky, V. B. Lushchik, S. I. Klenin, V. E. Bychkova and O. B. Ptitsyn, (1995). Domain coil-globule transition in homopolymers. *Macromolecules*, **28**(22),7519-7524

45. S. Fujishige, K. Kubota and I. Ando, (1989). Phase-transition of aqueous-solutions of poly(*N*-isopropylacrylamide) and poly(*N*-isopropylmethacrylamide). *Journal of Physical Chemistry*, **93**(8),3311-3313

46. Y. Xia, X. Yin, N. A. D. Burke and H. D. H. Stöver, (2005). Thermal response of narrow-disperse poly(*N*-isopropylacrylamide) prepared by atom transfer radical polymerization. *Macromolecules*, **38**(14),5937-5943

47. Z. Tong, F. Zeng, X. Zheng and T. Sato, (1999). Inverse molecular weight dependence of cloud points for aqueous poly(*N*-isopropylacrylamide) solutions. *Macromolecules*, **32**(13),4488-4490

48. H. Vihola, A. Laukkanen, L. Valtola, H. Tenhu and J. Hirvonen, (2005). Cytotoxicity of thermosensitive polymers poly(*N*-isopropylacrylamide), poly(*N*-vinylcaprolactam) and amphiphilically modified poly(*N*-vinylcaprolactam). *Biomaterials*, **26**(16),3055-3064

49. T. Sun and H. E. King, Jr., (1996). Pressure-induced reentrant phase behavior in the poly(*N*-vinyl-2-pyrrolidone)–water system. *Physical Review E*, **54**(3),2696-2703

50. Y. Maeda, (2001). Ir spectroscopic study on the hydration and the phase transition of poly(vinyl methyl ether) in water. *Langmuir*, **17**(5),1737-1742

51. D. E. Meyer, B. C. Shin, G. A. Kong, M. W. Dewhirst and A. Chilkoti, (2001). Drug targeting using thermally responsive polymers and local hyperthermia. *Journal of Controlled Release*, **74**(1-3),213-224

52. A. Chilkoti, M. R. Dreher, D. E. Meyer and D. Raucher, (2002). Targeted drug delivery by thermally responsive polymers. *Advanced Drug Delivery Reviews*, **54**(5),613-630

53. J. E. Chung, M. Yokoyama, M. Yamato, T. Aoyagi, Y. Sakurai and T. Okano, (1999). Thermo-responsive drug delivery from polymeric micelles constructed using block copolymers of poly(*N*-isopropylacrylamide) and poly(butylmethacrylate). *Journal of Controlled Release*, **62**(1-2),115-127

54. C. Choi, S. Y. Chae and J. W. Nah, (2006). Thermosensitive poly(*N*-isopropylacrylamide)-b-poly(epsilon-caprolactone) nanoparticles for efficient drug delivery system. *Polymer*, **47**(13),4571-4580

55. C. Chang, H. Wei, C. Y. Quan, Y. Y. Li, J. Liu, Z. C. Wang, S. X. Cheng, X. Z. Zhang and R. X. Zhuo, (2008). Fabrication of thermosensitive PCL-PNIPAAm-PCL triblock copolymeric micelles for drug delivery. *Journal of Polymer Science Part a-Polymer Chemistry*, **46**(9),3048-3057

56. S. Q. Liu, Y. Y. Yang, X. M. Liu and Y. W. Tong, (2003). Preparation and characterization of temperature-sensitive poly(*N*-isopropylacrylamide)-*b*-poly(D,L-lactide) microspheres for protein delivery. *Biomacromolecules*, **4**(6),1784-1793

57. M. Yang, L. Y. Chu, H. D. Wang, R. Xie, H. Song and C. H. Niu, (2008). A thermoresponsive membrane for chiral resolution. *Advanced Functional Materials*, **18**(4),652-663

58. E. S. Gil and S. M. Hudson, (2004). Stimuli-responsive polymers and their bioconjugates. *Progress in Polymer Science*, **29**(12),1173-1222

59. J. E. Elliott, M. Macdonald, J. Nie and C. N. Bowman, (2004). Structure and swelling of poly(acrylic acid) hydrogels: effect of pH, ionic strength, and dilution on the crosslinked polymer structure. *Polymer*, **45**(5),1503-1510

60. Y. Osada, K. Honda and M. Ohta, (1986). Control of water permeability by mechanochemical contraction of poly(methacrylic acid)-grafted membranes. *Journal of Membrane Science*, **27**(3),327-338

61. Y. Ito, Y. S. Park and Y. Imanishi, (2000). Nanometer-sized channel gating by a self-assembled polypeptide brush. *Langmuir*, **16**(12),5376-5381

62. J. Lindqvist, D. Nystrom, E. Ostmark, P. Antoni, A. Carlmark, M. Johansson, A. Hult and E. Malmstrom, (2008). Intelligent dual-responsive cellulose surfaces via surface-initiated ATRP. *Biomacromolecules*, **9**(8),2139-2145

63. Y. L. Xu, L. Q. Shi, R. J. Ma, W. Q. Zhang, Y. L. An and X. X. Zhu, (2007). Synthesis and micellization of thermo- and pH-responsive block copolymer of poly (*N*-isopropylacrylamide)-*block*-poly(4-vinylpyridine). *Polymer*, **48**(6),1711-1717

64. J. G. Zeng, K. Y. Shi, Y. Y. Zhang, X. H. Sun, L. Deng, X. Z. Guo, Z. J. Du and B. Zhang, (2008). Synthesis of poly(*N*-isopropylacrylamide)-*b*-poly(2-vinylpyridine) block

copolymers via RAFT polymerization and micellization behavior in aqueous solution. *Journal of Colloid and Interface Science*, **322**(2),654-659

65. H. Ghandehari, P. Kopečková and J. Kopecek, (1997). In vitro degradation of pH-sensitive hydrogels containing aromatic azo bonds. *Biomaterials*, **18**(12),861-872

66. N. Murthy, J. R. Robichaud, D. A. Tirrell, P. S. Stayton and A. S. Hoffman, (1999). The design and synthesis of polymers for eukaryotic membrane disruption. *Journal of Controlled Release*, **61**(1-2),137-143

67. R. Salgado-Rodriguez, A. Licea-Claverie and K. F. Arndt, (2004). Random copolymers of N-isopropylacrylamide and methacrylic acid monomers with hydrophobic spacers: pH-tunable temperature sensitive materials. *European Polymer Journal*, **40**(8),1931-1946

68. Y. S. Kim, J. Y. Lim, H. J. Donahue and T. L. Lowe, (2005). Thermoresponsive terpolymeric films applicable for osteoblastic cell growth and noninvasive cell sheet harvesting. *Tissue Engineering*, **11**(1-2),30-40

69. S. A. Angelopoulos and C. Tsitsilianis, (2006). Thermo-reversible hydrogels based on poly(*N*,*N*-diethylacrylamide)-*block*-poly(acrylic acid)-*block*-poly(*N*,*N*-diethylacrylamide) double hydrophilic triblock copolymer. *Macromolecular Chemistry and Physics*, **207**(23),2188-2194

70. N. González, C. Elvira and J. S. Román, (2005). Novel dual-stimuli-responsive polymers derived from ethylpyrrolidine. *Macromolecules*, **38**(22),9298-9303

71. J. P. Montheard, M. Chatzopoulos and D. Chappard, (1992). 2-Hydroxyethyl methacrylate (HEMA): chemical properties and applications in biomedical fields. *Journal of Macromolecular Science, Part C: Polymer Reviews*, **32**(1),1-34

72. J. P. H. Pérez, E. López-Cabarcos and B. López-Ruiz, (2006). The application of methacrylate-based polymers to enzyme biosensors. *Biomolecular Engineering*, **23**(5),233-245

73. M. Y. Arıca, H. A. Öktem, Z. Öktem and S. A. Tuncel, (1999). Immobilization of catalase in poly(isopropylacrylamide-co-hydroxyethylmethacrylate) thermally reversible hydrogels. *Polymer International*, **48**(9),879-884

74. Z. Cao, W. Liu, G. Ye, X. Zhao, X. Lin, P. Gao and K. Yao, (2006). *N*-isopropylacrylamide/2-hydroxyethyl methacrylate star diblock copolymers: synthesis and thermoresponsive behavior. *Macromolecular Chemistry and Physics*, **207**(24),2329-2335

75. X. Zhao, W. Liu, D. Chen, X. Lin and W. W. Lu, (2007). Effect of block order of ABA- and BAB-type NIPAAm/HEMA triblock copolymers on thermoresponsive behavior of solutions. *Macromolecular Chemistry and Physics*, **208**(16),1773-1781

76. M. M. Fares and A. A. Othman, (2008). Lower critical solution temperature determination of smart, thermosensitive *N*-isopropylacrylamide-*alt*-2-hydroxyethyl methacrylate copolymers: kinetics and physical properties. *Journal of Applied Polymer Science*, **110**(5),2815-2825

77. J. V. M. Weaver, I. Bannister, K. L. Robinson, X. Bories-Azeau, S. P. Armes, M. Smallridge and P. McKenna, (2004). Stimulus-responsive water-soluble polymers based on 2-hydroxyethyl methacrylate. *Macromolecules*, **37**(7),2395-2403

78. D. W. Scott, (1946). Thermal rearrangement of branched-chain methylpolysiloxanes. *Journal of the American Chemical Society*, **68**(3),356-358

79. R. H. Baney, M. Itoh, A. Sakakibara and T. Suzuki, (1995). Silsesquioxanes. *Chemical Reviews*, **95**(5),1409-1430

80. R. Y. Kannan, H. J. Salacinski, J. E. Ghanavi, A. Narula, M. Odlyha, H. Peirovi, P. E. Butler and A. M. Seifalian, (2007). Silsesquioxane nanocomposites as tissue implants. *Plastic and Reconstructive Surgery*, **119**(6),1653-1662

81. M. Z. Asuncion and R. M. Laine, (2007). Silsesquioxane barrier materials. *Macromolecules*, **40**(3),555-562

82. S. M. Lee, G. Matamis, D. G. Cahill and W. P. Allen, (1998). Thin-film materials and minimum thermal conductivity. *Microscale Thermophysical Engineering*, **2**(1),31-36

83. R. Franco, A. K. Kandalam, R. Pandey and U. C. Pernisz, (2002). Theoretical study of structural and electronic properties of methyl silsesquioxanes. *Journal of Physical Chemistry B*, **106**(7),1709-1713

84. W. J. Lin, W. C. Chen, W. C. Wu, Y. H. Niu and A. K. Y. Jen, (2004). Synthesis and optoelectronic properties of starlike polyfluorenes with a silsesquioxane core. *Macromolecules*, **37**(7),2335-2341

85. A. Lee, J. Xiao and F. J. Feher, (2005). New approach in the synthesis of hybrid polymers grafted with polyhedral oligomeric silsesquioxane and their physical and viscoelastic properties. *Macromolecules*, **38**(2),438-444

86. Z. P. Zhang, G. Z. Liang and X. L. Wang, (2007). The effect of POSS on the thermal properties of epoxy. *Polymer Bulletin*, **58**(5-6),1013-1020

87. X. Z. Zhang, Y. D. Huang, T. Y. Wang and L. Liu, (2006). Effects of polyhedral oligomeric silsesquioxane coatings on the interface and impact properties of carbon-fiber/polyarylacetylene composites. *Journal of Applied Polymer Science*, **102**(6),5202-5211

88. C. Zhang, F. Babonneau, C. Bonhomme, R. M. Laine, C. L. Soles, H. A. Hristov and A. F. Yee, (1998). Highly porous polyhedral silsesquioxane polymers. synthesis and characterization. *Journal of the American Chemical Society*, **120**(33),8380-8391

89. R. M. Laine, J. Choi and I. Lee, (2001). Organic–inorganic nanocomposites with completely defined interfacial interactions. *Advanced Materials*, **13**(11),800-803

90. C. Zhang and R. M. Laine, (2000). Hydrosilylation of allyl alcohol with $[HSiMe_2OSiO_{1.5}]_8$: Octa(3-hydroxypropyldimethylsiloxy)octasilsesquioxane and its

octamethacrylate derivative as potential precursors to hybrid nanocomposites. *Journal of the American Chemical Society*, **122**(29),6979-6988

91. Q. S. Zhang, L. S. Zha, J. H. Ma and B. R. Liang, (2007). Synthesis and characterization of novel, temperature-sensitive microgels based on *N*-isopropylacrylamide and *tert*-butyl acrylate. *Journal of Applied Polymer Science*, **103**(5),2962-2967

92. J. D. Lichtenhan, Y. A. Otonari and M. J. Carr, (1995). Linear hybrid polymer building blocks: methacrylate-functionalized polyhedral oligomeric silsesquioxane monomers and polymers. *Macromolecules*, **28**(24),8435-8437

93. S. H. Phillips, T. S. Haddad and S. J. Tomczak, (2004). Developments in nanoscience: polyhedral silsesquioxane (POSS)-polymers oligomeric. *Current Opinion in Solid State & Materials Science*, **8**(1),21-29

94. G. R. Pan, J. E. Mark and D. W. Schaefer, (2003). Synthesis and characterization of fillers of controlled structure based on polyhedral oligomeric silsesquioxane cages and their use in reinforcing siloxane elastomers. *Journal of Polymer Science Part B-Polymer Physics*, **41**(24),3314-3323

95. C. H. Chou, S. L. Hsu, S. W. Yeh, H. S. Wang and K. H. Wei, (2005). Enhanced luminance and thermal properties of poly(phenylenevinylene) copolymer presenting side-chain-tethered silsesquioxane units. *Macromolecules*, **38**(22),9117-9123

96. C. H. Chou, S. L. Hsu, K. Dinakaran, M. Y. Chiu and K. H. Wei, (2005). Synthesis and characterization of luminescent polyfluorenes incorporating side-chain-tethered polyhedral oligomeric silsesquioxane units. *Macromolecules*, **38**(3),745-751

97. A. Tsuchida, C. Bolln, F. G. Sernetz, H. Frey and R. Mulhaupt, (1997). Ethene and propene copolymers containing silsesquioxane side groups. *Macromolecules*, **30**(10),2818-2824

98. D. B. Drazkowski, A. Lee and T. S. Haddad, (2007). Morphology and phase transitions in styrene-butadiene-styrene triblock copolymer grafted with isobutyl-substituted polyhedral oligomeric silsesquioxanes. *Macromolecules*, **40**(8),2798-2805

99. J. Wu, T. S. Haddad, G. M. Kim and P. T. Mather, (2007). Rheological behavior of entangled polystyrene-polyhedral oligosilsesquioxane (POSS) copolymers. *Macromolecules*, **40**(3),544-554

100. R. A. Mantz, P. F. Jones, K. P. Chaffee, J. D. Lichtenhan, J. W. Gilman, I. M. K. Ismail and M. J. Burmeister, (1996). Thermolysis of polyhedral oligomeric silsesquioxane (POSS) macromers and poss-siloxane copolymers. *Chemistry of Materials*, **8**(6),1250-1259

101. K. B. Chen, H. Y. Chen, S. H. Yang and C. S. Hsu, (2006). Synthesis and opto-electrical properties of stellar polyfluorene derivatives containing polyhedral oligomeric silsesquioxanes as the center core. *Journal of Polymer Research*, **13**(3),237-245

102. R. O. R. Costa, W. L. Vasconcelos, R. Tamaki and R. M. Laine, (2001). Organic/inorganic nanocomposite star polymers via atom transfer radical polymerization of methyl methacrylate using octafunctional silsesquioxane cores. *Macromolecules*, **34**(16),5398-5407

103. Y. H. Liu, X. T. Yang, W. A. Zhang and S. X. Zheng, (2006). Star-shaped poly(epsilon-caprolactone) with polyhedral oligomeric silsesquioxane core. *Polymer*, **47**(19),6814-6825

104. A. Sellinger and R. M. Laine, (1996). Silsesquioxanes as synthetic platforms .3. photocurable, liquid epoxides as inorganic/organic hybrid precursors. *Chemistry of Materials*, **8**(8),1592-&

105. R. Tamaki, Y. Tanaka, M. Z. Asuncion, J. W. Choi and R. M. Laine, (2001). Octa(aminophenyl)silsesquioxane as a nanoconstruction site. *Journal of the American Chemical Society*, **123**(49),12416-12417

106. J. F. Mu and S. X. Zheng, (2007). Poly(*N*-isopropylacrylamide) nanocrosslinked by polyhedral oligomeric silsesquioxane: temperature-responsive behavior of hydrogels. *Journal of Colloid and Interface Science*, **307**(2),377-385

107. Y. H. Liu, F. L. Meng and S. X. Zheng, (2005). Poly (4-vinylpyridine) nanocrosslinked by polyhedral oligomeric silsesquioxane. *Macromolecular Rapid Communications*, **26**(11),920-925

108. I. S. Isayeva and J. P. Kennedy, (2004). Amphiphilic membranes crosslinked and reinforced by poss. *Journal of Polymer Science Part a-Polymer Chemistry*, **42**(17),4337-4352

109. T. Zhang, K. Xi, H. Chen and X. H. Yu, (2004). Synthesis and properties of self-crosslinkable polyurethane-urea with silsesquioxane formation. *Journal of Applied Polymer Science*, **91**(1),190-195

110. C. U. Pittman, G. Z. Li and H. L. Ni, (2003). Hybrid inorganic/organic crosslinked resins containing polyhedral oligomeric silsesquioxanes. *Macromolecular Symposia*, **196**(301-325

111. M. S. Soh, A. U. J. Yap and A. Sellinger, (2007). Methacrylate and epoxy functionalized nanocomposites based on silsesquioxane cores for use in dental applications. *European Polymer Journal*, **43**(2),315-327

112. K. Takahashi, S. Sulaiman, J. M. Katzenstein, S. Snoblen and R. M. Laine, (2006). New aminophenylsilsesquioxanes - synthesis, properties, and epoxy nanocomposites. *Australian Journal of Chemistry*, **59**(8),564-570

113. P. G. Harrison, (1997). Silicate cages: precursors to new materials. *Journal of Organometallic Chemistry*, **542**(2),141-183

114. F. Xiao, Y. Y. Sun, Y. H. Xiu and C. P. Wong, (2007). Preparation, thermal and mechanical properties of poss epoxy hybrid composites. *Journal of Applied Polymer Science*, **104**(4),2113-2121

115. J. E. Mark, (2003). Some unusual elastomers and experiments on rubberlike elasticity. *Progress in Polymer Science*, **28**(8),1205-1221

116. B. S. Hsiao, H. White, M. Rafailovich, P. T. Mather, H. G. Jeon, S. Phillips, J. Lichtenhan and J. Schwab, (2000). Nanoscale reinforcement of polyhedral oligomeric silsesquioxane (POSS) in polyurethane elastomer. *Polymer International*, **49**(5),437-440

117. G. Z. Li, L. C. Wang, H. Toghiani, T. L. Daulton, K. Koyama and C. U. Pittman, (2001). Viscoelastic and mechanical properties of epoxy/multifunctional polyhedral oligomeric silsesquioxane nanocomposites and epoxy/ladderlike polyphenylsilsesquioxane blends. *Macromolecules*, **34**(25),8686-8693

118. G. Z. Li, L. Wang, H. Toghiani, T. L. Daulton and C. U. Pittman, (2002). Viscoelastic and mechanical properties of vinyl ester (VE)/multifunctional polyhedral oligomeric silsesquioxane (POSS) nanocomposites and multifunctional POSS-styrene copolymers. *Polymer*, **43**(15),4167-4176

119. Y. H. Xu, J. B. Peng, J. X. Jiang, W. Xu, W. Yang and Y. Cao, (2005). Efficient white-light-emitting diodes based on polymer codoped with two phosphorescent dyes. *Applied Physics Letters*, **87**(19),3

120. M. Y. Lo, K. Ueno, H. Tanabe and A. Sellinger, (2006). Silsesquioxane-based nanocomposite dendrimers with photo-luminescent and charge transport properties. *Chemical Record*, **6**(3),157-168

121. J. Lee, H. J. Cho, N. S. Cho, D. H. Hwang, J. M. Kang, E. Lim, J. I. Lee and H. K. Shim, (2006). Enhanced efficiency of polyfluorene derivatives: organic-inorganic hybrid polymer light-emitting diodes. *Journal of Polymer Science Part a-Polymer Chemistry*, **44**(9),2943-2954

122. Y. Xiao, L. Liu, C. B. He, W. S. Chin, T. T. Lin, K. Y. Mya, J. C. Huang and X. H. Lu, (2006). Nano-hybrid luminescent dot: synthesis, characterization and optical properties. *Journal of Materials Chemistry*, **16**(9),829-836

123. R. H. Lee and H. H. Lai, (2007). Enhancing electroluminescence performance of MEH-PPV based polymer light emitting device via blending with organosoluble polyhedral oligomeric silsesquioxanes. *European Polymer Journal*, **43**(3),715-724

124. L. Fenenko, Y. Nakanishi, S. Tokito and A. Konno, (2006). Electronic characterization of new bright-blue-light-emitting poly(9,9-dioctylfluorenyl-2,7-diyl)-end capped with polyhedral oligomeric silsesquioxanes. *Japanese Journal of Applied Physics Part 1-Regular Papers Brief Communications & Review Papers*, **45**(1B),550-554

125. S.-i. Yamamoto, F. Minami, T. Masuda, O. Moriya, M. Kashio and T. Sugizaki, (2006). Preparation of polysilsesquioxane having dimethylamino group and grafted thermoresponsive polymer. *Polymer*, **47**(22),7693-7701

126. T. Masuda, S. I. Yamamoto, O. Moriya, M. Kashio and T. Sugizaki, (2008). Preparation of stimuli-responsive polysilsesquioxane grafted block copolymer of acrylamide monomers. *Polymer Journal*, **40**(2),126-136

127. O. Moriya, M. Kuga, S. Yamamoto, M. Kashio, A. Kamejima and T. Sugizaki, (2006). Preparation of polysilsesquioxane grafted thermoresponsive polymer by use of mercapto group. *Polymer*, **47**(6),1837-1844

128. H. Hussain, K. Y. Mya, Y. Xiao and C. B. He, (2008). Octafunctional cubic silsesquioxane (CSSQ)/poly(methyl methacrylate) nanocomposites: synthesis by atom transfer radical polymerization at mild conditions and the influence of CSSQ on nanocomposites. *J. Polym. Sci., Part A: Polym. Chem.*, **46**(3),766-776

129. H. Hussain, B. H. Tan, C. S. Gudipati, Y. Xiao, Y. Liu, T. P. Davis and C. B. He, (2008). Synthesis and characterization of organic/inorganic hybrid star polymers of 2,2,3,4,4,4-hexafluorobutyl methacrylate and octa(aminophenyl)silsesquioxane nano-cage made via atom transfer radical polymerization. *J. Polym. Sci., Part A: Polym. Chem.*, **46**(22),7287-7298

130. L. J. Fetters, A. D. Kiss, D. S. Pearson, G. F. Quack and F. J. Vitus, (1993). Rheological behavior of star-shaped polymers. *Macromolecules*, **26**(4),647-654

131. T. H. Mourey, S. R. Turner, M. Rubinstein, J. M. J. Frechet, C. J. Hawker and K. L. Wooley, (1992). Unique behavior of dendritic macromolecules: intrinsic viscosity of polyether dendrimers. *Macromolecules*, **25**(9),2401-2406

132. A. W. Bosman, R. Vestberg, A. Heumann, J. M. J. Fréchet and C. J. Hawker, (2002). A modular approach toward functionalized three-dimensional macromolecules: from synthetic concepts to practical applications. *Journal of the American Chemical Society*, **125**(3),715-728

133. X. Zhang, J. H. Xia and K. Matyjaszewski, (2000). End-functional poly(*tert*-butyl acrylate) star polymers by controlled radical polymerization. *Macromolecules*, **33**(7),2340-2345

134. K. Y. Mya, X. Li, L. Chen, X. Ni, J. Li and C. He, (2005). Core-corona structure of cubic silsesquioxane-poly(ethylene oxide) in aqueous solution: fluorescence, light scattering, and tem studies. *The Journal of Physical Chemistry. B*, **109**(19),9455-9462

135. S. X. Xiong, P. T. Jia, K. Y. Mya, J. Ma, F. Boey and X. H. Lu, (2008). Star-like polyaniline prepared from octa(aminophenyl) silsesquioxane: enhanced electrochromic contrast and electrochemical stability. *Electrochimica Acta*, **53**(9),3523-3530

136. I. M. Saez, J. W. Goodby and R. M. Richardson, (2001). A liquid-crystalline silsesquioxane dendrimer exhibiting chiral nematic and columnar mesophases. *Chemistry – A European Journal*, **7**(13),2758-2764

137. K. Tanaka, K. Inafuku, K. Naka and Y. Chujo, (2008). Enhancement of entrapping ability of dendrimers by a cubic silsesquioxane core. *Organic & Biomolecular Chemistry*, **6**(21),3899-3901

138. K. Zeng, Y. Fang and S. X. Zheng, (2009). Organic-inorganic hybrid hydrogels involving poly(*N*-isopropylacrylamide) and polyhedral oligomeric silsesquioxane:

preparation and rapid thermoresponsive properties. *Journal of Polymer Science, Part B: Polymer Physics*, **47**(5),504-516

139. L. Wang, K. Zeng and S. Zheng, (2011). Hepta(3,3,3-trifluoropropyl) polyhedral oligomeric silsesquioxane-capped poly(*N*-isopropylacrylamide) telechelics: synthesis and behavior of physical hydrogels. *ACS Applied Materials & Interfaces*, **3**(3),898-909

140. J. Wang, A. Sutti, X. Wang and T. Lin, (2011). Fast responsive and morphologically robust thermo-responsive hydrogel nanofibres from poly(*N*-isopropylacrylamide) and poss crosslinker. *Soft Matter*, **7**(9),4364-4369

141. W. A. Zhang, L. Liu, X. D. Zhuang, X. H. Li, J. R. Bai and Y. Chen, (2008). Synthesis and self-assembly of tadpole-shaped organic/inorganic hybrid poly(*N*-isopropylacrylamide) containing polyhedral oligomeric silsesquioxane via RAFT polymerization. *Journal of Polymer Science, Part A: Polymer Chemistry*, **46**(21),7049-7061

142. C. H. Ni, G. Wu, C. P. Zhu and B. L. Yao, (2010). The preparation and characterization of amphiphilic star block copolymer nano micelles using silsesquioxane as the core. *Journal of Physical Chemistry C*, **114**(32),13471-13476

143. C. Ni, G. Wu, C. Zhu and B. Yao, (2010). The preparation and characterization of amphiphilic star block copolymer nano micelles using silsesquioxane as the core. *The Journal of Physical Chemistry C*, **114**(32),13471-13476

144. K. Matyjaszewski and J. Xia, (2001). Atom transfer radical polymerization. *Chemical Reviews*, **101**(9),2921-2990

145. N. V. Tsarevsky and K. Matyjaszewski, (2007). "Green" atom transfer radical polymerization: from process design to preparation of well-defined environmentally friendly polymeric materials. *Chemical Reviews*, **107**(6),2270-2299

146. J. Qiu, B. Charleux and K. Matyjaszewski, (2001). Controlled/living radical polymerization in aqueous media: Homogeneous and heterogeneous systems. *Progress in Polymer Science (Oxford)*, **26**(10),2083-2134

147. M. F. Cunningham, (2002). Living/controlled radical polymerizations in dispersed phase systems. *Progress in Polymer Science (Oxford)*, **27**(6),1039-1067

148. M. Kamigaito, T. Ando and M. Sawamoto, (2004). Metal-catalyzed living radical polymerization: discovery and developments. *Chemical Record*, **4**(3),159-175

149. J. T. Rademacher, M. Baum, M. E. Pallack, W. J. Brittain and W. J. Simonsick Jr, (2000). Atom transfer radical polymerization of *N*,*N*-dimethylacrylamide. *Macromolecules*, **33**(2),284-288

150. M. Teodorescu and K. Matyjaszewski, (1999). Atom transfer radical polymerization of (meth)acrylamides. *Macromolecules*, **32**(15),4826-4831

151. K. Zhang, J. Ma, B. Zhang, S. Zhao, Y. P. Li, Y. X. Xu, W. Z. Yu and J. Y. Wang, (2007). Synthesis of thermoresponsive silica nanoparticle/pnipam hybrids by aqueous surface-initiated atom transfer radical polymerization. *Materials Letters*, **61**(4-5),949-952

152. K. Zhang, J. Ma, B. Zhang, S. Zhao, Y. Li, Y. Xu, W. Yu and J. Wang, (2007). Synthesis of thermoresponsive silica nanoparticle/pnipam hybrids by aqueous surface-initiated atom transfer radical polymerization. *Materials Letters*, **61**(4-5),949-952

153. D. J. Kim, B. Kong, Y. H. Jung, K. S. Kim, W. J. Kim, K. B. Lee, S. M. Kang, S. Jeon and I. S. Choi, (2004). Formation of thermoresponsive surfaces by surface-initiated, aqueous atom transfer radical polymerization of *N*-isopropylacrylamide: application to cell culture. *Bulletin of the Korean Chemical Society*, **25**(11),1629-1630

154. D. J. Kim, J. Y. Heo, K. S. Kim and I. S. Choi, (2003). Formation of thermoresponsive poly(*N*-isopropylacrylamide)/dextran particles by atom transfer radical polymerization. *Macromolecular Rapid Communications*, **24**(8),517-521

155. G. Masci, L. Giacomelli and V. Crescenzi, (2004). Atom transfer radical polymerization of *N*-isopropylacrylamide. *Macromolecular Rapid Communications*, **25**(4),559-564

156. T. Wu, Y. Zhang, X. Wang and S. Liu, (2008). Fabrication of hybrid silica nanoparticles densely grafted with thermoresponsive poly(*N*-isopropylacrylamide) brushes of controlled thickness via surface-initiated atom transfer radical polymerization. *Chemistry of Materials*, **20**(1),101-109

157. T. Ishizone, K. Yoshimura, A. Hirao and S. Nakahama, (1998). Controlled anionic polymerization of *tert*-butyl acrylate with diphenylmethyl anions in the presence of dialkylzinc. *Macromolecules*, **31**(25),8706-8712

158. T. Ishizone, K. Yoshimura, E. Yanase and S. Nakahama, (1999). Controlled anionic polymerization of *tert*-butyl acrylate with diphenylmethylpotassium in the presence of triethylborane. *Macromolecules*, **32**(3),955-957

159. H. Deng and K. Soga, (1996). Isotactic polymerization of *tert*-butyl acrylate with chiral zirconocene. *Macromolecules*, **29**(5),1847-1848

160. K. A. Davis and K. Matyjaszewski, (2000). Atom transfer radical polymerization of *tert*-butyl acrylate and preparation of block copolymers. *Macromolecules*, **33**(11),4039-4047

161. S. Strandman, P. Pulkkinen and H. Tenhu, (2005). Effect of ligand on the synthesis of star polymers by resorcinarene-based ATRP initiators. *Journal of Polymer Science, Part A: Polymer Chemistry*, **43**(15),3349-3358

162. K. L. Beers, S. Boo, S. G. Gaynor and K. Matyjaszewski, (1999). Atom transfer radical polymerization of 2-hydroxyethyl methacrylate. *Macromolecules*, **32**(18),5772-5776

163. J. K. Oh and K. Matyjaszewski, (2006). Synthesis of poly(2-hydroxyethyl methacrylate) in protic media through atom transfer radical polymerization using

activators generated by electron transfer. *Journal of Polymer Science Part A: Polymer Chemistry*, **44**(12),3787-3796

164. K. L. Robinson, M. A. Khan, M. V. de Paz Báñez, X. S. Wang and S. P. Armes, (2001). Controlled polymerization of 2-hydroxyethyl methacrylate by ATRP at ambient temperature. *Macromolecules*, **34**(10),3155-3158

165. H. C. Kolb, M. G. Finn and K. B. Sharpless, (2001). Click chemistry: diverse chemical function from a few good reactions. *Angewandte Chemie International Edition*, **40**(11),2004-2021

166. C. Hein, X. M. Liu and D. Wang, (2008). Click chemistry, a powerful tool for pharmaceutical sciences. *Pharmaceutical Research*, **25**(10),2216-2230

167. N. V. Tsarevsky, K. V. Bernaerts, B. Dufour, F. E. Du Prez and K. Matyjaszewski, (2004). Well-defined (co)polymers with 5-vinyltetrazole units via combination of atom transfer radical (co)polymerization of acrylonitrile and "click chemistry"-type postpolymerization modification. *Macromolecules*, **37**(25),9308-9313

168. X. Wan, J. Xu and S. Liu, (2010). Facile synthesis of dendrimer-like star-branched poly(*N*-isopropylacrylamide) via combination of click chemistry and atom transfer radical polymerization. *Science China Chemistry*, **53**(12),2520-2527

169. O. Altintas, A. L. Demirel, G. Hizal and U. Tunca, (2008). Dendrimer-like miktoarm star terpolymers: A_3-$(B\text{-}C)_3$ via click reaction strategy. *Journal of Polymer Science Part A: Polymer Chemistry*, **46**(17),5916-5928

170. M. Ciampolini and N. Nardi, (1966). Five-coordinated high-spin complexes of bivalent cobalt, nickel, and copper with tris(2-dimethylaminoethyl)amine. *Inorganic Chemistry*, **5**(1),41-44

171. J. E. Chung, M. Yokoyama, T. Aoyagi, Y. Sakurai and T. Okano, (1998). Effect of molecular architecture of hydrophobically modified poly(*N*-isopropylacrylamide) on the formation of thermoresponsive core-shell micellar drug carriers. *Journal of Controlled Release*, **53**(1-3),119-130

172. W. A. Zhang, B. Fang, A. Walther and A. H. E. Müller, (2009). Synthesis via RAFT polymerization of tadpole-shaped organic/inorganic hybrid poly(acrylic acid) containing polyhedral oligomeric silsesquioxane (POSS) and their self-assembly in water. *Macromolecules*, **42**(7),2563-2569

173. Y. L. Yu, R. Xie, M. J. Zhang, P. F. Li, L. Yang, X. J. Ju and L. Y. Chu, (2010). Monodisperse microspheres with poly(*N*-isopropylacrylamide) core and poly(2-hydroxyethyl methacrylate) shell. *Journal of Colloid and Interface Science*, **346**(2),361-369

174. P. Weda, B. Trzebicka, A. Dworak and C. B. Tsvetanov, (2008). Thermosensitive nanospheres of low-density core - an approach to hollow nanoparticles. *Polymer*, **49**(6),1467-1474

175. T. M. Quynh, M. Yoneyamab, Y. Maki and T. Dobashi, (2012). Poly(*N*-isopropylacrylamide-co-hydroxyethyl methacrylate) graft copolymers and their application as carriers for drug delivery system. *Journal of Applied Polymer Science*, **123**(4),2368-2376

176. T. L. Wang, Y. Z. Liu, B. C. Jeng and Y. C. Cai, (2005). The effect of initiators and reaction conditions on the polymer syntheses by atom transfer radical polymerization. *Journal of Polymer Research*, **12**(2),67-75

177. Y. Bai, J. Wei, L. P. Yang, C. B. He and X. H. Lu, (2012). Temperature and pH dual-responsive behavior of polyhedral oligomeric silsesquioxane-based star-block copolymer with poly(acrylic acid-block-*N*-isopropylacrylamide) as arms. *Colloid & Polymer Science*, **290**(6),507-515

PUBLICATIONS

1) **Yu Bai**, Jia Wei, Liping Yang, Chaobin He, Xuehong Lu, Temperature and pH dual-responsive behavior of polyhedral oligomeric silsesquioxane-based star-block copolymer with poly(acrylic acid-block-*N*-isopropylacrylamide) as arms, *Colloid & Polymer Science*, **2012**, *290*: 507-515.

2) **Yu Bai**, Liping Yang, Cher Ling Toh, Chaobin He, Xuehong Lu, Temperature and pH dual-responsive behavior of dendritic poly(*N*-isopropylacrylamide) with a polyoligomeric silsesquioxane core and poly(2-hydroxyethyl methacrylate) shell. *Macromolecular Chemistry and Physics*, **2012**, DOI: 10.1002/macp.201200578.

3) Jia Wei, Beng H. Tan, **Yu Bai**, Jan Ma, Xuehong Lu, Self-assembly behaviors of telechelic poly(styrene-ran-sodium styrenesulfonate) with polyhedral oligomeric silsesquioxane as end groups. *The Journal of Physical Chemistry B*. **2011**, *115*, 1929-1935.

4) Jia Wei, Shanxin Xiong, **Yu Bai**, Pengtao Jia, Jan Ma, Xuehong Lu, Polyaniline nanoparticles doped with star-like poly(styrene sulfonate): synthesis and electrochromic properties. *Solar Energy Materials & Solar Cells*, **2012**, *99*, 141-147.